FERMILAB-PUB-11-915-A

accepted to ApJS for *Kepler* special issue

Transit Timing Observations from *Kepler* : I. Statistical Analysis of the First Four Months

Eric B. Ford[1], Jason F. Rowe[2,3], Daniel C. Fabrycky[4], Joshua A. Carter[6], Matthew J. Holman[6], Jack J. Lissauer[3], Darin Ragozzine[6], Jason H. Steffen[7], Natalie M. Batalha[8], William J. Borucki[3], Steve Bryson[3], Douglas A. Caldwell[2,3], Thomas N. Gautier III[10], Jon M. Jenkins[2,3], David G. Koch[3], Jie Li[2,3], Philip Lucas[11], Geoffrey W. Marcy[12], Sean McCauliff[9], Fergal R. Mullally[2,3], Elisa Quintana[2,3], Martin Still[13,3], Peter Tenenbaum[2,3], Susan E. Thompson[2,3], Joseph D. Twicken[2,3]

eford@astro.ufl.edu

ABSTRACT

The architectures of multiple planet systems can provide valuable constraints on models of planet formation, including orbital migration, and excitation of orbital eccentricities and inclinations. NASA's *Kepler* mission has identified 1235 transiting planet candidates (Borucki et al. 2011). The method of transit timing variations (TTVs) has already confirmed 7 planets in two planetary systems (Holman et al. 2010; Lissauer et al. 2011a). We perform a transit timing analysis of the *Kepler* planet candidates. We find that at least ∼11% of planet candidates currently suitable for TTV analysis show evidence suggestive of TTVs, representing at least ∼65 TTV candidates. In all cases,

[1]Astronomy Department, University of Florida, 211 Bryant Space Sciences Center, Gainesville, FL 32111, USA

[2]SETI Institute, Mountain View, CA, 94043, USA

[3]NASA Ames Research Center, Moffett Field, CA, 94035, USA

[4]UCO/Lick Observatory, University of California, Santa Cruz, CA 95064, USA

[5]Hubble Fellow

[6]Harvard-Smithsonian Center for Astrophysics, 60 Garden Street, Cambridge, MA 02138, USA

[7]Fermilab Center for Particle Astrophysics, P.O. Box 500, MS 127, Batavia, IL 60510

[8]San Jose State University, San Jose, CA 95192, USA

[9]Orbital Sciences Corporation/NASA Ames Research Center, Moffett Field, CA 94035, USA

[10]Jet Propulsion Laboratory/California Institute of Technology, Pasadena, CA 91109, USA

[11]Centre for Astrophysics Research, University of Hertfordshire, College Lane, Hatfield, AL10 9AB, England

[12]University of California, Berkeley, Berkeley, CA 94720

[13]Bay Area Environmental Research Institute/NASA Ames Research Center, Moffett Field, CA 94035, USA

the time span of observations must increase for TTVs to provide strong constraints on planet masses and/or orbits, as expected based on n-body integrations of multiple transiting planet candidate systems (assuming circular and coplanar orbits). We find the fraction of planet candidates showing TTVs in this data set does not vary significantly with the number of transiting planet candidates per star, suggesting significant mutual inclinations and that many stars with a single transiting planet should host additional non-transiting planets. We anticipate that *Kepler* could confirm (or reject) at least ∼12 systems with multiple transiting planet candidates via TTVs. Thus, TTVs will provide a powerful tool for confirming transiting planets and characterizing the orbital dynamics of low-mass planets. If *Kepler* observations were extended to at least seven years, then TTVs would provide much more precise constraints on the dynamics of systems with multiple transiting planets and would become sensitive to planets with orbital periods extending into the habitable zone of solar-type stars.

Subject headings: planetary systems; planets and satellites: detection, dynamical evolution and stability; methods: statistical; techniques: miscellaneous

1. Introduction

NASA launched the *Kepler* space mission on March 6, 2009, to measure the frequency of small exoplanets. In its nominal mission *Kepler* will observe over 100 square degrees nearly continuously for three and a half years, so it can detect multiple transits of planets in the habitable zones of solar-type stars. The spacecraft carries consumables that could support an extended mission which would improve sensitivity for detecting small planets and would dramatically improve the constraints from transit timing studies. *Kepler* began collected engineering data ("quarter" 0; Q0) for stars brighter than *Kepler* magnitude (K_p) 13.6 on May 2, 2009, and science data for over 150,000 stars on May 13, 2009. The first "quarter" (Q1) of *Kepler* data extends through June 15, 2009 and the second quarter (Q2) runs from June 20 to September 16, 2009. On February 1, 2011, the *Kepler* team released light curves during Q0, Q1 and Q2 for all planet search targets via the Multi-Mission Archive at the Space Telescope Science Institute (MAST; `http://archive.stsci.edu/kepler/`). The *Kepler* team has performed an initial transiting planet search to identify Kepler Objects of Interest (KOIs) that show transit-like events during Q0-2 (Borucki et al. 2011; hereafter B11). B11 lists 1235 KOIs as active planet candidates. Other KOIs are recognized as likely astrophysical false positives (e.g., blends with background eclipsing binaries) and are reported in B11 Table 4. As the team performs tests of KOIs, a "vetting flag" is used to indicate which KOIs are the strongest and weakest planet candidates with the expected reliability ranging from ≥98% for confirmed planets to ≥60% for those which have yet to be fully vetted. Table 2 of B11, lists the putative orbital period, transit epoch, transit duration, planet size, and vetting flag for KOIs which are active planet candidates and were observed to transit in Q0-2. The current sample of planet candidates is incomplete due to selection effects. In particular, planets with long orbital periods ($P > 125$d),

small planets ($R_p \leq 2R_\oplus$), and planets around faint, active and/or large stars are affected (B11). Further candidates will likely be identified as additional data are analyzed and the *Kepler* pipeline is refined.

The light curve of two eclipsing objects can be very sensitive to perturbations that result in non-Keplerian motion. The variability in the times of eclipsing binaries have been studied for decades. Typically, an "O-C" diagram, highlighting the difference between the observed ephemeris and the ephemeris calculated from a constant period, has been used to detect additional bodies, apsidal motion, and other effects (Bozkurt & Değirmenci 2007 and reference therein; Slawson et al. 2011). The application of this technique to planetary transits is known as Transit Timing Variations (TTVs) which have been studied extensively both theoretically and observationally over the past several years. Astrophysically interesting deviations from a linear transit ephemeris that are potentially observable by *Kepler* can be caused most readily by a perturbing planet (e.g., Miralda-Escudé 2002; Agol et al. 2005; Holman & Murray 2005; Ford & Holman 2007) or moon (e.g., Simon et al. 2007; Kipping et al. 2009), though perturbations by a stellar companion or higher-order gravitational effects can occasionally be significant (e.g., Carter & Winn 2010). In principle, variations in transit duration, depth, or overall shape can also be used to study various astrophysical properties (e.g., Miralda-Escudé 2002; Ragozzine & Wolf 2009; Carter & Winn 2010). The physics of TTV is very similar to eclipse timing variations (ETVs) for binary stars, which are not uncommon in the Kepler Binary Star Catalog (Prsa et al. 2011; Slawson et al. 2011; Orosz et al. 2011). The symmetry of transits (even for large eccentricities) means that transit times are much less susceptible to degeneracies than other transit parameters (e.g., duration, impact parameter and limb darkening; Colón & Ford 2009). Thus, transit times can be measured with the highest precision and accuracy, and are generally expected to be the first recognizable signs of dynamical perturbations. In cases where TTVs are detected, a follow-up investigations of transit duration variations would be warranted.

In this paper, we analyze putative transit times (TTs) by *Kepler* planet candidates that show at least three transits in Q0-2. We describe our methods for measuring transit times and constructing ephemerides in §2. We discuss the results of several statistical analyses applied to each of the planet candidates under consideration in §3. We present a list of planet candidates with early indication of TTVs in §4.1. We compare the expected and observed TTVs for candidate multiple transiting planet systems in §4.2. Finally, we discuss the implications of these early results for planet formation and the future of the TTV method in §5.

2. Measurement of Transit Times from Kepler Data

2.1. Bulk Transit Time Measurements

A combination of pipelines is used to identify KOIs as described in Latham et al. (2011). We measure transit times based on the long cadence (LC), optimal aperture photometry performed by

the *Kepler* SOC pipeline version 6.2 (Jenkins et al. 2010). The pipeline produces both "calibrated" light curves (PA data) for individual analysis and "corrected" light curves (PDC) which are used to search for transits. This paper presents a bulk set of transit times measured from PDC data. For a detailed analysis of an individual system, we strongly recommend that users inspect both PA and PDC data to determine which is best suited for their target star and applications. For example, the TTV detections of Kepler-9b & c and Kepler-11 b-f were based on PA data (Holman et al. 2010; Lissauer et al. 2011a).

We fold light curves at the orbital period reported in B11. Next, we fit a limb-darkened transit model to the folded light curve, allowing the epoch, planet-star radius ratio, transit duration, and impact parameter to vary. We use the best-fit transit model as a fixed template to measure the transit time of each individual transit (while holding other parameters fixed). The best-fit transit times are determined by Levenberg-Marquardt minimization of χ^2 (Press et al. 1992). In a few cases, we iterate the procedure, aligning transits based on the measured period in order to generate an acceptable light curve model. For a small fraction of candidates (KOI 2.01, 403.01, 496.01, 508.01, 559.01, 617.01, 625.01, 678.01, 687.01, 777.01), we measure TTs during Q1 only, due to complications in the Q2 light curves (e.g., stellar noise, and/or grazing short-period events). Two other types of complications merit some explanation. For bright stars that saturate the CCD, causing electrons to bleed into neighboring pixels. When the spacecraft rotates each quarter, a target moves from one CCD to another and the aperture mask specifying which pixels are downloaded changes. If the aperture mask does not capture all the electrons, this can cause the transit light curve to vary from quarter to quarter, breaking the code used for measuring transit times. Another complication that interfered with measuring TTs during Q2 arises since the Q2 photometry for most targets is not as high quality as the Q1 photometry, due to a variety of technical issues (e.g., replacing guide stars that were discovered to be variable or binary resulted in the use of even more problematic guide stars, causing high-frequency spacecraft motion). For a few KOIs with small signal-to-noise per transit, this prevented accurate measurement of TTs during Q2. The photometric quality in subsequent quarters has improved significantly, as demonstrated in publically availiable light curves for Kepler-9, 10 and 11.

We estimate the uncertainty in each transit time from the covariance matrix. For most planet candidates, typical scatter in its TT relative to a linear ephemeris is comparable to the median timing uncertainty (see Fig. 1). Even when the transit model used for transit time measurements is not ideal, good TTVs and errors can be extracted using this technique, since the transit time is the only free parameter and only a roughly correct shape is needed to identify accurate times and errors. Subsets of the observed times reported in Table 1 were tested with different transit time estimation codes, which employ different techniques. While a more thorough analysis can sometimes reduce the timing uncertainty or minimize the number of apparent TTV outliers, the results are consistent across different algorithms.

For target stars where multiple transiting planet candidates have been identified, we sequentially fit each transit separately. Prior to fitting for TTVs, we remove the best-fit transit-models

for additional candidates present in the light curve. For example, if there are 3 planet candidates in the system, then the fitting procedure would first fit for the template light curves in the following order: 1) fit candidate .01, 2) remove .01 from the light curve, 3) fit candidate .02 from residuals, 4) remove .02 from light curve, 5) fit candidate .03 from residuals, and 6) remove .03 from light curve. In most cases, the sequence .01, .02, ... is from the highest to the lowest signal to noise (integrated over all transits). Next, we would measure the transit times according to the following plan: 1) remove .02 and .03 from original light curve, 2) fit for .01 template, 3) measure TTs for candidate .01, 4) remove .01 and .03 from original light curve, 5) fit for .02 template, 6) measure TTs for candidate .02, 7) remove .01 and .02 from original light curve, 8) fit for .03 template, and 9) measure TTs for candidate .03. In some cases, we repeat the measurement of TTs by aligning the transits using the first set of TTs before generating the template.

2.2. Transit Timing Models

Once each set of individual transit times (TTs) has been measured, we calculate multiple sets of TTVs by comparing them to multiple ephemerides. The TTVs reported in Table 1 are measured relative to the linear ephemeris published in B11 (E_L5). A postive TTV corresponds to a transit occuring later than the ephemeris. Second, we considered the TTVs relative to the best-fit linear ephemeris calculated from TTs in Q0-2 (E_L2; Table **??**). The E_L5 ephemerides differ from the E_L2 ephemerides in that epoch ($\hat{E}_0$) and period ($\hat{P}$) were determined using *Kepler* data up to and including Q5, rather than Q2. Finally, we also considered TTVs relative to the best-fit quadratic ephemeris calculated from TTs in Q0-2 (E_Q2). The quadratic ephemeris is given by

$$\hat{t}_n = \hat{E}_0 + n\hat{P}(1 + n\hat{c}), \tag{1}$$

where $\hat{E}_0$ is the best-fit time of the zeroth transit, $\hat{P}$ is the best-fit orbital period, and $\hat{c}$ is the best-fit value of the curvature. For a linear ephemeris, $\hat{c} = 0$.

3. Assessing the Significance of Transit Timing Variations

Transit times for each planet candidate considered are provided in the electronic version of Table 1. Times are measured relative to the E_L5 ephemerides given in Borucki et al. 2011b. We perform several tests to determine if TTVs are statistically significant. These address three questions: 1) "Is the observed scatter in TTs greater than expected?", 2) "Is there is a long-term trend in the TTs?", and 3) "Is there a simple periodic variation in the TTs?".

3.1. Scatter in Transit Times

First, we calculated $X^2 \equiv \sum_{n\in\ Q0-2} \left(\left(t_n - \hat{t}_n \right) / \sigma_n \right)^2$ for $\hat{t}_n$ calculated from both the E_L2 and E_L5 ephemerides. As X^2 closely resembles a χ^2 variable, we first apply a χ^2 test, but based on X^2. If we assume that X^2 follows a χ^2 distribution, then a χ^2 test based would result in a p-value less than 0.001 for 15-17% of candidates. As expected, the fraction is lower if we use the E_L2 ephemerides, since the same times are being used for the model fit and the calculation of X^2. If the errors in the TT measurements, normalized by the estimated timing uncertainty, were accurately described by a standard normal distribution, then one would expect only a few false alarms. However, we note that a disproportionate fraction (42%) of the planet candidates with seemingly significant scatter in their transit times have an average signal to noise (S/N) in each transit of less than 3, while planet candidates with such a small S/N per transit represent only ($\sim$23%) of planet candidates considered. While it is possible that planets with low S/N transit are more likely to have significant TTVs, we opt for a more conservative interpretation that the distribution of errors in our transit times measurements for low S/N transits are not accurately described by a normal distribution with a dispersion given by the estimated timing uncertainties. In particular, when measuring the times of low S/N transits, the X^2 surface as a function of t_n can be bumpy due to noise in the observed light curve, resulting in a much greater probability of measuring a significantly discrepant transit time than assumed by our normal model.

To avoid a high rate of false alarms due to random noise, we focus our attention on planet candidates where the typical S/N in a transit exceeds 3. If we assume that X^2 follows a χ^2 distribution, then results in $\sim$11-13% (86 or 103/805) of the remaining planet candidates having a p-value less than 0.001. We observe that for many of these cases, the contribution to X^2 is dominated by a small fraction of the TTs. Based on the inspection of many light curves around these isolated discrepant transit times, we find that occasionally the measured TTs can be significantly skewed by a couple of deviant photometric measurements. In principle, this could occur due to random noise, but for high S/N transits, stellar variability or improperly corrected systematic errors are the more likely culprits. For example, systematic errors often appear after events such as reaction wheel desaturations, reaction wheel zero crossings, and data gaps (see data release notes at MAST for details; `http://archive.stsci.edu/kepler/data_release.html`).

To further guard against a few discrepant TTs leading to a spurious detection of TTVs, we calculate a statistic that is similar to X^2, but one that is more robust to outliers,

$$X'^2 \equiv \frac{\pi\ N_{TT}\ (\ \mathrm{MAD})^2}{2\sigma_{TT}^2}, \tag{2}$$

where N_{TT} is the number of TTs measured in Q0-2, σ_{TT} is the median TT measurement uncertainty. Here MAD is the median absolute deviation of the measured TTs from an ephemeris, given by

$$\mathrm{MAD} \equiv \mathrm{median}_{i=1}^{N_{TT}} \left(\left| t_i - \hat{t}_i \right| \right), \tag{3}$$

where $\hat{t}_i$ is the time predicted by a given ephemeris. The X'^2 statistic can be viewed as the ratio of a robust variance of the transit times to the square of the typical measurement uncertainty for

transit times. We calculate alternative p-values for rejecting the null hypothesis that there are no deviations from a linear ephemeris by replacing χ^2 with X'^2. Since the distribution of X'^2 may deviate from a χ^2 distribution, the p-values and resulting significance levels are not reliable. Our X'^2 test merely provides a means of filtering the list of KOIs to identify those with potentially significant TTVs. The advantage of X'^2 for our application is that X'^2 is much less sensitive to the assumption that measurement errors are well characterized by a normal distribution. A small fraction of significant outliers can greatly increase X^2 but has a minimal effect on X'^2. While this is more robust than a standard χ^2 test, the statistical significance will not be accurately estimated if the measurement errors are severely non-Gaussian. Of course, the increased robustness comes at a price: X'^2 is not useful for recognizing TTV signals where only a small fraction of TTs deviate from a standard linear ephemeris. We expect this is a good trade, given the predicted TTV signatures (Veras et al. 2011) and the characteristics of our TT measurements.

We identify planet candidates showing strong indications of a TTV signal based on an ad hoc threshold which would correspond to a p-value of $p \leq 10^{-3}$, if X'^2 followed a χ^2 distribution. Restricting our attention to planet candidates for which the individual transits are detected in the light curve with a S/N greater than 3, this test identifies roughly ∼4-5% (29 or 39/805) as showing excess scatter relative to a linear ephemeris. We find the larger fraction (∼5%) when comparing to the E_L2 ephemerides (rather than the E_L5 ephemerides). We speculate that this may be due to the E_L5 ephemerides being more robust to a small number of outlying TTs in Q2 which would have a greater effect on the E_L2 ephemerides. We discuss these candidates further in §4.1. A summary of these and other summary statistics for all planet candidates considered appears in Table 4.

We also considered calculating X^2, but based on "clipped" TTs from Q0-2, where we reject TTs with either a formal uncertainty greater than twice the median timing uncertainty or with an absolute deviation greater than three times the MAD of TTs. This results in ∼4% of planet candidates with at least 3 transits during Q0-2 and a S/N per transit greater than 3 as showing excess scatter relative to the E_L2 ephemeris. While the rate of TTV candidates is consistent with the results of the X'^2 statistic described above, the exact systems flagged differ from those identified basedon X'^2 test. Roughly half of these are cases with less than 10 transits during Q0-2, in which case the threshold for clipping is poorly defined. Therefore, we prefer the tests based on X'^2 for the present dataset.

3.2. Long Term Trends in Transit Times

3.2.1. Difference in Best-fit Orbital Periods

Next, we search the TTs in Q0-2 for evidence of a long-term trend. As a first test, we compare the orbital periods we measure from our E_L2 ephemeris to the period of the E_L5 ephemeris reported in B11 that is based on data from Q0-5. We find period differences greater than three times the formal uncertainty in the orbital periods for roughly 14% (111/805) of planet candidates with a

S/N per transit greater than 3 and at least 3 transits during Q0-2. Most of these have only three transits in Q0-2 or only slightly exceed the threshold, perhaps due to a slight underestimate of the uncertainty in the orbital period. Of the planet candidates for which the periods disagree very significantly and there are at least four transits in Q0-2, most show an easily recognizable long-term trend and were identified as interesting based on X'^2, as described in §3.1.

For planet candidates with an apparently discrepant period and no more than 5 transit times measured in Q0-2, often the E_L2 ephemeris could have been significantly affected by a single outlying TTV point during Q0-2. KOI 1508.01 has 6 transits, and may also have been affected by an outlier. Two planet candidates have large and nearly linear residuals suggesting an inaccurate ephemeris was given in B11. Similarly, further analysis has revealed that the orbital period of KOI 730.03 is much more likely to be very nearly twice that of the value given in B11. Based on data through Q0-2 only, we provide alternative ephemerides of: $(107.5984 \pm 0.0090) + n(19.7198 \pm 0.0044)$ for KOI 730.03, $(118.05868 \pm 0.00011) + n(2.8153306 \pm 0.0000084)$ for KOI 767.01 and $(147.41414 \pm 0.00085) + n(1.2094482 \pm 0.000038)$ for KOI 1540.01. After discarding the cases above, the most compelling candidates with at least five transit times observed in Q0-2 that were identified by this method and not based on X'^2 test are **KOI-524.01** and **662.01**. KOI-961.01 is formally highly significant, but we caution that the short transit duration may affect the TT measurements. **KOIs 226.01, 238.01, 248.01, 564.01, 700.02, 818.01** and **954.01** are also identified based on an apparent discrepancy ($\geq 4 - \sigma$) between the periods of the E_L2 and E_L5 ephemerides. KOIs 295.01, 339.02 and 834.03 also meet this criteria, but are even less secure since they have a S/N per transit of less than three. If the putative signals are real, then they should become obvious with a longer time span of TT observations.

3.2.2. Difference in Best-fit Epochs

We can perform a test similar to §3.2.1, but comparing the epochs we measure from our E_L2 ephemeris to the epoch from the E_L5 ephemeris reported in B11. This test identifies 30 planet candidates for which the best-epoch for Q0-2 differs from that reported for Q0-5 from B11 at the $\geq 4\sigma$ level (excluding some with known issues regarding the TT measurements). Of these, 16 had not been identified based on X'^2 or the test for a difference in orbital periods between Q0-2 and Q0-5: **10.01, 94.02, 137.02, 148.03, 217.01, 279.01, 377.02, 388.01, 417.01, 443.01, 658.01, 679.01** and **1366.01**. In addition, the test based on X'^2 flagged KOIs 1169.01 and 360.01 that have poor TT measurements due to low S/N, 800.02 that may be affected by an outlier. While 279.01 and 679.01 have only three TTs during Q0-2, that is sufficient for testing whether the epoch matches the B11 ephemeris. Particularly interesting are KOIs 279.01, and 658.01 and 663.02 that are in systems with two planet candidates and 94.02, 137.02, 148.03, 377.02, 884.02 and 961.01 that are in systems with three planet candidates (see §4.1.3 & 4.2).

3.2.3. $\mathcal{F}$-test for Comparing Quadratic and Linear Models

While TTV signatures can be quite complex, the time scale for resonant dynamical interactions among planetary systems is typically orders of magnitude longer than the orbital period. Thus, we expect that the dominant TTV signature of many resonant planetary systems can be well approximated by a gradual change in the orbital period over timescales of months to years. Indeed, such a pattern led to the confirmation of Kepler-9 b&c (Holman et al. 2010). (There is also a pattern of alternating transit arriving earlier and later than the quadratic ephemeris. However this "chopping" signature occurs on an orbital timescale, but a much smaller amplitude.) Thus, we fit both linear and quadratic ephemerides (see §2.2) to the Q0-2 data, calculate $X^2_{E_L 2}$ and $X^2_{E_Q 2}$ for the two models, respectively. We perform a variant of the F-test to assess whether including a curvature term significantly improves the quality of the fit. We use a test statistic as $\mathcal{F} \equiv (N_{TT} - 3)X_{E_L 2} / \left[(N_{TT} - 2)X_{E_Q 2}\right]$. This is similar to an F-statistic, but we use $\mathcal{F}$ since it is based on a ratio of X statistics that do not necessarily follow χ^2 distributions. This method has the advantage of being less sensitive to the accuracy of the TT uncertainty estimates, as they affect both the numerator and denominator of the $\mathcal{F}$ statistic similarly. If we assumed that $\mathcal{F}$ followed an F distribution, then an F-test would not result in a p-value less than 10^{-3} for any of the KOIs that are still viable planet candidates. For our application, the $\mathcal{F}$-test has limited power, since we fit only TTs measured in Q0-2, resulting in a shorter time span for a gradual change in the period to accumulate. We note that the $\mathcal{F}$-test does strongly favor the quadratic model for two KOIs previously identified as being due to stellar binary or triple systems (KOI-646.01, Fabrycky et al. in prep; 1153.01), where the curvature is sufficiently large that the period changes appreciably during Q0-2.

Next, we consider systems for which $\mathcal{F}$ would imply a p-value of 0.05 or less, if $\mathcal{F}$ were to follow an F distribution. Quadratic ephemerides for these KOIs are given in Table 4. Approximately 1% of KOIs considered are identified. Half of these correspond to candidates with only 4 or 5 transits in Q0-2, so it is impractical to assess the quality of a three-parameter model accurately. Of the remaining systems, KOI 142.01 and 227.01 were already identified by the X'^2 test, while KOI-528.01 and 1310.01 were not. Upon visual inspection, **528.01** appears to be a plausible detection of TTVs, but 1310.01 does not, as the TTs and uncertainties are also consistent with a linear ephemeris. These candidates are discussed further in §4.1.

3.3. Periodic Variations in Transit Times

Over long time scales, dynamical interactions in two-planet systems can result in complex TTV signatures characterized by many frequencies. However, on short time scales, TTV signatures can often be well described by a single periodic term. For example, for closely packed, but non-resonant, planetary systems, the TTV signature is often dominated by the reflex motion of the star due to other planets. In this case, we would expect a typically small TTV signal on an orbital time scale.

Given the relatively short time span of the observations, we search for planet candidates with a TTV signature that can be approximated by a single sinusoid,

$$\hat{t}_n = \hat{E}_0 + n\hat{P} + \hat{A}\sin(2\pi\ n\hat{P}/\hat{P}_{TTV}) + \hat{B}\cos(2\pi\ n\hat{P}/\hat{P}_{TTV}), \quad (4)$$

$\hat{A}$ and $\hat{B}$ determine the amplitude and phase of the TTV signal, while $2\pi/\hat{P}_{TTV}$ gives the frequency of the model TTV perturbation. For a given $\hat{P}_{TTV}$, finding the best-fit (i.e., minimum X^2) model is a linear minimization problem. Thus, we perform a brute force search over $\hat{P}_{TTV}$ to identify the best-fit simple harmonic model (Ford et al. 2011). Assessing whether the best-fit harmonic model is significantly better than a standard linear ephemeris is notoriously difficult (e.g., Ford & Gregory 2007), even when the distribution and magnitude of measurement uncertainties are well understood. Therefore, we plotted the cumulative distribution of summary statistics and recognized a break in the distribution corresponding to a tail that included approximately 2% of the planet candidates considered, which also included several KOIs which have since been moved to the false positives list. One quarter of the KOIs in this tail had eight or fewer TTs measured in Q0-2, so it was not practical to assess the quality of a five-parameter fit accurately. Of the remaining KOIs with a possible periodic signal, 90% have some other evidence suggesting that they are a stellar binary. Three KOIs remain: KOI-258.01 (most significant), 1465.01, and 1204.01 (least significant). The first two were also identified by the X'^2 analysis described in §3.1. KOI-258.01 appears to show a periodic pattern with amplitude ∼40 minutes and time scale of either ∼28 or 58 days (see Fig. 2), however there is also a hint of a secondary eclipse for KOI-258.01. For KOI-1465.01 the combination of a short transit duration and long cadence observations might have resulted in the PDC data having artifacts that render the TTs unreliable. For KOI-1204.01, there is only a hint of a periodicity and additional observations will be necessary to assess the significance of the putative signal.

4. Planet Candidates of Particular Interest

In this section, we investigate KOIs of particular interest, including those which were identified as potentially having transit timing variations based on one of the statistical tests described in §3 and several in multiple transiting planet candidate systems.

4.1. Planet Candidates with Potential Transit Timing Variations

We provide a summary of the planet candidates identified by our statistical tests in Table 6. For completeness sake, the table includes all planet candidates from B11, with some indication of TTVs and at least three transits in Q0-2. However, we regard many as weak candidates. For a strong candidate, we typically require: 1) a S/N per transit of at least 4, 2) at least 5 TTs observed in Q0-2 for most tests, and 3) no indications of potential difficulties measuring the transit times (e.g., near data gap, short duration, PDC artifacts, heavily spotted star). When comparing the best-fit

epochs, we require only three transits during Q0-2. Many of these candidates were identified by the X'^2 statistic which appears to provide a balance of sensitivity and robustness when searching for excess scatter in the present data set. Those detected by other tests have already been discussed in §3.2 & §3.3 or are indicated with a flag of 6 in Table 6. As the number of transits observed by *Kepler* increases, it is expected that model fitting will eventually provide superior results (Ford & Holman 2007). For example, Kepler 9b&c, and Kepler 11b-f were confirmed by transit timing variations, but only Kepler-9c shows TTVs in the Q0-2 data. For Kepler-9b, the TTVs are not detectable during Q0-2, as the libration timescale (∼10 years) is much greater than the time span of observations (Holman et al. 2009). The TTVs of planets in Kepler-11 are much smaller and demonstrate the benefits of fitting a dynamical model to TTs of all planets simultaneously (Lissauer et al. 2011a).

The analysis presented in this manuscript considers each candidate individually. For multi-candidate systems, it is possible that there exists a significant anti-correlation in TTV signals (Ford et al. in prep; Steffen et al. in prep), even though the individual signals do not reach the various significance thresholds given in Section 3. If the relationship between TTVs of multi-candidate systems can be proven to be non-random, it significantly weakens the probability that the candidate signals are due to false positives (Ragozzine & Holman 2010), even if the properties of the planets cannot be directly inferred. This method of confirming planets will become much stronger with additional data.

4.1.1. False Positives

KOI 928.01 attracted the early attention of the *Kepler* Transit Timing Working Group, despite its low S/N per transit. A detailed analysis suggesting that this is likely a stellar triple system will be presented in Steffen et al. (2011). Several other single TTV candidates were identified as false positives and removed from the B11 planet candidate list.

4.1.2. Weak TTV Candidates

KOIs 156.02, 260.01, 346.01, 579.01, 751.01, 756.02, 786.01, 1019.01, 1111.01, 1236.02, 1241.02, 1396.02, 1508.01 and 1512.01 appear to have excess scatter based on the X'^2 test. However, the small S/N in each transit makes the TT measurements and uncertainties unreliable. Similarly, KOI 295.01, 339.02, 700.02, 800.02, and 834.03 appear to have a change in orbital period and/or epoch between Q0-2 and Q0-5, but may be affected by the small S/N in each transit. In particular, KOI 260.01, 346.01, 800.02, 1111.01, 1508.01 and 1512.01 appear to be affected by an outlier.

Several relatively weak TTV candidates will receive further attention once more TTs are available. For example, KOIs 124.02, 148.03 (see Fig. 2), 209.01 and 707.03 also appear to have excess scatter and have host stars with multiple transiting planet candidates. These planet candidates are less likely to be affected by random noise, given their higher S/N transits, but it is difficult to

assess whether the scatter is significant, since they have only three or four TTs measured in Q0-2.

Of the TTV candidates with only 3 or 4 transits observed in Q0-2, **KOI 148.03, 279.01** and **377.02** stand out, as all three have host stars with multiple transiting planet candidates and a significant offset in epoch relative to the B11 ephemeris. This is suggestive of long-term trends emerging during Q0-5. Indeed, KOI 377.02 has already been confirmed as Kepler-9b (Holman et al. 2011). In the case of KOI 148.03, the scatter in the TTs of the other planet candidates is small, but there may be a feature in common near 160 days, perhaps due to dynamics. Clearly, a more detailed analysis incorporating TTs beyond Q0-2 is merited.

4.1.3. Strong TTV Candidates

Based on Q0-2 data, the largest timing variations for active planet candidates are **KOIs 227.01, 277.01, 1465.01, 884.02, 103.01, 142.01,** and **248.01** (starting with largest magnitude of TTVs). Each of these has well-measured transit times due to a high S/N in each transit, a transit duration of over three hours (minimizing complications due to long cadence and PDC corrections), and a star with limited variability. Each shows a clear trend of TTVs, indicating at least a period change between Q0-2 and Q0-5. Fig. 2 (top row) shows the TTVs of two examples, KOI 103.01 and 142.01. For KOIs 142.02 and 227.01, the period derivative can be measured from Q0-2 data alone (see Table 4). Each of these candidates has been tested with centroid motion tests, high-resolution imaging (except 884 and 1465), and at least some spectroscopic observations. Only KOI 142 shows any indications of the KOI being due to a blend with an eclipsing binary star. Given the large magnitude of the period derivatives, the transiting body must be strongly perturbed, by a companion that is massive, close and/or in a mean-motion resonance (MMR). Despite the clear timing variations, we do not consider these confirmed planets, out of an abundance of caution. Confirming them would require excluding nearly all known possible false positives, as was done for Kepler-9d (Torres et al. 2011) and Kepler-10c (Fressin et al. 2011).

For example, it is possible that some (or all) of these may be examples of physically bound triple systems consisting of the bright target star and a low-mass eclipsing binary. Eclipse timing variations are not uncommon in the Kepler Binary Star Catalog (Prsa et al. 2011; Slawson et al. 2011; Orosz et al. 2011). If this is the case, then it may eventually be possible to detect eclipses of additional bodies due to orbital precession, as observed in the triply eclipsing triple system, KOI-126 (Carter et al. 2011). Indeed, some of the first KOIs investigated by the *Kepler* Transit Timing Working Group have timing variations of a similar magnitude and time scale but turned out to be triple systems (KOIs 646, 928). Since these systems were selected to have the largest amplitude TT variations during Q0-2, it would not be surprising if they were atypical of multiple transiting planet candidate systems. The *Kepler* Science Team will investigate these systems further to determine which are indeed planets and which are multiple star systems. If they are planets, then the planet radii are $\sim 2-3R_{\oplus}$, assuming stellar radii from the Kepler Input Catalog (Brown et al. 2011). Even if all were to turn out to be false positives, the timing variations will play a critical role in

understanding the nature of these KOIs.

Several other planet candidates were identified as having significant scatter in their TTs by the X'^2 test or a difference between our E_L2 ephemeris and the E_L5 ephemeris of B11. Further information for these is given in Table 6. A few, such as **KOI 151.01** and **270.01**, appear to have hints of a pattern in the TTs, but large timing uncertainties make interpretation difficult at this time. We expect that further TT observations will clarify which are real signals and enable confirmation and/or complete dynamical model modeling. One potential source of astrophysical false positives that could masquerade as planets with dynamical TTVs is an isolated star+planet (or eclipsing binary) combined with stellar activity and/or spots. This is a particular concern for planet candidates that appear to have excessive scatter of their TTVs, rather than a long-term trend or periodic pattern. The *Kepler* Follow-up Observation Program will be conducting a variety of follow-up measurements to help eliminate potential false positives and likely confirming many of the multiple transiting planet candidates.

4.1.4. Strong TTV Candidates in Multiple Transiting Planet Candidate Systems

Here we identify only planet candidates with a S/N per transit of at least 4, five or more TTs measured in Q0-2 and a host star with multiple transiting planet candidates: **KOIs 137.02, 153.01, 244.02, 248.01, 270.01, 528.01, 528.03, 564.01, 658.01, 663.02, 693.02, 884.02, 935.01** and **954.01**. For most of these, there is no obvious pattern in the TTVs, perhaps due to measurement errors, or perhaps due to a complex TTV signature. Visual inspection does reveal several planet candidates with tantalizing patterns in the observed TTs.

KOI 884.02 shows the most pronounced pattern, with a min-to-max variation of over an hour within Q0-2. Any TTVs of KOI 884.01 are only suggestive at this time. The period ratio with KOI 884.01 is $P_{884.02}/P_{884.01} = 2.17$, near, but well beyond the nominal 1:2 MMR.

KOI 137.02 shows a significant shift in epoch between the E_L2 and E_L5 ephemerides. The variations in KOI 137.01 are not statistically significant on their own, but are suggestive. The period ratio with KOI 137.01 is $P_{137.02}/P_{137.01} = 1.94$, slightly inside the nominal 1:2 MMR. A detailed analysis of this system will be presented in Cochran et al. (2011).

KOI 244.02 shows a significant shift in epoch between the E_L2 and E_L5 ephemerides, but KOI 244.01 does not. The period ratio with KOI 244.01 is $P_{244.02}/P_{244.01} = 2.04$, near the nominal 1:2 MMR.

KOI 663.02 and **KOI 248.01** show significant shifts in both period and epoch between the E_L2 and E_L5 ephemerides. KOI 663.02 is not near a low-order period commensurability with another transiting planet candidate. KOI 248.01 is near the 3:2 MMR withi 248.02, with a period ratio $P_{248.02}/P_{248.01} = 1.52$.

KOI 528.01 appears to have a long-term trend and/or a periodic pattern of TTVs with a ∼20-30 minute min-to-max in Q0-2. There are not sufficient transits of the other candidates in Q0-2 for a comparison of their TTVs. KOI 528.01 is slightly beyond the nominal 1:2 MMR with KOI 528.03 with a period ratio $P_{528.03}/P_{528.01} = 2.15$.

KOI 270.01 could have a sizable TTV amplitude (∼40 minutes), but relatively large TT measurement uncertainties prevent such a pattern from being clearly recognized in the present data. The period ratio with KOI-270.02 is $P_{270.02}/P_{270.01} = 2.68$.

4.2. Candidate Multiple Transiting Planet Systems

We discuss a few particularly interesting systems with multiple transiting planet candidates. In order to form an order-of-magnitude estimate of the magnitude of TTVs that are likely to arise in systems with multiple transiting planets, we performed an n-body integration for each of these systems. We assume coplanar and circular initial conditions and assign masses according to

$$M_p/M_\oplus = (R_p/R_\oplus)^{2.06}, \tag{5}$$

as described in Lissauer et al. (2011b). As an example, the TTs predicted by the baseline model for the four of the planet candidates of KOI 500 are presented in Fig. 4. The magnitude of TTVs predicted by this baseline model for all stars with multiple transiting planet candidates are reported in Table 7. As the TTV signature can be very sensitive to masses and initial conditions (Veras et al. 2011), we do not expect that these simulations will accurately model the TTV observations. However, they can help us develop intuition for interpreting TT observations. For example, we can often predict a timescale and associated amplitude of TTVs to within a factor of $\sim$ 2, but the phase of the associated TTVs is more sensitive to the detailed initial conditions. For systems with at least one eccentric planet, there can be additional TTV frequencies with much larger amplitudes. the exact phases

4.2.1. Non-detection of TTVs in Multiple Transiting Planet Candidate Systems

Our n-body simulations of multiple transiting planet candidate systems indicate that we should not be surprised that many multiple transiting systems have not yet been detected by TTVs. For our assumed mass-radius relation and circular, coplanar orbits, only KOI 137.01 and 250.02 would have TTVs more than twice the median TT uncertainty and at least three transits during Q0-2. The only indication of TTVs in KOI 137.01 is from the X^2 statistics calculated using the clipped TTs relative to the E_2L ephemeris. Interestingly, we do not detect significant TTVs for 250.02. One possible explanation is that the planets have smaller masses, resulting in TTVs with a smaller amplitude and/or longer timescale. Alternatively, the planets may have eccentricities that significantly affect the TTV signal during Q0-2. Or, there may be additional non-transiting

planets that significantly affect the orbital dynamics. Yet another possibility is that one or both of these KOIs are actually a blend of two planetary systems (or one planetary system and one background eclipsing binary), rather than multiple planets in a single planetary system. Since we chose these two systems based on the predicted TTV signature being among the largest during Q0-2, it would not be surprising if they were atypical of the multiple transiting planet candidate systems. Fortunately, simulations predict that the RMS amplitude will grow to over 17 (137.01) and 5 (250.02) times the median timing uncertainty, so further observations are very likely to resolve the nature of these systems.

Looking at the predicted TTVs over the 3.5 year nominal mission lifetime for all the multiple transiting planet candidate systems, we find that at least 25 transiting planet candidates in 12 systems would be expected to have detectable TTVs. The number of multiple transiting planet systems with detectable TTVs could increase considerably if significant eccentricities are common (Steffen et al. 2010; Veras et al. 2011; Moorhead et al. 2011).

4.2.2. Dynamical Instability & Multiple Transiting Planet Candidate Systems

Our n-body integrations show that the nominal circular, coplanar models of only three KOIs (191, 284 and 730) are violently unstable (Lissauer et al. 2011b). As it is unlikely that a (presumably old) planetary system would go unstable on a timescale much less than the age of the system, we presume that this is an artifact of our choice of masses and/or orbital parameters. This also demonstrates the power of dynamical studies to help constrain the masses and orbits of systems of transiting planet candidates. Alternatively, these KOIs could be a blend of two stars, each with one transiting planet. This would be the natural conclusion, if a future, more thorough investigation were to find that all plausible masses and orbits would quickly result in instability. Indeed, we note that KOI 191.02, 284.02 and 284.03 were assigned a vetting flag of 3 in B11, indicating that there is a increased probability of confusion for these candidates. However, the close commensurabilities of the orbital periods of the planet candidates in KOI 191 (5:4) and 730 (8:6:4:3) make it extremely unlikely for these to be blend scenarios. The dynamics of systems like KOI-730 is discussed in Fabrycky et al. (in prep). Assuming KOI 191, 284 and 730 are stable multiple transiting planet systems, they could have very large TTVs due to their strong mutual gravitational interactions that place them near the edge of instability. As the time span of *Kepler* TT observations increases, TTVs become increasingly sensitive to the masses and orbits of such planetary systems.

4.2.3. Specific Systems

We do not analyze KOI 377 (Kepler-9; Holman et al. 2010), KOI 72 (Kepler-10; Batalha et al. 2011), KOI 157 (Kepler-11; Lissauer et al. 2011a), KOI 137 (Cochran et al. in prep) or KOI 730 (Fabrycky et al. in prep) further, as more thorough analyses have already been published using

data beyond Q0-2 or are in preparation.

KOI-500 hosts five transiting planet candidates. If confirmed, they would be even more tightly packed than the planets of Kepler-11 and would indicate that planetary systems like Kepler-11 are not extremely rare (Lissauer et al. 2011b). The TTs during Q0-2 are shown in Fig. 4. KOI 500.01 was identified as a TTV candidate due to the difference in the best-fit epoch during Q0-2 from that during Q0-5, as reported in B11. While the apparent discrepancy is suggestive, the Q0-2 data is not sufficient to confirm the planetary nature of the KOI. This is not surprising as confirming 5 of the 6 planets orbiting Kepler-11 with TTVs required data extending over Q0-6 (Lissauer et al. 2011a). Fortunately, the nominal model predicts that much larger TTVs (∼hour) will become apparent for four of the 5 planet candidates in future *Kepler* data. The large amplitude is very likely related to the near period commensurabilities of the orbital periods of the outer four planet candidates (4:6:9:12). Each neighboring pair of planets has a period ratio slightly greater than the nominal MMR, as is typical for near-resonant systems identified by *Kepler* (Lissauer et al. 2011b). Further, each pair deviates from the nominal resonance by a similar amount, strongly suggesting that the four bodies are dynamically interacting. Unfortunately, *Kepler* 's nominal mission lifetime is shorter than the dominant timescale of TTVs predicted for KOI-500. In order to establish that a TTV signal is periodic, one needs to observe $\geq$ 2 cycles. Hopefully, the *Kepler* mission can be extended, as the increased time baseline would dramatically enhance the sensitivity of TTV observations to the planet masses and orbital parameters.

5. Discussion

5.1. Precision of Transit Times from Kepler

Our analysis of TT measurements during Q0-Q2 demonstrate that *Kepler* is capable of providing precise transit times which can be expected to enable the dynamical confirmation of transiting planet candidates and detection of non-transiting planets. After discarding those planet candidates with S/N per transit of less than 4 or just a few transits in Q0-2, the median absolute deviation (MAD) of transit times from a linear ephemeris during Q0-2 is as small as ∼20 seconds for Jupiter-size planets, and 1.5 minutes for Neptune and super-Earth-size planets. The median (taken over planet candidates) MAD of TTs is approximately ∼11 minutes for super-Earth-size planets, ∼6.5 minutes for Neptune-size planets, and ∼1.5 minutes for Jupiter-size planets. Since large planets can be detected around fainter stars at low signal-to-noise, each class includes some candidates with relatively poor timing precision (up to an hour).

All the TT measurements presented in this paper were based on LC data only and were performed in a semi-automated fashion. Experience with systems subjected to detailed TTV studies suggests that TT precision could often be significantly improved, if individual attention to devoted to mitigating systematic effects and choosing which transits yield the best templates. This work can serve as a broad, but shallow survey of *Kepler* planet candidates. Our results can help scientists

choose the most interesting systems for follow-up work to perform more detailed light curve modeling (as well as other types of follow-up such as observations from other observatories, theoretical investigations and observations using short cadence mode).

In addition to LC observations, *Kepler* collects photometry in short cadence mode ($\approx$ 1 minute samples) for a small fraction of its targets. In some cases, short cadence data may further improve timing precision (e.g., Batalha et al. 2011; Carter et al. 2011). It is expected that the differences in the times and errors inferred from the two data types are small for purely white, Gaussian noise and adequate transit phase coverage. However, when either precondition is not met, the accuracy of TTs can depend on whether LC or SC data are used.

Short cadence times show improved accuracy and smaller errors for situations where the ingress/egress phases are short in duration and largely unresolved in the long cadence photometry. In the case of KOI-137, this improvement is significant, with timing errors differing by nearly a factor of two at some epochs. In a similar vein, the short cadence times are more robust against deterministic (as opposed to stochastic) trends that have characteristic timescales less than the long cadence integration time. In particular, brightening anomalies occurring during transit associated with the occultation of a cool spot on the star by the planet will be unresolved with long cadence photometry and will likely result in a timing bias.

For several planet candidates, the orbital period is a near multiple of the long cadence integration time. The result is sparse transit phase coverage that is not improved as the number of observed epochs increases. In these cases, the short cadence photometry provides a more complete phase coverage and, subsequently, times with smaller error bars.

For low signal-to-noise transit events, stochastic temporally-correlated noise may dominate on short cadence timescales. As a result, the short cadence timing uncertainties may be unrealistically optimistic if they were inferred assuming a "white" noise model. Here, the long cadence photometry will give more reliable errors when assessed with the same noise model by effectively averaging over high frequency noise. Short cadence times estimated for Kepler-10b seem to be affected by correlated noise, under the expectation of a linear ephemeris, given the relatively small timing errors and the relatively large deviates (compared to the long cadence times).

5.2. Frequency of TTV Signals & Multiple Planet Systems

While TTVs have been used to confirm transiting planet candidates, TTVs have yet to provide a solid detection of a non-transiting planet. In principle, one strength of the TTV method is that it is sensitive to planets which do not transit the host star (Agol et al. 2005; Holman & Murray 2005). A longer time baseline will be required before TTVs yield strong detections. Yet, we can already use the multiple transiting planet candidate systems and the number of preliminary TTV signals to estimate the frequency of multiple planet systems.

Doppler planet searches find that systems with multiple giant planets are common ($\geq$ 28%; Wright et al. 2009). *Kepler* is probing new regimes of planet mass and orbital separation, so it will be interesting to compare the frequency of multiple planet systems among systems surveyed by Doppler and *Kepler* observations. B11 estimates the false alarm rate of *Kepler* planet candidates to range from $\leq$ 2% for the confirmed planets ("vetting flag"=1) to $\leq$ 20% for well-vetted candidates (vetting flag=2) to $\leq$ 40% for those that are yet to be fully vetted (vettting flag=3 or 4). Morton & Johnson (2011) use the specifications for *Kepler* to predict that even incomplete vetting could result in a false positive rate of less than ∼10% for planet candidates larger than $1.3R_{\oplus}$ and a typical host star. The most common mode of false positive involves a blend of multiple stars which are closely superimposed on the sky (Torres et al. 2011). Contriving such scenarios for KOIs with multiple planet candidates is more difficult. The odds of three or more physically unassociated stars being blended together is extremely small. In many cases, requiring dynamical stability excludes the possibility of multiple transit-like events being due to a multiply eclipsing star systems. The most common types of false positives for a candidate multiple transiting systems are expected to be either a blend of two stars each with one transiting planet or a blend of one star with a transiting planet and one eclipsing binary (Torres et al. 2011). Even these scenarios become highly improbable for pairs of planets that are close to a MMR. Thus, candidate multiple transiting planet systems, and especially near-resonant candidate multiple planet systems, are expected to have very few false positives (Holman et al. 2010; Latham et al. 2011; Lissauer et al. 2011b).

Given the low rate of expected false positives, we can use the frequency of stars with multiple transiting planet candidates to estimate a lower bound on the frequency of systems with multiple planets (with sizes and orbits detectable by *Kepler* using the present data), assuming that all systems are coplanar. Table 7 lists the number of stars with at least one transiting planet candidate (N_{st}) and the number of transiting planet candidates (N_{tr}), separated by the number of candidates per star (N_{cps}). The probability that at least two coplanar candidates transit for a randomly positioned observer is simply $R_{\star}/a_{(2)}$, where $a_{(2)}$ is the semi-major axis of the planet with the second smallest orbital period. Among the planet candidates in B11, the average $a/R_{\star}$ for single planet candidates is ∼30. For stars with two (multiple) transiting planet candidates, the average $a_{(2)}/R_{\star}$ is 44 (39). Thus, the difference in the detection rates due to purely geometric considerations would be modest if the two planets are stricly coplanar. The fraction of *Kepler* planet candidate host stars with at least two (exactly two) transiting planets (with sizes and orbits detectable by *Kepler* using the present data) is at least ∼23% (17%). For stars with at least three transiting planet candidates, the average $a_{(3)}/R_{\star}$ is 50, so purely geometric considerations are more significant even if the orbits are strictly coplanar. While only $\sim 5.6\%$ of *Kepler* planet candidate host stars have at least three candidates, adopting a minimum geometric correction factor of 50/30, yields a fraction of *Kepler* planet candidate host stars with at least three similar transiting planets of at least $\sim 9.4\%$. Such a high occurance rate of multiple candidate systems requires that there be large numbers of systems with one transiting planet where additional (more distant) planets are not seen to transit, even in the most conservative coplanar case. Of course, the true rates of multiplicity could be much higher, if systems have significant mutual inclinations. Lissauer et al. (2011b) provide more

detailed analysis of the observed rate of multiple transiting planet systems and its implications for their inclination distribution and multiplicity rate.

Next, we make use of the fact that TTV observations are sensitive to non-transiting planets. Table 7 includes multiple values of the number of planet candidates ($N_{\rm TTV}$) that were identified as likely having TTVs by various sets of tests described in §3 and the number of planet candidates which these tests were applied to ($N_{\rm tr}$). We evaluate the robustness of our results by applying various sets of tests for TTVs to different samples of planet candidates. In Table 7 the columns labeled sSnN refer only to planet candidates with a single transit S/N of at least S and at least N TTs measured during Q0-2. Some planet candidates in the s4n3 sample have too few transits to apply the X'^2 test, $\mathcal{F}$-test and period comparison test. Similarly, for the epoch and period comparison tests, we required a S/N per transit of at least 4, so these tests were not applied to all the planet candidates in the s3n5. The s4n5 sample is the smallest, but is the least likely to result in false alarms when searching for TTV signals. To further reduce the risk of false alarms, we do not include the X'^2 test for excess scatter when analyzing the s4n5 sample. The columns labeled "% TTV" give the fraction of planet candidates that were identified by the tests for TTVs that were applied to the given sample.

We find that ∼11-20% of planet candidates suitable for TTV analysis show some evidence for TTVs, depending on the tests applied (see Table 7). We obtain similar rates when we consider only systems with $N_{cps} = 1 - 3$ transiting planet candidates. For $N_{cps} \geq 4$, the accuracy of the resulting rates are limited by small number statistics.

Of planet candidates which are near a 1:2 MMR with another planet candidate, 25% show some evidence for a long-term trend. This could be due to planets near the 1:2 MMR being more likely to have large TTVs, but we caution that this results is based on a small sample size and an early estimate for the frequency of TTVs.

Regardless of which sample and tests are chosen, we do not find significant differences in the fraction of planet candidates which show TTV signals as a function of N_{cps}. This suggests stars with a single transiting planet are nearly as likely to have additional planets that cause TTVs, as stars with multiple transiting planets are to have masses and orbits that result in detectable TTVs. Since large TTVs most naturally arise for systems that are densely packed and/or have pairs of planets in or near a MMR, a system with a single transiting planet that shows TTVs is likely to have a significant dispersion of orbital inclinations. A dispersion of inclinations has the effect of increasing the probability that a randomly located observer will observe a single planet to transit and decreasing the probability of observing multiple planets to transit. Thus, a dispersion of inclinations may help explain the relatively small frequency of systems with two transiting planet candidates relative to the frequency of systems with one transiting planet candidate. However, simply increasing the inclination dispersion to match the ratio of two transiting planet candidate systems to one transiting planet candidate systems fails to produce the observed rate of systems with three or more transiting planet candidates. This suggests that a single population model is

insufficient to explain the observed multiplicity frequencies (Lissauer et al. 2011b).

5.3. Frequency of False Positives and Planets in Close Binaries

The small fraction of systems with very large TTVs is consistent with the notion that the *Kepler* planet candidate list has a small rate of false positives. In particular, physically bound triple systems are one of the most difficult types of astrophysical false positives to completely eliminate (i.e., an eclipsing binary that is diluted by light from a third star). In many cases, wide triple systems would be recognized based on centroid motion during the transit (B11). For KOIs that are not near the threshold of detection there is a relatively narrow range of orbital periods that would escape detection by the centroid motion test and be dynamically stable (for stellar masses). In many cases, such a triple system would exhibit eclipse timing variations, as are often seen in the *Kepler* binary star catalog (Prsa et al. 2011; Slawson et al. 2011; Orosz et al. 2011). We identify only a handful of systems with large period derivatives that are consistent with a stellar triple system. This suggests that the *Kepler* planet list contains few physical triple stars with eclipsing timing variations and that the current *Kepler* planet candidates are rarely in a tight binary systems.

5.4. Future Prospects for TTVs

We identify over 60 transiting planet candidates that show significant evidence of TTVs, even on relatively short timescales. Even for the early TTV candidates identified here, an increased number of transits and time span of *Kepler* observations will be necessary before TTVs can provide secure detections of non-transiting planets. Additionally, follow-up observations to determine the stellar properties and reject possible astrophysical false positives will also be important for confirming planets to be discovered by TTVs.

We expect the number of TTV candidates to increase considerably as the number and timespan of *Kepler* observations increase. For non-resonant systems (e.g., Kepler-11), TTVs typically have timescales of order the orbital period, but relatively small amplitudes (Nesvorný 2009; Veras et al. 2011). In this case, *Kepler* will be most sensitive when the planets are closely spaced (e.g., Kepler-11). Our analysis of TTs during Q0-2 identified no periodic signals at a confidence level of ≤ 0.01. When searching for a simple periodic signal in time series, the minimum detectable signal decreases dramatically as the number of observations increases beyond $\sim$12 observations and continues to decrease faster than classical $\sim N^{-1/2}$ scaling even as the number of observations grows to $\sim$40 observations. Thus, over the 3.5 year nominal lifetime of *Kepler* the increased number of TT observations will significantly improve *Kepler's* sensitivity to closely spaced, non-resonant systems. In this regime, *Kepler* will be most sensitive to TTVs of short-period planets, since they will provide enough transits during the mission lifetime to detect a periodic signal. Some TTV candidates identified by *Kepler* will become targets for ground-based follow-up in the post-*Kepler*

era.

For planetary systems near a MMR (e.g., Kepler-9), both the amplitude and timescale of the TTVs can be quite large. Fortunately, continued observations provide the double benefit of increased number of observations and an increasing signal size. To illustrate this point, we used n-body integrations to predict the RMS TTV of multiple transiting planet candidate systems identified in B11 for a nominal circular, coplanar model (see Fig. 5). During Q0-2 less than 2% had a TTV signature with an RMS more than 10 minutes, but the fraction grows to over 10% over the 3.5 year mission lifetime (see Table 7). Both this result and the ∼12% of suitable planet candidates showing evidence for a long-term drift in TTs suggest that the TTV method will become a powerful tool for detecting non-transiting planets as well as confirming transiting planets. For systems with multiple transiting planets, the additional information makes the interpretation of TTVs even more powerful for confirming their planetary nature and that they orbit the same host star (e.g., Holman et al. 2010; Lissauer et al. 2011a). With continued observations, TTVs become very sensitive to the planet mass and orbital parameters.

Based on the distribution of orbital periods of *Kepler* transiting planet candidates in B11, at least ∼16% of multiple transiting planet candidate systems contain at least one pair of transiting planets close to a 2:1 period commensurability ($1.83 \leq P_{\rm out}/P_{\rm in} \leq 2.18$). If we assume that planets near the 1:2 MMR are nearly coplanar, then true rate of detectable planets near the 1:2 MMR (if both had a favorable inclination) is at least ∼ 25%. If a significant fraction of these systems are not in the low inclination regime, then the true rate of pairs of planets near the 1:2 MMR would be even larger (Lissauer et al. 2011b). This rate is approximately double the rate of systems that show TTVs basd on our initial analysis of early *Kepler* data, implying that the number of systems with TTVs could double over the course of the mission.

In conclusion, transit timing is extremely complementary to Doppler observations form confirming planets. On one hand, transit timing only works for planets with detectable TTVs. On the other hand, TTVs can be quite sensitive to low-mass planets that are extremely challenging for Doppler confirmation. Additionally, TTVs are likely to be particularly useful for confirming some of the *Kepler* planet candidates with host stars that are problematic for confirmation via Doppler observations (e.g., faint stars, active stars, hot and/or rapidly rotating stars).

Of particular interest for the *Kepler* mission is whether the transit timing method might be able to discover or confirm rocky planets in the habitable zone. Due to the TT uncertinaties for Earth-size planets, a detection of TTVs of the rocky planet itself would require a large signal which is only likely if the small planet is near a resonance with another planet. Further complicating matters, planets in the habitable zone will have only a few transits for solar-mass stars. Fortunately, *Kepler* is detecting many systems with multiple transiting planets, which would open the door to TT measurements of both the planet in the habitable zone and an interior planet (see Fig. 6). Indeed, *Kepler* has identified over a dozen planet candidates that are in or near the habitable zone and are associated with stars that have multiple transiting planet candidates. In most cases,

the period ratio between the transiting planet candidates is large, so the TTVs could be small (unless there are additional non-transiting planets). However, N-body integrations suggest that continued *Kepler* observations of several pairs could prove very useful for confirming (or rejecting) these planet candidates based on TT. Of course, many other stars with a planet candidate in or near the habitable zone may harbor additional non-transiting planets. The distribution of period ratios of *Kepler* transiting planet candidates shows that planets near the 1:2, 2:3 and 1:3 MMRs are not uncommon. For reference, Kepler-9 b & c were confirmed on the basis on 9(b)+6(c)=15 TT observations. Obtaining 15 TTs for two planets in a 1:2 MMR requires observing for 5-6 times the orbital period of the outer planet. Thus, it is feasible that a transiting planet in the habitable zone identified by *Kepler* could be confirmed using TTVs, provided that there is another transiting planet near an interior MMR and that the *Kepler* mission were extended to $\geq$ 6 years. The prospects improve significantly for stars less massive than the sun, thanks to the shorter orbital period at the habitable zone.

Funding for this mission is provided by NASA's Science Mission Directorate. We thank the entire Kepler team for the many years of work that is proving so successful. We thank David Latham for a careful reading of the manuscript. E.B.F acknowledges support by the National Aeronautics and Space Administration under grant NNX08AR04G issued through the Kepler Participating Scientist Program. This material is based upon work supported by the National Science Foundation under Grant No. 0707203. D. C. F. and J. A. C. acknowledge support for this work was provided by NASA through Hubble Fellowship grants #HF-51272.01-A and #HF-51267.01-A awarded by the Space Telescope Science Institute, which is operated by the Association of Universities for Research in Astronomy, Inc., for NASA, under contract NAS 5-26555.

Facilities: Kepler.

REFERENCES

Agol, E., Steffen, J., Sari, R., & Clarkson, W. 2005, MNRAS, 359, 567

Batalha, N. M., et al. 2011, ApJ, 729, 27

Borucki, W.J. et al. 2011, accepted to ApJ. arXiv:1101.0541.

Bozkurt, Z., & Değirmenci, Ö. L. 2007, MNRAS, 379, 370

Carter, J. A., & Winn, J. N. 2010, ApJ, 716, 850

Carter, J. A., et al. 2011, Science, 331, 562

Colón, K. D., & Ford, E. B. 2009, ApJ, 703, 1086

Fabrycky, D. et al. 2011, in prep

Ford, E. B., & Gregory, P. C. 2007, Statistical Challenges in Modern Astronomy IV, 371, 189

Ford, E. B., & Holman, M. J. 2007, ApJ, 664, L51

Ford, E. B., et al. 2011, submitted to Bayesian Analysis.

Ford, E. B. et al. 2011, in prep

Fressen, F., et al. 2011 accepted tp ApJ, arXiv:1105.4647

Jenkins, J. M., et al. 2010, ApJ, 713, L87

Kipping, D. M., Fossey, S. J., & Campanella, G. 2009, MNRAS, 400, 398

Latham, D. W., et al. 2011, ApJ, 732, 24.

Lissauer, J.J. et al. 2011a, 2011, Nature, 470, 53-58.

Lissauer, J.J. et al. 2011b, submitted to ApJ, arXiv:1101.0543.

Miralda-Escudé, J. 2002, ApJ, 564, 1019

Moorhead, A.V. et al. 2011, accepted to ApJ, arXiv:1101.0547.

Morton, T. D., & Johnson, J. A. 2011, arXiv:1101.5630

Nesvorný, D. 2009, ApJ, 701, 1116

Orosz, J.A. et al. 2011, in preparation.

Press, W. H., Teukolsky, S. A., Vetterling, W. T., & Flannery, B. P. 1992, Cambridge: University Press, —c1992, 2nd ed.,

Prsa, A., et al. 2011, AJ, 141, 83.

Ragozzine, D., & Holman, M. J. 2010, submitted to ApJ, arXiv:1006.3727

Ragozzine, D., & Wolf, A. S. 2009, ApJ, 698, 1778

Slawson, R. W., et al. 2011, submitted to AJ, arXiv:1103.1659

Simon, A., Szatmáry, K., & Szabó, G. M. 2007, A&A, 470, 727

Steffen, J. H., et al. 2010, ApJ, 725, 1226

Steffen, J. et al. 2011, in prep

Steffen, J. et al. 2011b, in prep

Torres, G., et al. 2011, ApJ, 727, 24

Veras, D., Ford, E. B., & Payne, M. J. 2011, ApJ, 727, 74

Wright, J. T., Upadhyay, S., Marcy, G. W., Fischer, D. A., Ford, E. B., & Johnson, J. A. 2009, ApJ, 693, 1084

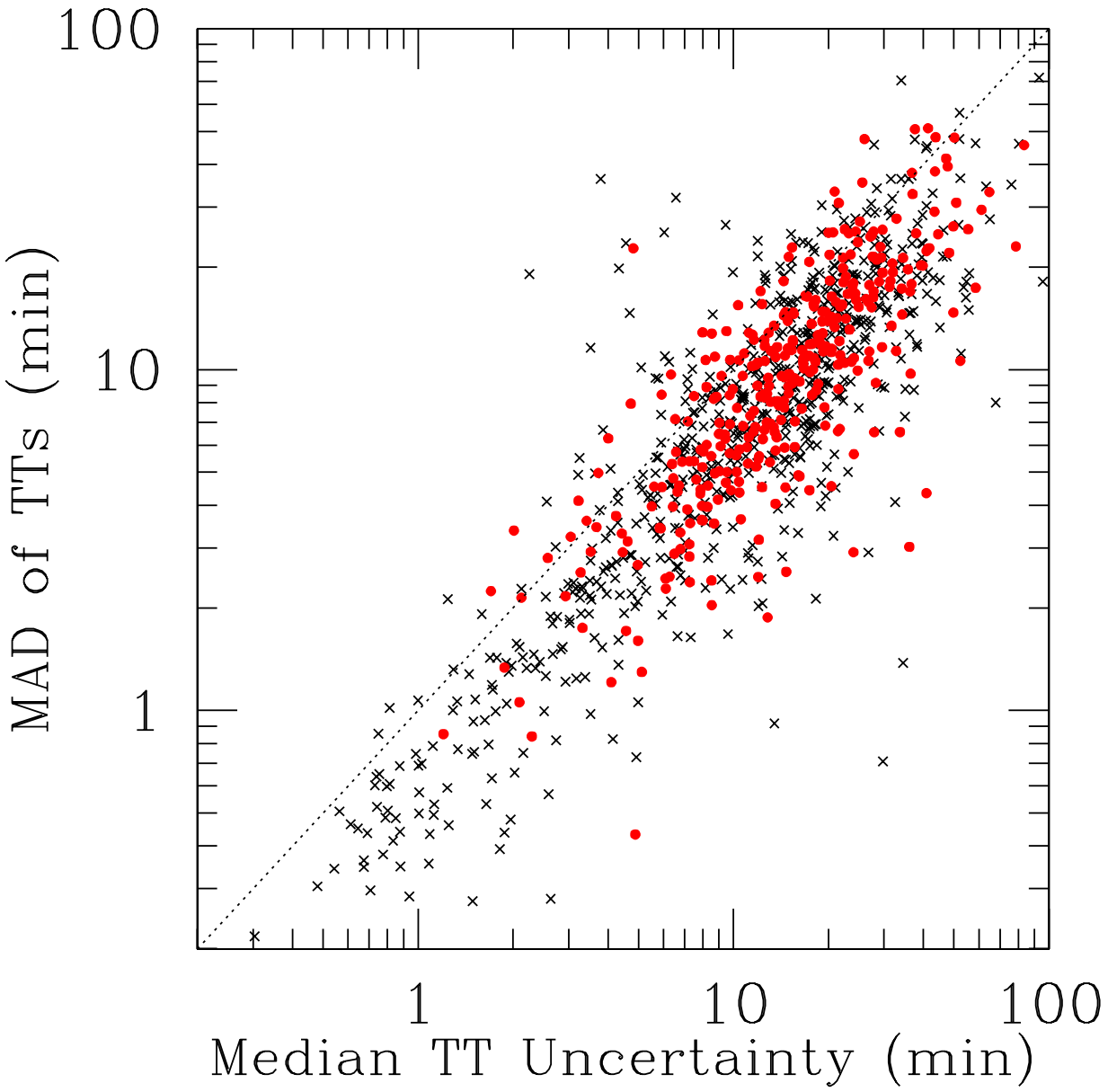

Fig. 1.— Median absolution deviation of transit times from the ephemeris of B11 versus the median uncertainty in transit time observations during Q0-2. Systems with one planet candidate are marked with an X, and multiple planet candidate systems are marked with a (red) disk.

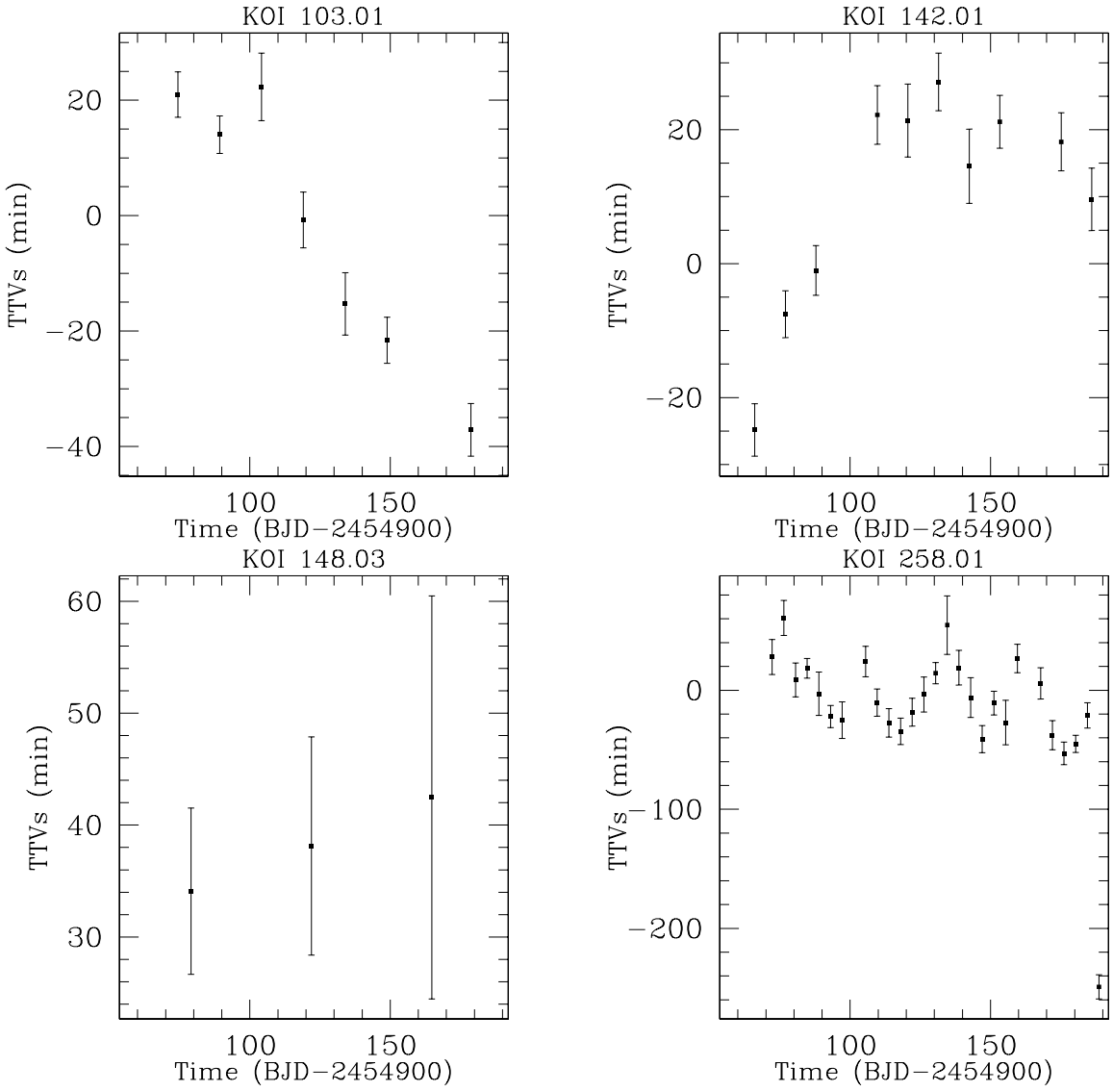

Fig. 2.— Transit timing measurements for four examples of strong TTV candidates: KOI 103.01, 142.01, 148.03, 258.01. Note that the TTs are measured relative to the EL5 ephemerides given in Borucki et al. 2011b and this is based on transit times measured through Q5. KOI 103.01 shows TTVs indicative of a long-term change in the orbital period. KOI 142.01 already shows significant curvature during Q0-2, suggesting an orbital period or libration timescale not much longer than the timespan of observations. While the TTs of KOI 148.03 appear consistent with a constant orbital period, they are significantly offset relative to the ephemeris of B11, suggesting a long-term change in the orbital period. KOI 258.01 appears to show periodic TTVs on a relatively short timescale. There are preliminary indications that KOI 258.01 may show an occultation or secondary eclipse.

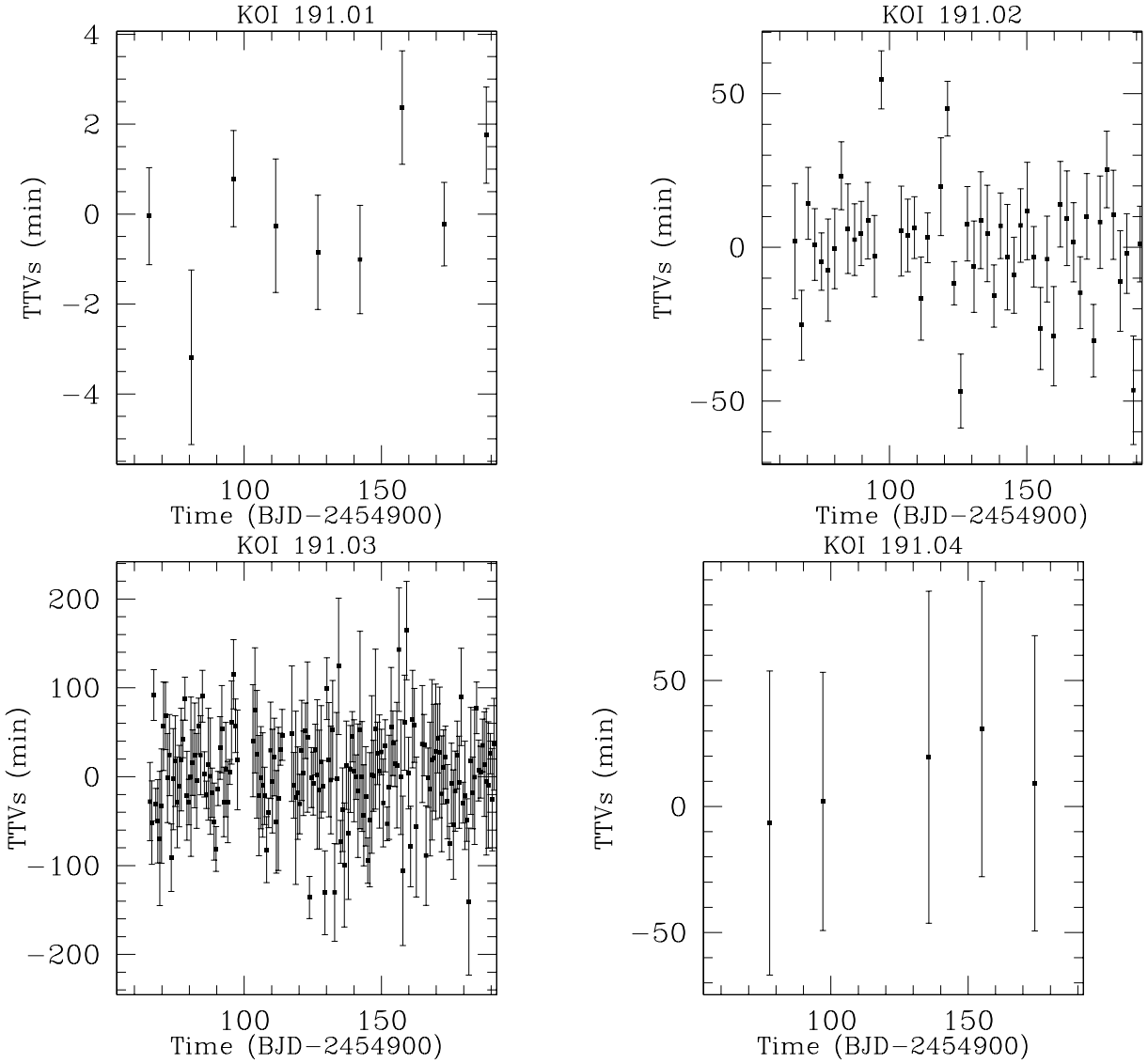

Fig. 3.— Transit timing measurements for four transiting planet candidates associated with KOI 191. These provide examples of datasets for which we do *not* find significant evidence of TTVs.

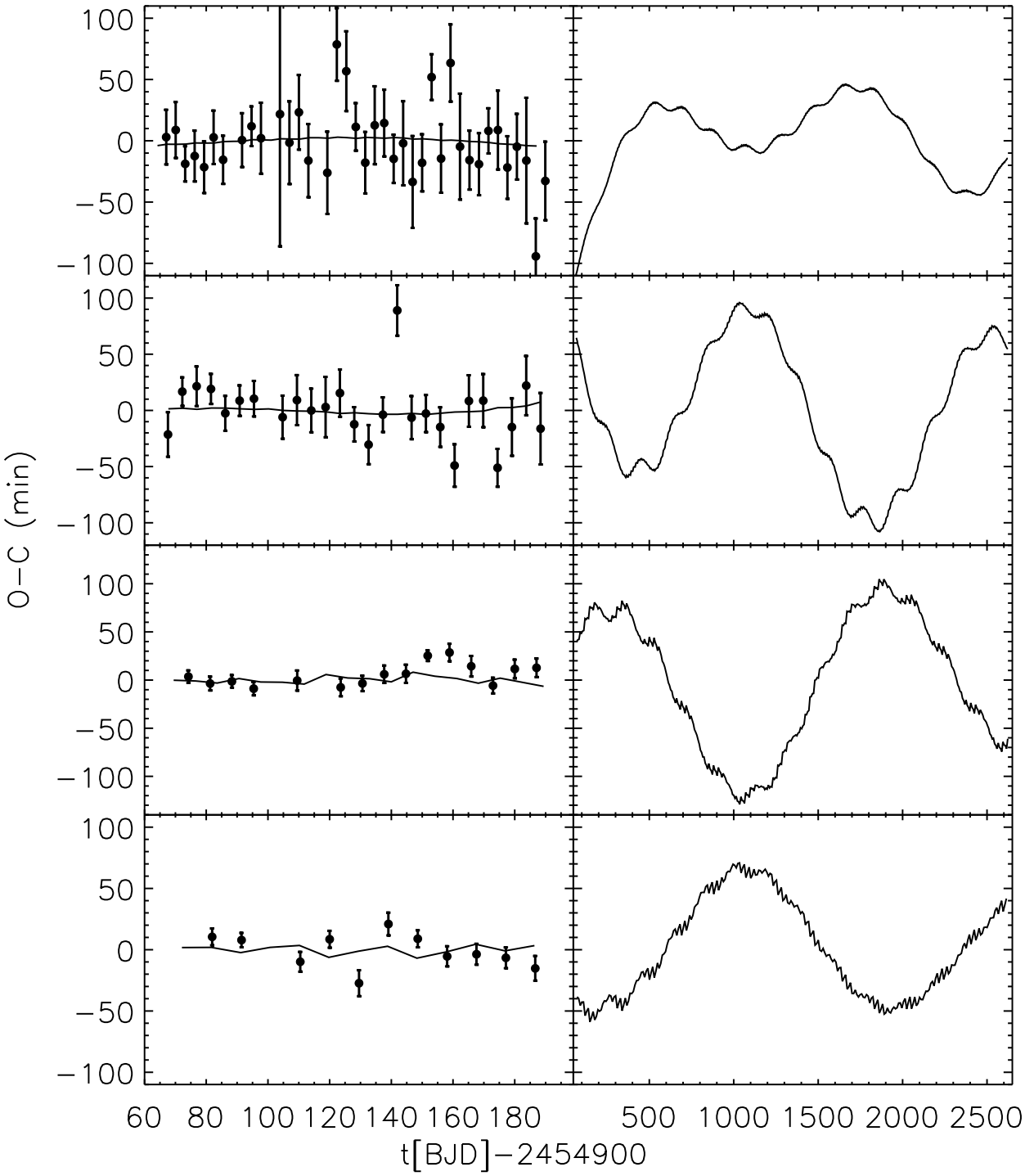

Fig. 4.— Transit timing observations (points, left column only) and the TTVs predicted by n-body integrations (lines). This is not a fit, but rather the output for a nominal circular orbital model (Lissauer et al. 2011). The right-hand column shows the predictions over 7-years, while the left-hand column zooms in on the first two quarters reported here. Rows are for KOI 500.03 (top), 500.04 (upper middle), 500.01 (lower middle) and 500.02 (bottom). KOI 500.05 is not shown, as the TT error bars are ∼hour and the model TTVs are less than a second.

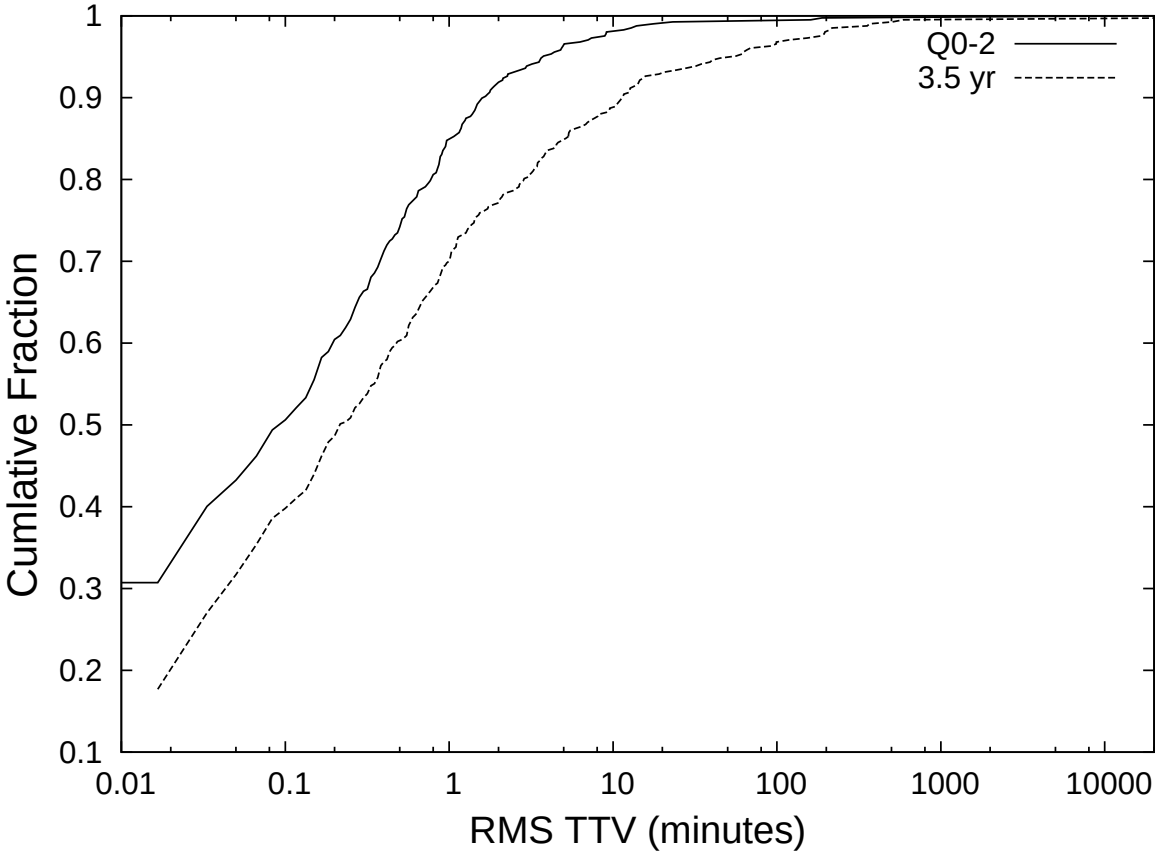

Fig. 5.— Cumulative distribution of the predicted RMS TTVs for systems of multiple transiting planets over the four months of Q0-2 (solid) and the 3.5 years mission lifetime (dashed). The predictions are based on n-body integrations starting from coplanar and circular orbits. Actual TTV amplitudes could be much higher for even modest eccentricities. Even for the case of all circular orbits, over half have a TTV amplitude that is measurable with ground-based follow-up. At least 10% of current multiple transiting planet candidates are expected to have amplitudes of $\sim$10 minutes or more, allowing for detailed dynamical modeling based on TTV observations.

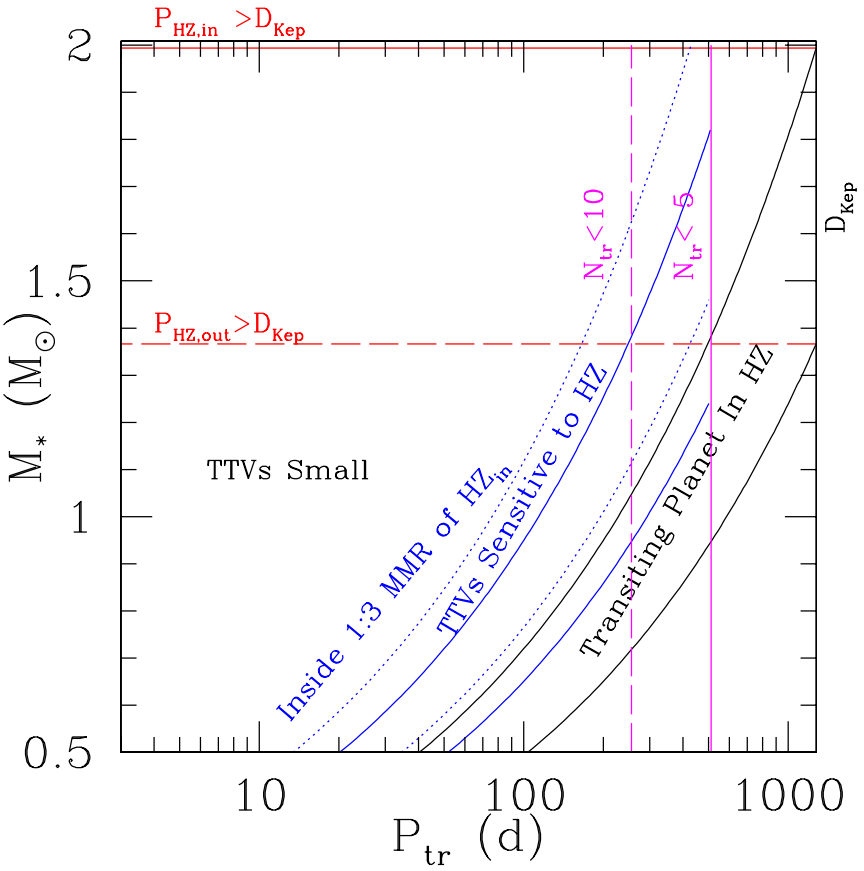

Fig. 6.— Orbital periods and stellar masses for which confirmation of a transiting planet in the habitable zone is practical. The x-axis is the orbital period of a transiting planet ($P_{\rm tr}$), limited by the nominal mission lifetime ($D_{\rm Kep}$ =3.5 years). The black curve approximate the orbital periods corresponding to the inner and outer edge of the habitable zone. The solid (dotted) magenta lines indicate the orbital period beyond which *Kepler* would observe no more than 5 (10) transits during $D_{\rm Kep}$. It would be extremely difficult to interpret TTVs for planets to the right of these curves. Therefore, it is unlikely that the nominal 3.5 year *Kepler* mission would measure the masses of planets in the HZ of stars more massive than the sun based on their TTVs. The solid (dotted) blue curves indicate the orbital period of a planet near the 1:2 (1:3) MMR with the inner and outer edges of the habitable zone. A second planet significantly to the left of the blue curves will not typically result in detectable TTV signature due to interactions with a planet in the habitable zone. The solid (dotted) line indicates the stellar mass ($M_\star$) above which the orbital period at the inner (outer) edge of the habitable zone exceeds $D_{\rm Kep}$. The most promising prospects for TTVs confirming a planet in the habitable zone involve a system with one transiting planet in the habitable zone (between black curves) and a second transiting planet that is between the blue and black curves.

Table 1. Transit Times for *Kepler* Transiting Planet Candidates during Q0-2

KOI	n	t_n BJD-2454900	TTV_n (d)	σ_n (d)
1.01	0	65.645036	-0.000204	0.000073
1.01	1	68.115649	-0.000058	0.000051
1.01	2	70.586262	-0.000001	0.000079
1.01	3	73.056875	-0.000042	0.000186
1.01	4	75.527488	0.000045	0.000098
1.01	5	77.998101	-0.000020	0.000103
1.01	6	80.468714	-0.000041	0.000071
1.01	7	82.939327	-0.000091	0.000080
1.01	8	85.409940	0.000004	0.000074
1.01	9	87.880553	-0.000123	0.000054

Note. — Note that the TTs are measured relative to the EL5 ephemerides given in Borucki et al. 2011b and this is based on transit times measured through Q5. In some cases, a long-term trend manifests itself as all the reported values of TTs having the same sign. Table 1 is published in its entirety in the electronic edition of the *Astrophysical Journal Supplement*. A portion is shown here for guidance regarding its form and content. An electronic version is availiable online at: `http://astro.ufl.edu/$sim$eford/data/kepler/`

Table 2. Linear Ephemerides Used for TTV analysis

KOI	Epoch[a] (d)	Period (d)
1.01	55.762580	2.47061310
2.01	54.357810	2.20473550
3.01	57.812270	4.8878177
4.01	90.526100	3.849370
5.01	65.973500	4.7803247
7.01	56.611260	3.213682
10.01	54.118090	3.522297
12.01	79.597720	17.855038
13.01	53.564980	1.7635892
17.01	54.485750	3.2347003

[a]BJD-2454900

Note. — Table 6 is published in its entirety in the electronic edition of the *Astrophysical Journal Supplement*. A portion is shown here for guidance regarding its form and content.

Table 3. Metrics for Transit Timing Variations of *Kepler* Planet Candidates.

KOI	σ_{TT} (min)	(E_L5,T2) MAD[a] (min)	WRMS[b] (min)	MAX[c] (min)	$p_{X'^2}$[d]	(E_L2,T2) MAD[a] (min)	WRMS[b] (min)	MAX[c] (min)	$p_{X'^2}$[d]	$\frac{\lvert\Delta P\rvert}{\sigma_P}$[e]	$\frac{\lvert\Delta E\rvert}{\sigma_E}$[f]
1.01	0.2	0.1	0.1	2.4	0.99999727	0.1	0.1	2.5	0.99989265	1.3	1.1
2.01	0.3	0.2	0.3	0.7	0.66745223	0.1	0.3	0.8	0.99935567	1.4	1.4
3.01	0.7	0.3	0.4	3.2	0.99982414	0.3	0.4	3.1	0.99929283	1.2	0.6
4.01	3.5	2.4	3.5	8.6	0.84167045	2.8	3.4	9.4	0.35265519	0.0	2.4
5.01	1.9	1.4	1.6	3.1	0.711099	1.7	1.5	3.0	0.11421086	2.2	0.6

Note. — Table 4 is published in its entirety in the electronic edition of the *Astrophysical Journal Supplement*. A portion is shown here for guidance regarding its form and content.

[a]Median Absolute Deviation of transit times in Q0-2 from ephemeris

[b]Weighted Root Mean Square deviation of transit times in Q0-2 from ephemeris

[c]MAXimum absolute deviation of transit times in Q0-2 from ephemeris

[d]p-value for a χ^2-like-test assuming X'^2 follows a χ^2 distribution, as described in §3.1

[e]Absolute value of difference of best-fit periods for L_2,T2 and L_5,T2 ephemerides normalized by formal uncertainty

[f]Absolute value of difference of best-fit transit epochs for L_2,T2 and L_5,T2 ephemerides normalized by formal uncertainty

Table 4. Quadratic Ephemerides for Kepler Objects of Interest based on transit times during Q2.

KOI	E[a] (d)	σ_E (d)	P (d)	σ_P (d)	c[b]	σ_c	MAD[c] (d)	WRMS[d] (d)	MAX[e] (d)	$p_{X'^2}$[f]	$p_{\mathcal{F}}$[g]
42.01	149.89207	0.002317258	17.835806	0.000999096	-7.93E-05	4.83E-05	0.000224292	0.000465821	0.00087804	0.98156568	0.053661725
124.02	107.5387	0.004856891	31.713798	0.003447988	0.000155781	9.53E-05	0.000101866	8.70E-05	0.000177141	0.96675223	0.018503953
142.01	120.58229	0.0014794	10.912549	0.000260135	6.28E-05	7.86E-06	0.001685495	0.002572359	0.00727168	0.67069648	0.005875349
227.01	122.54014	0.001542628	17.678654	0.000469767	-7.68E-05	1.55E-05	0.000969901	0.001511303	0.003312192	0.82842292	0.028645506
314.01	124.63071	0.001690889	13.780802	0.000429775	3.71E-05	1.52E-05	0.002035933	0.001290098	0.003126117	0.35704363	0.078718429
467.01	151.46194	0.001891538	18.007959	0.000842961	-4.92E-05	2.47E-05	6.71E-05	6.55E-05	0.000102345	0.93992411	0.029226395
528.01	138.41866	0.003407732	9.578232	0.000663483	-5.97E-05	2.13E-05	0.002067159	0.003516547	0.007456802	0.99547272	0.035870139
649.01	139.37393	0.010461445	23.447238	0.004043237	-0.000165971	0.000148364	0.000121626	0.000120244	0.000228574	0.98082178	0.017380622
878.01	130.40553	0.007549669	23.615695	0.006189283	-0.000667528	0.000214225	0.001208953	0.001048118	0.001790873	0.79282356	0.067398588
935.01	133.86998	0.003139609	20.860536	0.001445591	8.34E-05	5.89E-05	6.38E-05	0.000120015	0.000214038	0.99919724	0.002730505
941.03	146.68417	0.00254628	24.664449	0.002533906	0.000158955	9.16E-05	0.000255548	0.000235014	0.000381217	0.87610092	0.07150007
960.01	125.95369	0.000313363	15.800727	0.000146537	1.07E-05	5.90E-06	0.000135125	0.000123596	0.000210589	0.88030747	0.054869155
1308.01	126.11344	0.008972545	23.597302	0.004072063	0.00039199	0.000147879	0.003606992	0.003070563	0.005514918	0.73324413	0.061761557
1310.01	129.81925	0.009257043	19.130778	0.00267195	6.13E-05	8.77E-05	0.000511397	0.001120656	0.002320763	0.99997768	0.020817298

[a]Epoch

[b]curvature; see Eqn. 1

[c]Median Absolute Deviation of TTs from quadratic ephemeris

[d]Weighted Root Mean Square deviation of TTs from quadratic ephemeris

[e]MAXimum absolute deviation of TTs from quadratic ephemeris

[f]p-value for a chi^2-test based on X'^2 relative to quadratic ephemeris, as described in §3.1

[g]p-value for an F-like-test that compares linear and quadratic ephemerides, assuming that $\mathcal{F}$ follows an F-distribution, as described in §3.1

Table 5. Notes for *Kepler* Planet Candidates with Putative Transit Timing Variations.

KOI	P (d)	R_p[a] ($R_\oplus$)	S/N[b]	T_{dur}[c] (hr)	nTT[d]	nPC[e]	TTV[f] Flag	Comment
10.01	3.52230	10.5	22.6	3.3	35	1	2	epoch offset
13.01	1.76359	20.4	130.7	3.2	35	1	3	outlier
42.01	17.83278	2.6	10.8	4.5	5	1	2	quadratic?
94.02	10.42361	4.0	10.1	5.3	3	3	2	offset
103.01	14.91155	2.3	14.5	3.4	7	1	1	Period & epoch differ

Note. — Table 6 is published in its entirety in the electronic edition of the *Astrophysical Journal Supplement*. A portion is shown here for guidance regarding its form and content.

[a]Putative radius of planet in Earth radii (from B11)

[b]Typical Signal to Noise Ratio of an individual transit

[c]Transit duration (from B11)

[d]Number of transit times measured in Q0-2

[e]Number of transiting planet candidates for host star

[f]1=pattern to eye, 2=trend or periodicity, 3=excess scatter and no trend, 4=low S/N per transit and/or few transits, 5=note about difficulty measuring TTs, 6=excess scatter significant only after clipping

Table 6. Predicted Transit Time Variation Magnitude for *Kepler* Transiting Planet Candidates

KOI	RMS Q2 (s)	Min-to-Max Q2 (s)	RMS 3.5yr (s)	Min-to-Max 3.5yr (s)	RMS 7yr (s)	Min-to-Max 7yr (s)
70.01	1.2	3.5	1.3	5.1	1.3	5.2
70.02	1.4	5	1.3	6	1.3	6
70.03	···	···	3.4	9.7	3.4	10
70.04	23	71	23	91	23	94
72.01	0.0003	0.001	0.003	0.01	0.01	0.05
72.02	0.01	0.03	0.2	0.5	0.2	0.5

Note. — We report the magnitude (root mean square and min-to-max) of transit timing variations expected based on n-body integrations using estimated nominal masses and initially circular orbits (Lissauer et al. 2011b). We assume that all members of multiple planet candidate systems are true planets and orbit the same star. Integrations extend for the duration of the first two quarters of *Kepler* data, the nominal 3.5 year mission life time and 7.5 years, representative of a hypothetical extended mission. Eccentric models can dramatically affect both the predicted TTV magnitude and timescale. Table 7 is published in its entirety in the electronic edition of the *Astrophysical Journal Supplement*. A portion is shown here for guidance regarding its form and content.

Table 7. TTV Candidates & Transiting Planet Candidates

N_{cps}[a]	N_{st}[b]	$N_{\rm tr}$[c]	$N_{\rm tr}$[d] s4n3	$N_{\rm tr}$[e] s3n5	$N_{\rm tr}$[f] s4n5	$N_{\rm TTV}$[g] s4n3	$N_{\rm TTV}$[h] s3n5	$N_{\rm TTV}$[i] s4n5	% TTV[j] s4n3	% TTV[k] s3n5	% TTV[l] s4n5
1	809	809	462	453	371	95	59	45	21%	13%	12%
2	115	230	121	110	83	24	16	13	20%	15%	16%
3	45	135	71	67	57	14	8	6	20%	12%	11%
4	8	32	15	14	10	2	1	1	13%	7%	10%
5	1	5	2	3	2	1	1	0	50%	33%	0%
6	1	6	4	3	3	0	0	0	0%	0%	0%
All	979	1217	675	650	526	136	85	65	20%	13%	12%

Note. — Number and fractions of systems with evidence showing for TTVs separated by the number of transiting planet candidates in the system

[a]Number of candidates per star

[b]Number of stars

[c]Number of transiting planet candidates (only those used for this analysis)

[d]Number of transiting planet candidates with a S/N per transit $\geq$ 4 and at least 3 transits in Q0-2

[e]Number of transiting planet candidates with a S/N per transit $\geq$ 3 and at least 5 transits in Q0-2

[f]Number of transiting planet candidates with a S/N per transit $\geq$ 4 and at least 5 transits in Q0-2

[g]Number of transiting planet candidates from s4n3 sample that show indications of TTVs

[h]Number of transiting planet candidates from s3n5 sample that show indications of TTVs, excluding epoch offset test

[i]Number of transiting planet candidates from s4n5 sample that show indications of TTVs, excluding X'^2 test

[j]% of planets from s4n3 sample that show indications of TTVs

[k]% of planets from s3n5 sample that show indications of TTVs, excluding the epoch offset test

[l]% of planets from s4n5 sample that show indications of TTVs, ecluding X'^2 test

Table 4. Metrics for Transit Timing Variations of *Kepler* Planet Candidates.

KOI	σ_{TT} (min)	(E_L5,T2) MAD[a] (min)	WRMS[b] (min)	MAX[c] (min)	$p_{X'^2}$[d]	(E_L2,T2) MAD[a] (min)	WRMS[b] (min)	MAX[c] (min)	$p_{X'^2}$[d]	$\frac{\lvert\Delta P\rvert}{\sigma_P}$[e]	$\frac{\lvert\Delta E\rvert}{\sigma_E}$[f]
1.01	0.2	0.1	0.1	2.4	0.99999727	0.1	0.1	2.5	0.99989265	1.3	1.1
2.01	0.3	0.2	0.3	0.7	0.66745223	0.1	0.3	0.8	0.99935567	1.4	1.4
3.01	0.7	0.3	0.4	3.2	0.99982414	0.3	0.4	3.1	0.99929283	1.2	0.6
4.01	3.5	2.4	3.5	8.6	0.84167045	2.8	3.4	9.4	0.35265519	0.0	2.4
5.01	1.9	1.4	1.6	3.1	0.711099	1.7	1.5	3.0	0.11421086	2.2	0.6
7.01	3.5	2.1	3.4	18.3	0.98587454	2.1	3.2	15.8	0.97553341	1.5	1.4
10.01	0.8	18.3	21.0	35.2	0	6.2	7.1	12.7	0.015052582	2.6	
12.01	1.0	0.7	1.3	2.1	0.60479879	0.7	0.7	1.0	0.28837559	0.8	1.3
13.01	4.1	0.8	3.1	20.9	1	0.9	3.0	19.7	1	0.5	3.0
17.01	0.7	0.3	0.3	0.5	0.93944266	0.3	0.3	0.5	0.85296174	0.3	1.1
18.01	0.7	0.9	1.0	1.7	0.030577461	0.4	0.5	0.8	0.65314361	0.3	2.2
20.01	0.5	0.3	0.5	1.5	0.90732023	0.4	0.5	1.4	0.71942255	0.6	0.6
22.01	0.6	0.5	1.0	4.2	0.22568081	0.2	0.9	4.6	0.99376928	1.6	0.8
41.01	9.4	9.1	9.2	19.3	0.14659777	7.2	8.0	22.8	0.32234503	0.2	0.4
42.01	4.7	14.7	14.8	19.7	4.00E-15	3.1	3.5	5.3	0.33467081	1.3	0.5
46.01	4.3	1.6	5.6	15.4	0.99998638	1.7	5.6	15.3	0.99987464	0.2	0.2
49.01	7.4	4.9	5.7	12.7	0.73992243	2.2	3.6	7.9	0.99415475	0.1	0.6
51.01	2.0	0.5	0.9	1.9	0.96389448	0.5	0.7	1.4	0.61883068	17.3	0.0
63.01	3.2	1.2	2.7	19.5	0.98868323	1.3	2.5	17.2	0.92756729	1.4	0.1
64.01	3.8	2.3	3.5	9.4	0.99640901	2.4	3.3	9.0	0.98389423	1.8	0.1
69.01	3.1	2.2	3.1	6.2	0.73181601	2.4	3.1	5.7	0.47472802	0.6	0.2
70.01	3.0	3.2	4.2	10.4	0.061133419	2.8	3.6	11.4	0.10361429	0.9	1.9
70.02	6.7	4.6	7.3	57.6	0.86573929	5.0	7.0	55.0	0.55873677	0.4	2.8
70.04	33.7	6.6	37.7	138.1	1	9.3	37.4	136.7	0.99999533	0.6	0.8
72.01	8.2	6.0	9.4	48.5	0.91550494	6.4	9.4	48.3	0.55708987	0.9	0.9
72.02	4.9	0.4	0.7	1.1	0.99812806	0.0	0.0	0.1	0.99496589	3.4	2.3
82.01	3.2	4.1	4.2	6.0	0.017313477	4.1	4.0	5.2	0.003764048	0.4	0.7
82.02	9.0	5.0	12.0	111.4	0.931708	4.2	11.1	114.8	0.9520552	0.2	0.8
84.01	3.5	1.9	3.4	11.5	0.93794108	2.3	2.9	7.5	0.63089441	1.6	1.5
85.01	5.0	2.7	4.5	11.0	0.98441823	2.4	4.0	10.2	0.98986235	1.0	1.0
85.02	52.4	10.6	22.2	112.3	1	12.7	22.1	115.3	1	0.7	0.1
85.03	15.0	9.7	21.2	44.6	0.82709803	8.5	21.2	46.4	0.86674621	0.1	0.6

Table 4—Continued

KOI	σ_{TT} (min)	(E_L5,T2) MAD[a] (min)	WRMS[b] (min)	MAX[c] (min)	$p_{X'^2}$[d]	(E_L2,T2) MAD[a] (min)	WRMS[b] (min)	MAX[c] (min)	$p_{X'^2}$[d]	$\frac{\lvert\Delta\ P\rvert}{\sigma_P}$[e]	$\frac{\lvert\Delta\ E\rvert}{\sigma_E}$[f]
94.02	9.5	13.0	13.0	15.6	0.032338604	12.3	12.5	13.1	0.005123416	317.0	13.6
97.01	0.8	0.4	0.5	1.4	0.99648639	0.4	0.5	1.1	0.98688162	0.5	0.6
98.01	4.9	0.7	1.5	3.2	1	0.7	1.3	3.0	1	0.5	0.1
100.01	6.7	5.9	6.0	12.5	0.25415671	4.7	4.9	14.8	0.49515881	2.5	1.5
102.01	3.0	1.8	3.0	7.8	0.99847261	1.7	2.8	8.2	0.99971355	1.1	0.9
103.01	4.6	23.5	24.9	36.2	0	1.7	4.9	15.9	0.90263724	10.1	4.2
104.01	5.9	1.9	6.4	26.0	1	2.1	6.3	27.1	0.99999972	0.1	0.4
105.01	3.3	2.3	3.1	7.3	0.69657599	1.9	2.9	6.7	0.79593361	0.5	0.4
107.01	6.6	4.4	4.8	11.0	0.81665114	4.6	4.4	10.7	0.63276108	0.9	1.1
108.01	5.1	2.4	2.5	4.3	0.94863752	2.2	2.5	4.4	0.88138773	0.6	0.2
110.01	4.8	2.2	3.6	16.8	0.98650951	2.5	3.6	16.4	0.89613764	0.5	0.4
111.01	5.8	3.4	4.5	9.2	0.86038256	3.6	4.4	9.1	0.64421757	0.1	0.0
111.02	6.5	7.2	8.3	13.7	0.080308799	8.7	8.2	12.9	0.002192174	0.6	0.5
112.02	18.5	12.6	22.5	63.1	0.85910829	11.8	22.2	64.8	0.90299725	0.8	0.6
115.01	5.1	1.3	3.7	15.7	0.99999994	1.2	3.7	15.7	0.99999988	0.2	0.1
115.02	13.6	4.0	9.2	19.4	0.99996113	5.2	8.9	21.7	0.99602082	0.2	0.1
116.01	7.5	8.4	7.7	15.6	0.048012264	3.0	5.1	14.9	0.91819163	1.6	1.1
116.02	7.3	2.8	6.4	10.6	0.86961288	4.4	5.7	8.0	0.18353792	1.6	0.6
117.01	8.7	5.0	8.2	13.4	0.82915219	3.2	5.2	14.3	0.91921374	2.0	0.0
117.02	21.5	8.8	21.2	60.1	0.99984958	16.2	19.2	51.2	0.4905386	0.6	0.9
117.03	20.7	13.9	36.7	150.0	0.90373914	18.4	36.2	141.4	0.097261158	0.6	1.1
117.04	83.5	45.6	96.7	449.7	0.96254145	56.1	92.8	421.1	0.65775779	0.1	1.4
118.01	12.9	5.4	8.5	15.6	0.92651619	4.5	8.2	15.2	0.81099207	0.6	0.7
122.01	5.3	2.2	5.0	10.2	0.9851732	4.2	4.7	7.6	0.27010843	1.0	0.1
123.01	8.0	3.6	11.5	37.8	0.99705529	6.4	10.1	30.0	0.31744605	1.4	1.6
123.02	7.3	2.4	6.8	13.1	0.98531875	6.8	6.2	10.5	0.081870505	0.9	0.3
124.01	13.6	10.9	15.3	43.8	0.43374707	5.3	14.7	43.4	0.96782263	1.0	0.3
124.02	8.8	8.3	7.5	9.0	0.23188899	7.9	6.8	8.8	0.080674869	1.6	0.7
127.01	0.7	0.4	0.7	1.8	0.9945318	0.4	0.7	1.9	0.97383084	2.3	0.3
128.01	0.6	0.5	0.6	2.0	0.78208277	0.4	0.6	2.0	0.79957506	0.3	1.5
131.01	1.2	2.1	2.5	6.5	2.62E-09	1.0	1.3	4.8	0.3515113	0.6	1.5
135.01	1.0	0.7	1.2	5.0	0.65077067	0.7	1.1	5.3	0.5818778	3.0	1.3

Table 4—Continued

KOI	σ_{TT} (min)	(E_L5,T2) MAD[a] (min)	WRMS[b] (min)	MAX[c] (min)	$p_{X'2}$[d]	(E_L2,T2) MAD[a] (min)	WRMS[b] (min)	MAX[c] (min)	$p_{X'2}$[d]	$\frac{\lvert\Delta\ P\rvert}{\sigma_P}$[e]	$\frac{\lvert\Delta\ E\rvert}{\sigma_E}$[f]
137.01	2.1	2.1	3.0	31.7	0.062049934	1.7	2.4	32.9	0.27840051	2.5	1.2
137.02	1.9	1.3	2.1	4.2	0.59047062	1.7	1.6	2.9	0.12931018	1.2	6.0
137.03	15.3	11.4	16.7	45.7	0.66658325	10.7	16.4	52.1	0.7311264	0.9	0.6
139.02	31.7	13.4	30.0	98.0	0.99999122	18.8	29.1	81.2	0.97306244	0.9	0.2
141.01	2.4	1.4	2.1	5.5	0.99001857	1.4	2.0	6.0	0.98610276	0.7	0.2
142.01	4.3	19.8	19.1	29.4	0	13.3	11.4	18.1	0	8.2	12.6
144.01	5.2	4.9	5.8	18.3	0.070405945	4.6	5.7	17.2	0.11307597	0.2	0.7
148.01	9.5	5.0	8.1	21.7	0.99463961	5.1	7.8	20.5	0.98479452	0.7	0.9
148.02	4.5	2.9	5.5	18.8	0.7801617	3.0	5.3	16.8	0.57864979	2.5	2.6
148.03	9.8	10.7	9.2	22.0	0.12958845	0.1	0.1	0.1	0.98595413	2.9	12.3
149.01	6.3	2.8	5.3	12.8	0.96157323	2.0	2.8	6.6	0.97222511	0.0	0.2
150.01	6.5	2.9	3.5	7.1	0.99313616	3.2	3.4	6.9	0.9449915	0.1	0.0
150.02	8.9	4.2	5.4	10.5	0.85116977	5.6	5.2	8.8	0.28966722	0.2	0.1
151.01	6.3	10.6	9.0	17.1	2.48E-06	3.0	4.1	11.4	0.89586618	4.6	0.2
152.02	9.7	6.9	7.9	11.6	0.55549867	3.0	3.3	5.4	0.85934384	1.5	0.2
152.03	12.4	6.3	9.1	17.1	0.92038904	4.8	5.9	11.6	0.93186358	1.3	0.4
153.01	5.6	4.5	7.2	14.4	0.41842245	7.3	6.6	10.5	0.000395973	1.2	0.6
153.02	7.1	3.9	8.4	45.7	0.99050896	4.0	8.1	43.5	0.97253653	1.3	0.5
155.01	7.0	3.1	5.9	30.2	0.99868204	2.9	5.9	30.6	0.9985353	0.8	0.5
156.01	9.7	8.4	11.1	22.8	0.28723819	8.7	9.5	26.6	0.13045819	1.6	1.3
156.02	14.4	18.2	27.8	109.4	0.000169556	13.6	26.5	109.6	0.062392491	2.0	1.1
156.03	4.1	1.2	2.3	6.9	0.99868967	1.2	2.2	6.1	0.99217569	0.3	0.8
157.01	7.2	7.1	9.8	16.8	0.12524872	4.7	9.1	16.9	0.55750364	1.2	0.2
157.02	6.6	4.4	4.0	6.8	0.63513028	4.2	4.0	6.8	0.37599593	0.4	1.9
157.03	4.0	6.3	6.2	9.4	0.003886391	1.5	1.7	3.4	0.63961181	3.3	0.5
157.06	18.0	15.3	18.1	44.0	0.32621514	14.6	17.9	42.3	0.2444876	0.4	0.1
159.01	9.1	8.9	11.6	29.2	0.11180289	6.4	11.3	26.8	0.51655727	0.1	0.6
161.01	3.9	2.6	4.0	15.4	0.91981851	2.4	4.0	15.2	0.96594571	0.6	0.6
162.01	8.5	5.0	6.8	14.6	0.84076704	5.1	6.8	14.7	0.65762625	0.5	0.5
163.01	7.0	6.2	11.0	52.2	0.2466841	5.5	10.7	47.6	0.30418995	0.3	1.1
165.01	7.0	5.8	6.5	10.5	0.36402274	4.3	6.1	12.3	0.58545823	0.2	0.3
166.01	7.1	9.4	11.5	21.3	0.002517424	9.0	8.0	16.7	0.00149333	3.0	1.6

Table 4—Continued

KOI	σ_{TT} (min)	(E_L5,T2) MAD[a] (min)	WRMS[b] (min)	MAX[c] (min)	$p_{X'^2}$[d]	(E_L2,T2) MAD[a] (min)	WRMS[b] (min)	MAX[c] (min)	$p_{X'^2}$[d]	$\frac{\lvert\Delta\ P\rvert}{\sigma_P}$[e]	$\frac{\lvert\Delta\ E\rvert}{\sigma_E}$[f]
167.01	9.8	7.0	12.1	30.9	0.73217302	6.8	12.0	31.0	0.7092131	0.9	0.4
168.01	13.1	6.9	16.3	50.6	0.93800877	6.6	14.5	39.9	0.88536273	1.6	4.0
168.02	47.8	39.5	69.7	213.9	0.36947977	40.2	69.2	218.6	0.2215729	0.5	0.4
168.03	44.6	24.9	44.4	81.4	0.94596753	28.6	35.0	83.7	0.71993969	1.4	1.1
171.01	10.6	6.7	10.9	25.7	0.90139707	6.7	10.8	23.9	0.81055481	0.4	0.1
172.01	8.5	8.6	12.7	24.7	0.11429709	14.1	11.8	18.6	4.90E-06	0.5	1.4
173.01	11.6	10.9	12.7	25.5	0.16662144	9.2	12.4	25.9	0.28728258	1.0	1.1
176.01	11.5	6.3	6.9	11.2	0.80254354	5.6	6.8	12.4	0.6077188	1.0	1.1
177.01	14.5	18.9	15.4	22.6	0.013871918	10.6	13.3	19.9	0.28435937	0.9	0.3
179.01	8.6	14.5	15.8	58.0	0.000152069	7.1	14.6	58.3	0.16910905	1.4	0.0
180.01	8.8	4.4	6.5	10.3	0.96193692	3.3	4.8	11.0	0.98309058	1.4	0.4
183.01	0.5	0.3	0.4	1.4	0.97199142	0.3	0.4	1.4	0.97756339	0.1	0.1
186.01	0.9	0.3	0.6	1.2	1	0.3	0.6	1.2	1	0.0	0.3
187.01	0.8	0.0	0.2	0.4	0.9997405	0.1	0.1	0.2	0.82041991	0.8	0.1
188.01	0.6	0.5	0.9	4.7	0.62137077	0.5	0.9	4.8	0.2870704	0.0	0.3
189.01	0.9	0.4	0.3	0.6	0.81130566	0.4	0.3	0.5	0.59756469	0.7	0.2
190.01	1.3	1.3	2.6	8.2	0.10105516	1.4	2.4	7.1	0.028657014	0.3	2.1
191.01	1.2	0.9	1.3	3.2	0.62638467	1.0	1.2	2.8	0.23891752	1.2	0.3
191.02	12.9	9.5	20.0	56.7	0.76852469	8.2	19.2	50.0	0.96687334	1.8	0.1
191.03	49.7	23.9	46.0	182.2	1	27.0	49.8	163.0	1	1.2	0.1
191.04	58.6	17.4	17.5	28.5	0.98344131	6.9	9.0	13.5	0.99090958	0.2	1.2
192.01	0.8	0.4	0.6	1.1	0.96172643	0.4	0.6	1.1	0.95632961	0.5	0.3
193.01	0.8	0.6	0.5	0.8	0.44634571	0.0	0.1	0.2	0.9028308	5.5	2.5
194.01	2.6	0.6	1.9	13.5	1	0.7	1.9	13.8	1	0.1	0.1
195.01	0.8	0.5	0.9	8.5	0.95338554	0.4	0.9	8.7	0.99467902	0.7	0.3
196.01	0.7	0.5	0.7	3.4	0.89949585	0.4	0.7	3.3	0.99874001	1.4	0.7
197.01	0.8	1.0	1.0	1.5	0.016176357	0.8	0.8	1.4	0.05078992	1.8	0.8
199.01	1.0	0.6	1.0	2.5	0.99272173	0.6	0.9	2.6	0.97103253	0.6	1.1
200.01	1.0	0.5	1.0	4.0	0.98877833	0.4	0.9	3.6	0.99159788	1.0	0.7
201.01	7.0	2.4	2.4	12.3	0.99999904	2.6	2.4	11.5	0.99996647	0.5	1.4
202.01	0.8	0.5	0.7	2.3	0.99696707	0.5	0.7	2.3	0.99101077	1.1	0.8
203.01	0.7	0.6	0.7	3.6	0.13312885	0.6	0.7	3.6	0.14251895	0.3	0.3

Table 4—Continued

KOI	σ_{TT} (min)	(E_L5,T2) MAD[a] (min)	WRMS[b] (min)	MAX[c] (min)	$p_{X'^2}$[d]	(E_L2,T2) MAD[a] (min)	WRMS[b] (min)	MAX[c] (min)	$p_{X'^2}$[d]	$\frac{\lvert\Delta\ P\rvert}{\sigma_P}$[e]	$\frac{\lvert\Delta\ E\rvert}{\sigma_E}$[f]
204.01	1.7	1.4	1.8	6.2	0.28684302	1.3	1.7	6.1	0.47764383	1.0	0.4
205.01	1.0	0.7	1.4	5.4	0.67359556	0.7	1.4	5.6	0.51141935	0.1	1.2
206.01	2.4	1.3	1.8	4.9	0.97739907	1.4	1.8	5.6	0.92797231	0.7	0.3
208.01	4.9	2.0	2.6	5.7	0.99999855	1.9	2.5	6.4	0.99999944	2.3	0.5
209.01	2.0	3.4	3.8	4.8	0.0042149	3.6	3.4	4.6	0.000108707	2.8	0.8
209.02	3.3	1.7	8.7	17.8	0.82500155	3.5	8.6	16.9	0.036904548	0.9	1.0
212.01	2.1	1.4	2.5	5.7	0.82471978	1.7	2.4	5.9	0.32559997	2.3	0.1
214.01	1.5	0.9	1.7	11.2	0.97335068	0.7	1.7	11.0	0.99993462	0.7	0.9
216.01	2.5	1.0	3.1	10.4	0.96109924	1.2	3.1	10.2	0.68320385	0.5	0.1
217.01	0.9	0.7	0.9	3.5	0.51371281	0.6	0.9	3.2	0.8999275	1.4	4.6
219.01	2.8	1.9	2.7	6.5	0.76605909	1.8	2.3	6.5	0.75358377	1.8	0.1
220.01	2.9	2.2	3.1	9.0	0.75810376	2.1	2.9	7.1	0.82267841	2.0	1.1
220.02	36.3	17.0	49.8	178.1	0.99962092	24.3	48.9	165.8	0.81476702	1.3	0.4
221.01	2.5	2.2	2.6	6.7	0.26978724	2.2	2.6	6.6	0.18869327	0.4	0.7
222.01	8.3	4.6	7.5	18.2	0.97286375	4.1	7.2	17.8	0.97959141	0.5	0.2
222.02	9.5	4.7	13.1	26.8	0.91449794	8.3	11.8	20.4	0.13388569	2.2	0.6
223.01	6.8	3.3	6.1	13.8	0.99973941	3.0	6.1	13.4	0.99995185	0.5	0.2
223.02	9.0	7.0	5.9	8.0	0.42000351	1.8	1.7	2.3	0.66919883	2.6	1.0
225.01	3.7	2.4	4.4	74.5	0.99926748	2.4	4.4	74.7	0.99825783	0.3	0.1
226.01	10.6	8.2	13.0	26.9	0.51275718	9.8	10.2	21.6	0.083977284	4.1	1.3
227.01	3.8	36.3	66.2	109.9	0	5.5	7.2	12.3	0.00028818	33.7	3.5
229.01	3.2	2.3	2.8	17.9	0.76705404	1.8	2.7	18.1	0.98574847	0.9	0.9
232.01	3.4	3.6	3.6	9.8	0.065699024	2.2	3.3	11.3	0.60090967	0.1	1.2
232.02	19.0	11.8	22.3	62.9	0.91500872	11.3	21.6	58.3	0.89842696	1.9	0.7
234.01	10.7	8.4	8.7	12.5	0.47207156	8.0	8.7	13.7	0.41948815	0.3	0.4
235.01	10.0	5.0	7.3	20.9	0.99502875	5.8	7.3	20.8	0.93208493	0.4	0.2
237.01	10.4	6.5	9.7	26.8	0.85926269	5.5	9.2	28.1	0.91264615	1.5	0.2
238.01	14.5	15.9	33.3	70.9	0.056591325	16.0	25.3	43.6	0.017408912	4.1	1.5
239.01	7.6	4.7	5.7	11.1	0.91629028	3.9	5.3	11.2	0.97376917	0.6	1.5
240.01	8.0	6.8	9.2	21.8	0.29843757	6.0	8.9	21.9	0.55647144	0.7	0.7
241.01	7.4	10.0	12.5	27.8	0.001313043	12.9	10.8	20.1	1.03E-07	2.7	1.6
242.01	3.5	2.2	3.4	7.5	0.87624967	2.9	3.3	7.0	0.23753434	0.1	0.5

Table 4—Continued

KOI	σ_{TT} (min)	(E_L5,T2) MAD[a] (min)	WRMS[b] (min)	MAX[c] (min)	$p_{X'2}$[d]	(E_L2,T2) MAD[a] (min)	WRMS[b] (min)	MAX[c] (min)	$p_{X'2}$[d]	$\frac{\lvert\Delta\ P\rvert}{\sigma_P}$[e]	$\frac{\lvert\Delta\ E\rvert}{\sigma_E}$[f]
244.01	1.7	2.2	2.0	6.4	0.005423181	1.5	1.8	7.7	0.14534664	0.6	0.5
244.02	3.7	5.0	4.5	9.9	6.67E-05	2.6	2.5	5.7	0.64186157	0.7	3.2
245.01	3.5	11.6	18.4	54.4	4.93E-11	5.7	17.4	60.4	0.000489352	1.7	8.1
246.01	4.3	4.1	4.5	12.0	0.092012543	3.9	4.5	11.4	0.098107351	0.5	0.4
247.01	6.8	2.5	10.0	19.8	0.98290209	3.9	9.8	19.9	0.60309425	0.5	0.1
248.01	7.3	3.5	8.1	25.3	0.99082216	3.6	6.8	18.7	0.9659645	4.5	3.4
248.02	8.5	5.6	13.7	94.6	0.7655133	9.0	12.5	98.7	0.022377549	1.0	0.9
248.03	15.4	9.1	22.1	58.0	0.99383516	8.9	21.2	54.8	0.99356392	2.9	1.3
249.01	4.2	2.4	3.1	6.6	0.87247006	0.9	1.9	6.8	0.99951576	2.3	0.9
250.01	4.6	3.1	4.1	9.9	0.68768223	1.3	3.5	8.6	0.99362271	0.1	1.7
250.02	5.9	4.5	5.1	10.2	0.48403266	4.5	4.7	8.2	0.24380497	1.5	1.0
250.03	34.2	14.5	37.6	149.6	0.99998435	14.3	36.4	138.4	0.99996183	0.1	1.4
251.01	4.1	2.7	4.7	23.2	0.9134354	3.1	4.7	23.0	0.48509255	0.2	0.5
252.01	8.7	7.0	10.6	17.6	0.42560986	5.6	8.8	17.6	0.41764123	1.5	1.4
253.01	5.9	6.1	6.8	13.8	0.034198778	5.1	6.4	16.3	0.18518009	0.9	0.4
254.01	0.8	0.6	0.8	4.8	0.69912465	0.6	0.7	4.9	0.58600301	0.5	0.8
255.01	7.7	5.0	3.9	5.7	0.61069408	2.9	2.1	4.0	0.63694653	1.0	1.2
257.01	4.7	2.9	4.2	14.3	0.89880058	3.0	4.1	15.1	0.76278922	0.2	0.4
258.01	11.9	21.5	59.8	240.9	1.11E-16	22.9	49.1	180.9	0	13.8	10.7
260.01	15.6	9.4	42.5	163.9	0.83864354	24.1	37.2	127.4	9.42E-06	3.4	0.6
261.01	6.1	10.9	6.8	19.2	7.97E-06	10.1	6.7	20.7	1.12E-05	0.1	0.5
262.01	15.4	4.4	14.8	31.8	0.99997831	8.3	14.5	33.3	0.90962008	0.3	0.8
263.01	16.3	5.5	28.0	54.1	0.97031368	20.8	19.9	47.7	0.005322006	1.9	0.6
265.01	36.1	12.7	36.4	100.8	0.99999395	17.5	34.1	83.0	0.99396981	1.3	2.7
269.01	18.9	4.0	7.4	13.4	0.99668965	2.8	7.2	12.1	0.982813	0.1	1.3
270.01	17.4	20.7	31.2	58.2	0.017533	26.9	29.9	49.3	1.92E-05	0.7	1.2
270.02	18.6	9.1	8.4	9.4	0.77071847	2.3	2.5	3.7	0.7852684	4.0	0.5
273.01	7.2	3.7	4.5	18.3	0.94650762	2.8	4.3	17.7	0.97785391	0.4	0.7
274.01	30.2	16.5	22.4	35.5	0.85626187	17.8	21.2	35.7	0.57198846	0.4	0.3
275.01	17.9	11.9	15.3	23.7	0.67885197	9.7	13.5	22.5	0.66939178	0.9	0.1
277.01	6.0	25.3	40.9	72.5	0	2.8	5.0	20.2	0.78961113	30.7	18.6
279.01	2.1	1.1	1.8	2.9	0.75286868	0.2	0.2	0.3	0.87269261	6.0	4.3

Table 4—Continued

KOI	σ_{TT} (min)	(E_L5,T2) MAD[a] (min)	WRMS[b] (min)	MAX[c] (min)	$p_{X'^2}$[d]	(E_L2,T2) MAD[a] (min)	WRMS[b] (min)	MAX[c] (min)	$p_{X'^2}$[d]	$\frac{\lvert\Delta\ P\rvert}{\sigma_P}$[e]	$\frac{\lvert\Delta\ E\rvert}{\sigma_E}$[f]
279.02	13.9	7.9	12.3	19.6	0.80896122	8.1	8.4	18.8	0.52530852	1.3	0.4
280.01	4.1	5.1	4.5	7.1	0.00817993	3.2	3.4	10.9	0.28122714	2.0	0.8
281.01	10.8	8.3	72.2	185.0	0.46050574	24.4	49.5	85.7	1.14E-08	8.9	10.9
282.02	29.6	11.6	19.9	40.8	0.99866543	11.3	18.2	50.9	0.99578796	0.2	1.2
283.01	6.7	1.7	4.9	12.3	0.99849279	2.1	2.8	5.6	0.95150632	1.5	1.2
284.01	12.9	12.8	12.0	17.7	0.15930845	5.9	6.2	10.7	0.73684589	2.0	1.3
284.02	18.0	10.8	30.5	102.0	0.91558857	11.2	28.9	124.3	0.79985904	2.0	0.0
284.03	21.1	15.8	25.1	61.6	0.60179869	14.3	25.0	61.5	0.66848418	0.1	0.7
285.01	5.7	5.5	5.2	8.9	0.17043247	4.2	4.4	7.9	0.31648963	0.5	0.0
288.01	10.0	19.3	18.2	34.8	5.32E-09	18.6	18.1	33.0	5.25E-09	1.1	2.7
289.01	7.2	8.8	8.1	9.6	0.070617943	2.3	2.8	3.8	0.48291515	11.0	1.1
291.01	12.8	1.9	2.3	4.0	0.99175963	0.4	0.3	0.5	0.94302319	1.7	0.7
291.02	20.4	11.3	20.9	50.9	0.94572719	13.1	17.7	33.7	0.70078787	2.2	0.1
292.01	11.4	7.5	13.1	31.7	0.95301857	7.9	12.9	31.9	0.82948616	0.5	0.2
295.01	9.9	7.0	12.0	33.2	0.74383871	4.5	11.2	35.1	0.99432057	4.2	5.8
296.01	9.9	4.3	5.4	7.5	0.83262163	2.8	4.2	6.4	0.53859068	2.0	0.3
297.01	16.7	12.8	17.9	34.2	0.54185771	13.7	17.8	29.9	0.26766006	1.3	1.8
298.01	13.5	0.9	6.7	17.0	0.99998685	4.6	5.4	10.0	0.82221406	1.2	2.9
299.01	14.6	10.1	14.7	41.0	0.954408	10.2	14.6	43.0	0.91283882	0.0	0.6
301.01	15.6	4.8	13.7	28.3	0.99999218	6.0	13.7	28.3	0.99896732	0.8	1.8
302.01	11.6	5.9	9.7	21.5	0.80443367	7.8	8.2	16.5	0.24714338	0.3	1.3
304.01	5.1	4.4	5.9	12.9	0.29255807	4.7	5.5	11.6	0.10832331	1.2	1.4
305.01	11.3	6.3	10.4	46.5	0.98350886	8.0	9.7	43.6	0.66128638	0.8	1.2
306.01	9.3	4.3	4.1	7.6	0.85816079	1.6	1.2	1.6	0.91540422	0.1	0.7
307.01	14.2	5.0	4.9	10.5	0.97858564	3.4	4.1	8.0	0.9706469	0.6	0.2
312.01	12.7	18.5	22.8	58.0	0.000238467	19.7	22.2	60.3	7.78E-06	1.2	0.2
313.01	7.9	3.6	3.0	5.2	0.9230473	2.0	2.2	9.8	0.96599497	0.5	0.3
313.02	15.7	7.0	6.4	14.0	0.98968182	7.2	6.0	12.7	0.95766491	0.2	1.9
314.01	4.4	3.3	4.0	7.3	0.53706149	3.8	4.0	7.6	0.1568915	0.5	1.5
314.02	6.4	4.8	4.9	5.6	0.48031383	2.8	2.5	3.2	0.55254082	0.9	1.3
316.01	8.5	5.5	6.0	9.9	0.69431684	4.3	5.4	13.0	0.6593251	0.3	2.3
317.01	9.8	5.4	5.5	7.5	0.79076483	2.1	3.4	6.2	0.94895477	1.0	0.1

Table 4—Continued

KOI	σ_{TT} (min)	(E_L5,T2) MAD[a] (min)	WRMS[b] (min)	MAX[c] (min)	$p_{X'^2}$[d]	(E_L2,T2) MAD[a] (min)	WRMS[b] (min)	MAX[c] (min)	$p_{X'^2}$[d]	$\frac{\lvert\Delta\ P\rvert}{\sigma_P}$[e]	$\frac{\lvert\Delta\ E\rvert}{\sigma_E}$[f]
318.01	6.7	2.6	5.1	9.4	0.8647526	2.5	2.6	2.7	0.42452061	10.1	1.0
321.01	17.1	12.9	21.3	58.9	0.69381398	14.5	21.1	58.8	0.19699072	1.0	0.8
323.01	19.1	30.3	32.9	269.6	1.95E-09	8.2	20.4	294.9	0.99756997	1.5	2.4
326.01	15.6	5.7	14.4	55.7	0.99888705	7.1	14.2	53.2	0.96123178	0.6	1.0
327.01	18.1	6.9	21.2	86.3	0.99999915	6.9	19.2	75.6	0.99999662	3.2	0.8
330.01	23.4	26.2	31.3	66.4	0.019163379	14.9	28.9	74.0	0.68586039	1.7	0.8
331.01	15.2	25.0	28.7	48.8	0.000285606	20.4	28.0	42.3	0.0020791	1.1	0.5
332.01	15.3	15.8	18.1	44.4	0.029722797	8.8	16.3	36.6	0.91978582	2.1	0.9
333.01	20.8	3.3	6.0	13.8	0.9999294	4.9	5.8	11.6	0.9874892	0.2	1.0
337.01	19.0	4.7	11.6	23.0	0.99694594	6.8	10.7	18.5	0.8765242	0.4	0.2
338.01	16.1	11.8	17.6	48.3	0.62896735	13.0	16.8	38.9	0.27695282	2.0	0.9
339.01	16.5	11.4	16.6	48.9	0.92466415	11.5	16.5	48.9	0.8782667	0.1	0.3
339.02	32.0	19.3	46.0	137.9	0.92225861	28.8	37.2	112.7	0.11686992	4.0	1.5
341.01	8.0	5.2	7.8	19.6	0.84196405	5.3	7.7	18.3	0.67938207	1.1	1.0
341.02	14.6	14.7	27.9	83.9	0.03264905	16.4	27.4	78.3	0.001386103	0.1	0.5
343.01	8.0	5.7	9.4	19.2	0.74180591	6.4	9.2	20.6	0.33597761	0.0	1.3
343.02	12.6	10.6	18.1	128.1	0.25296899	10.3	17.8	130.8	0.31082299	0.1	1.8
344.01	4.8	2.9	3.8	4.9	0.63781813	0.8	0.7	1.0	0.71920246	4.7	0.3
345.01	4.5	2.8	2.6	3.6	0.60321844	0.2	0.3	0.5	0.92761642	3.6	0.8
346.01	5.8	9.4	12.9	143.7	2.19E-05	5.3	9.3	148.4	0.09768589	0.8	2.0
348.01	3.9	6.7	7.7	8.9	0.002866661	6.4	5.2	6.7	0.000341499	12.6	0.5
349.01	7.9	5.9	6.4	13.0	0.54213099	4.0	5.3	11.5	0.78865011	1.5	0.3
350.01	12.0	2.0	3.9	9.7	0.99998823	3.1	3.5	8.1	0.99578222	0.1	1.5
352.01	17.8	9.3	16.3	27.4	0.78408029	10.6	10.5	14.2	0.32525663	0.2	1.4
354.01	10.0	8.8	10.2	15.1	0.28198592	4.1	8.8	15.4	0.87425425	0.3	2.0
355.01	12.4	10.7	16.8	210.2	0.26484271	8.0	13.1	213.5	0.81952665	1.9	3.8
356.01	4.9	3.5	5.7	22.9	0.85994343	3.3	5.7	22.9	0.93498712	0.4	0.3
360.01	25.3	16.1	32.5	66.3	0.86480396	15.7	22.5	58.7	0.79953737	3.5	4.8
361.01	22.9	14.3	35.2	90.7	0.97029257	12.7	34.5	81.5	0.99279663	0.2	0.2
369.01	16.7	11.0	18.6	76.8	0.84984314	8.3	18.4	73.3	0.98249068	0.4	0.1
377.01	2.3	0.8	0.8	1.3	0.93302904	0.0	0.0	0.1	0.99911082	0.4	0.6
377.02	4.7	7.9	8.6	12.6	0.004034632	0.2	0.3	0.4	0.91184439	16.7	11.8

Table 4—Continued

KOI	σ_{TT} (min)	(E_L5,T2) MAD[a] (min)	WRMS[b] (min)	MAX[c] (min)	$p_{X'^2}$[d]	(E_L2,T2) MAD[a] (min)	WRMS[b] (min)	MAX[c] (min)	$p_{X'^2}$[d]	$\frac{\lvert\Delta\ P\rvert}{\sigma_P}$[e]	$\frac{\lvert\Delta\ E\rvert}{\sigma_E}$[f]
377.03	27.0	17.7	32.1	112.6	0.98438344	21.8	28.7	89.8	0.35996862	2.5	0.1
379.01	17.2	6.3	26.3	52.4	0.99978219	11.2	24.8	47.9	0.73581608	2.5	0.1
384.01	24.5	13.8	27.7	55.1	0.97786462	20.0	26.8	53.5	0.29057731	0.5	1.4
385.01	17.4	13.1	24.6	44.6	0.53000198	22.1	23.1	35.9	0.001785453	2.5	2.3
386.01	8.3	4.0	6.0	10.8	0.78202625	1.9	3.1	5.6	0.62224905	0.2	1.6
387.01	7.1	6.0	5.7	14.1	0.34475107	6.8	5.3	9.9	0.070146273	0.5	1.1
388.01	233.5	19.7	77.2	233.5	1	46.5	71.7	196.0	0.99999985	0.4	9.2
392.01	34.5	1.4	9.9	15.4	0.99982619	6.6	7.4	9.0	0.67590567	0.6	0.3
393.01	25.0	7.7	11.7	22.1	0.98012123	8.2	10.6	19.9	0.8393572	0.5	0.0
398.02	7.5	5.4	21.9	101.8	0.75080186	6.6	21.5	98.0	0.14705779	0.5	1.2
401.01	3.5	2.9	3.6	4.9	0.35703515	0.2	0.2	0.3	0.89399968	7.6	0.4
408.01	6.6	5.7	7.8	28.2	0.27089792	4.7	7.4	30.3	0.529365	0.3	1.1
408.02	10.7	6.8	8.9	21.2	0.74717683	8.8	8.8	19.0	0.20193272	0.5	0.3
408.03	21.5	10.3	12.5	18.9	0.83475859	7.1	8.1	14.3	0.70960551	1.1	0.1
409.01	10.3	6.7	8.3	16.8	0.70440411	4.2	6.5	13.0	0.86692266	0.3	0.7
410.01	2.1	1.5	4.0	52.2	0.63016347	1.9	3.7	49.8	0.12548569	3.2	0.2
412.01	2.7	1.8	2.4	6.6	0.86625754	1.8	2.4	6.6	0.75402224	0.9	0.1
413.01	6.7	5.8	5.9	9.6	0.31477502	5.7	5.8	10.7	0.14885938	0.3	1.3
416.01	4.6	1.7	1.4	2.9	0.9270674	1.4	1.3	2.3	0.74074907	0.2	0.6
417.01	1.6	1.9	1.6	2.7	0.03425553	1.0	1.0	2.5	0.48742978	0.2	4.7
418.01	1.1	0.4	0.5	0.8	0.95409308	0.3	0.3	0.5	0.79089691	0.0	3.5
419.01	1.1	0.4	0.4	0.7	0.91015747	0.2	0.2	0.5	0.94191537	0.7	0.2
420.01	3.0	1.8	2.2	6.0	0.91804594	1.2	2.1	5.6	0.99884138	1.8	3.4
421.01	0.8	0.7	1.0	1.8	0.24906331	0.8	0.9	1.7	0.007655862	0.9	1.1
423.01	5.7	9.5	5.2	12.8	0.001534191	12.2	3.4	15.9	4.59E-07	0.2	4.5
425.01	1.5	1.1	1.2	12.5	0.74726068	1.0	1.1	12.2	0.74714386	1.2	0.1
426.01	8.0	7.7	9.6	13.9	0.17165855	7.1	8.8	16.4	0.12195087	0.2	1.7
427.01	6.9	4.5	5.6	8.6	0.56728722	4.5	4.2	4.5	0.15643663	5.8	2.2
428.01	2.7	1.5	2.0	15.4	0.96208307	1.4	2.0	15.3	0.94223268	0.2	0.0
429.01	3.3	1.9	2.9	6.6	0.90295149	2.4	2.8	6.1	0.45442385	0.1	0.3
430.01	6.4	4.6	6.1	14.0	0.58373105	4.6	5.7	11.0	0.34895771	0.8	0.9
431.01	10.2	5.0	5.4	12.5	0.89420223	3.7	4.3	9.9	0.8744959	0.6	0.4

Table 4—Continued

KOI	σ_{TT} (min)	(E_L5,T2) MAD[a] (min)	WRMS[b] (min)	MAX[c] (min)	$p_{X'^2}$[d]	(E_L2,T2) MAD[a] (min)	WRMS[b] (min)	MAX[c] (min)	$p_{X'^2}$[d]	$\frac{\lvert\Delta\ P\rvert}{\sigma_P}$[e]	$\frac{\lvert\Delta\ E\rvert}{\sigma_E}$[f]
431.02	10.4	15.5	14.1	18.6	0.014731084	9.2	10.2	13.1	0.052578611	9.4	0.2
432.01	5.5	3.4	4.4	10.2	0.92482495	3.4	4.3	10.2	0.85996414	0.3	0.1
435.01	7.5	7.5	11.2	23.9	0.16878142	6.1	10.8	21.4	0.15849289	0.3	1.8
438.01	8.8	3.4	6.2	16.3	0.99984276	3.6	5.8	14.1	0.99853816	0.6	0.1
439.01	3.9	2.6	3.9	10.7	0.97271579	2.5	3.9	10.7	0.98204165	0.1	0.1
440.01	9.1	6.0	7.1	13.1	0.69524064	5.8	7.0	12.1	0.48574946	1.2	1.6
440.02	9.2	9.6	15.9	86.8	0.019298327	9.8	15.8	83.8	0.006278561	1.7	1.5
442.01	16.9	16.5	20.8	36.7	0.15487012	19.4	18.0	24.5	0.011153454	1.4	0.4
442.02	27.8	17.0	35.0	84.5	0.99748556	21.6	33.5	75.8	0.52264078	3.1	1.7
443.01	11.9	10.0	13.3	23.6	0.35035917	11.8	10.9	15.9	0.055145468	0.1	4.8
444.01	14.1	16.5	16.2	28.9	0.028542834	11.9	12.0	17.1	0.17387623	2.4	0.6
446.01	12.6	11.7	13.0	19.9	0.22454881	11.3	11.4	22.5	0.10627174	0.4	0.6
446.02	19.5	6.8	6.9	9.4	0.90126799	6.4	6.7	8.1	0.47858245	1.4	0.8
448.01	9.7	5.7	5.9	9.6	0.86596018	5.2	5.9	9.6	0.80402208	0.1	0.1
452.01	17.4	9.1	12.8	29.4	0.99812642	9.1	12.5	33.3	0.99523835	1.2	0.7
454.01	17.3	12.9	10.0	18.3	0.47711128	13.8	9.7	16.1	0.1346324	0.6	1.6
456.01	8.7	8.2	9.2	17.6	0.1836453	8.9	8.4	15.8	0.040786373	1.1	0.5
456.02	27.4	15.2	43.7	159.0	0.9900628	17.8	42.9	148.3	0.85832222	0.3	1.9
457.01	8.2	4.9	13.6	54.6	0.95791458	5.1	13.1	50.7	0.88054998	1.8	1.2
459.01	8.7	3.5	5.7	14.0	0.93435174	1.1	3.8	9.0	0.98932126	1.0	0.3
459.02	39.8	20.2	68.4	153.7	0.97870628	20.3	67.2	139.6	0.94153324	0.5	1.0
460.01	6.3	4.6	4.6	6.9	0.54165358	3.5	3.8	7.8	0.58132447	1.1	0.0
463.01	3.6	5.0	5.1	7.2	0.019885053	3.2	2.7	5.3	0.082167005	0.9	1.9
464.02	9.4	6.3	9.6	28.6	0.85127256	6.1	9.4	25.2	0.79389944	1.1	0.6
466.01	4.1	3.4	5.0	9.2	0.37947528	4.1	4.9	8.4	0.033468389	1.4	1.4
467.01	3.2	4.9	3.5	5.1	0.00540304	4.1	3.2	4.5	0.006767789	1.1	1.3
468.01	4.5	1.9	3.0	5.1	0.88523556	2.0	2.0	2.6	0.52359204	0.8	1.0
469.01	3.5	2.8	2.7	4.6	0.48465293	2.8	2.6	4.4	0.27675031	0.2	0.4
470.01	3.6	1.6	3.9	54.5	0.99986482	1.1	3.9	53.4	0.99999986	0.7	0.7
471.01	16.9	6.4	9.1	13.7	0.95255963	7.7	8.0	10.0	0.65748835	2.1	2.0
472.01	8.1	4.1	9.0	34.0	0.99690006	4.3	8.7	31.8	0.98367111	0.3	0.1
473.01	11.1	2.9	9.1	19.3	0.99900783	5.7	5.5	9.0	0.76608567	3.4	3.5

Table 4—Continued

KOI	σ_{TT} (min)	(E_L5,T2) MAD[a] (min)	WRMS[b] (min)	MAX[c] (min)	$p_{X'^2}$[d]	(E_L2,T2) MAD[a] (min)	WRMS[b] (min)	MAX[c] (min)	$p_{X'^2}$[d]	$\frac{\lvert\Delta\ P\rvert}{\sigma_P}$[e]	$\frac{\lvert\Delta\ E\rvert}{\sigma_E}$[f]
474.01	13.5	6.6	11.7	38.9	0.9585778	4.9	11.0	34.4	0.9798315	0.1	0.3
474.02	16.5	7.7	10.6	15.1	0.88701966	4.6	6.2	17.3	0.89448862	1.0	0.7
475.01	15.0	8.5	13.5	28.3	0.91981521	10.9	12.8	30.5	0.44991643	0.6	0.5
475.02	14.6	4.5	20.7	45.0	0.99402922	8.6	10.5	18.0	0.58451596	3.2	0.3
476.01	12.6	19.0	17.6	25.7	0.001501655	13.3	17.2	29.2	0.031886526	0.9	1.1
477.01	12.1	9.4	19.0	89.0	0.46849007	10.5	15.0	105.5	0.14022034	1.8	3.2
478.01	4.3	4.4	5.2	8.5	0.10516056	4.6	5.0	9.7	0.021586518	0.7	0.8
480.01	8.5	4.8	6.2	13.3	0.98500519	4.9	6.1	11.9	0.95154402	0.1	0.5
481.01	7.9	4.3	7.8	48.1	0.95868756	4.1	7.3	44.5	0.94390425	1.0	0.3
481.02	14.9	11.5	18.6	56.8	0.61470174	10.7	18.3	54.2	0.84871317	0.6	1.3
483.01	10.3	6.3	11.6	27.7	0.93439962	6.5	11.3	31.7	0.84615555	0.7	1.6
484.01	9.6	1.7	7.2	13.2	0.99956065	8.1	6.2	8.6	0.15539003	0.7	1.2
486.01	12.6	8.3	43.1	107.7	0.6084807	41.7	29.1	44.5	1.11E-15	5.3	3.8
487.01	15.1	7.4	20.3	63.1	0.98438452	11.9	16.8	41.7	0.32709793	2.1	3.4
488.01	29.1	15.2	36.3	88.5	0.94353164	10.4	24.3	48.2	0.98793837	2.0	1.0
490.01	18.3	8.7	26.9	84.3	0.99900239	12.8	24.5	65.9	0.6998975	2.7	0.3
490.03	17.4	11.0	26.0	80.0	0.86479372	9.2	25.9	79.4	0.93063091	0.3	0.2
492.01	15.7	7.2	6.8	8.7	0.85618908	2.8	1.9	3.4	0.90554671	0.9	2.7
494.01	10.6	7.7	8.9	14.3	0.50270536	9.3	7.9	14.2	0.087665347	0.0	0.6
497.01	17.4	4.4	8.1	15.4	0.99961212	5.1	7.7	14.5	0.99113121	1.0	1.2
497.02	39.3	20.2	45.3	115.8	0.99609804	22.4	42.7	102.1	0.96213481	1.5	0.5
499.01	16.2	8.1	12.7	26.1	0.96862494	7.4	11.8	20.4	0.95033213	0.4	0.8
500.01	9.1	6.5	13.0	28.6	0.66811472	3.3	10.0	19.3	0.9976317	3.9	0.7
500.02	8.2	8.9	11.6	27.3	0.041456158	5.5	10.3	29.0	0.56740326	3.0	3.0
500.03	26.8	15.8	43.8	153.1	0.99085943	14.6	42.6	140.0	0.99573193	1.9	1.6
500.04	19.2	14.8	24.0	89.0	0.55763918	9.7	22.2	95.0	0.99265411	2.5	0.0
500.05	27.0	11.3	26.8	682.9	0.99999965	11.0	26.7	683.9	0.99999948	0.3	0.9
501.01	27.3	30.6	27.1	41.1	0.095444835	18.1	16.7	24.5	0.2527165	0.8	1.6
503.01	10.3	5.4	8.3	18.9	0.96596605	6.4	8.0	21.6	0.7396599	0.7	0.3
505.01	10.2	9.1	12.7	22.5	0.26069055	10.5	12.2	19.1	0.034752521	0.1	3.1
506.01	9.0	5.3	8.0	36.0	0.99945398	5.7	7.7	35.8	0.99092535	3.3	1.8
507.01	7.4	7.5	7.6	15.4	0.14869272	5.3	7.2	20.4	0.32021899	0.7	0.4

Table 4—Continued

KOI	σ_{TT} (min)	(E_L5,T2) MAD[a] (min)	WRMS[b] (min)	MAX[c] (min)	$p_{X'^2}$[d]	(E_L2,T2) MAD[a] (min)	WRMS[b] (min)	MAX[c] (min)	$p_{X'^2}$[d]	$\frac{\lvert\Delta\ P\rvert}{\sigma_P}$[e]	$\frac{\lvert\Delta\ E\rvert}{\sigma_E}$[f]
508.01	9.7	7.3	10.2	26.0	0.63762265	7.9	12.1	25.4	0.40794296	0.3	1.7
508.02	13.6	5.8	9.1	17.3	0.9443842	6.2	5.3	7.8	0.74338748	0.5	2.8
509.01	12.8	8.5	18.6	60.6	0.88320664	10.4	16.4	52.6	0.29466399	3.1	1.7
509.02	10.7	9.6	16.7	39.4	0.24750617	8.5	16.5	36.9	0.27267275	0.1	0.5
510.01	19.2	12.8	32.7	109.2	0.92516339	13.1	32.6	108.6	0.84339076	0.6	0.3
510.02	18.2	10.6	27.0	73.2	0.93442677	16.9	22.3	54.0	0.087291291	1.8	2.5
511.01	9.8	4.2	8.4	16.7	0.99476071	5.5	7.9	13.9	0.86410711	0.1	1.7
512.01	28.0	20.2	28.2	92.6	0.68196676	21.7	25.7	74.2	0.38997822	1.0	1.0
513.01	15.1	4.1	4.2	5.6	0.95203049	1.7	2.1	3.3	0.80259234	0.0	1.0
517.01	7.0	2.9	6.6	20.2	0.99999916	2.5	6.4	19.0	0.99999996	0.2	0.7
518.01	7.9	4.5	7.5	17.0	0.80706386	4.6	7.3	18.2	0.52363854	0.7	0.1
519.01	18.4	10.4	28.4	58.2	0.8528028	15.6	20.1	36.7	0.17093072	2.4	1.9
520.01	10.4	5.8	8.2	13.2	0.86339323	7.5	6.5	11.8	0.3663366	1.4	1.1
520.02	21.3	14.2	46.4	130.8	0.83510763	15.8	44.4	124.4	0.50649644	2.4	0.7
520.03	11.6	6.6	8.0	17.7	0.77136103	5.4	7.8	17.8	0.63763665	0.2	0.4
521.01	9.7	6.3	6.7	11.5	0.75906386	2.4	4.0	7.2	0.99863707	1.6	1.9
522.01	9.0	7.4	10.2	23.0	0.38735199	3.9	8.5	20.1	0.83324576	1.1	0.1
523.02	22.3	18.0	24.8	41.8	0.39246056	22.6	18.1	26.1	0.039848547	1.4	0.3
524.01	8.4	8.2	13.7	36.7	0.045522239	7.6	10.0	23.5	0.098775486	7.8	7.8
525.01	6.7	2.9	6.2	13.4	0.9781138	2.9	5.9	11.2	0.91450148	0.4	0.7
526.01	6.7	3.4	6.3	18.2	0.99996894	3.5	6.2	17.2	0.99984409	0.4	1.4
528.01	10.8	11.2	14.1	25.0	0.073023263	8.8	10.5	16.4	0.24679098	2.2	3.5
528.03	8.5	12.8	18.7	28.1	0.003594179	15.8	17.4	24.0	6.71E-06	1.1	0.8
530.01	19.1	8.8	16.4	32.0	0.97844579	10.9	16.1	35.9	0.77797262	0.2	0.4
531.01	3.3	5.5	9.4	27.7	1.11E-15	6.0	9.3	29.2	0	1.2	2.8
532.01	14.3	12.9	16.8	44.3	0.15738921	10.1	16.5	47.2	0.6786841	0.2	0.1
533.01	17.9	18.7	21.5	35.4	0.10178161	14.0	17.1	30.3	0.23942852	0.2	1.8
534.01	10.0	8.8	19.5	50.3	0.23496182	7.3	18.0	39.7	0.49883735	2.0	0.5
534.02	17.1	16.4	25.1	89.2	0.033643932	13.4	23.2	72.0	0.45345501	2.9	0.9
535.01	8.0	5.9	9.1	23.5	0.6175038	4.7	7.9	25.3	0.87463901	2.4	1.4
537.01	16.4	7.8	18.7	60.3	0.99993744	7.8	18.6	64.1	0.99986195	0.8	0.3
538.01	14.6	6.4	5.5	9.4	0.91314262	5.6	5.1	8.3	0.76262433	0.8	0.4

Table 4—Continued

KOI	σ_{TT} (min)	(E_L5,T2) MAD[a] (min)	WRMS[b] (min)	MAX[c] (min)	$p_{X'^2}$[d]	(E_L2,T2) MAD[a] (min)	WRMS[b] (min)	MAX[c] (min)	$p_{X'^2}$[d]	$\frac{\lvert\Delta\ P\rvert}{\sigma_P}$[e]	$\frac{\lvert\Delta\ E\rvert}{\sigma_E}$[f]
541.01	17.5	6.0	11.7	22.0	0.98884823	7.3	9.8	16.9	0.86244199	1.1	0.4
543.01	11.6	12.2	19.9	50.4	0.010678925	11.2	19.0	40.0	0.034419494	2.7	0.1
543.02	22.2	21.3	30.1	76.2	0.037649827	23.0	29.7	82.5	0.002904857	0.9	1.1
546.01	16.0	3.3	8.0	18.1	0.99692124	3.9	4.5	6.3	0.9282117	1.1	0.1
547.01	5.5	4.0	3.4	5.3	0.51022853	3.1	2.5	5.0	0.38528161	0.4	1.0
548.01	10.8	8.2	8.7	14.3	0.46204256	8.4	7.8	12.4	0.14936317	0.5	1.3
550.01	11.2	5.0	9.1	18.4	0.95015887	5.5	7.7	13.5	0.75875745	0.1	1.5
551.01	16.1	4.9	37.6	101.0	0.99830363	6.6	36.7	93.1	0.9333973	0.5	2.1
551.02	15.4	12.2	17.5	42.2	0.47940972	8.8	16.6	45.6	0.92219759	1.1	1.0
552.01	2.8	1.5	3.0	32.8	0.99876304	1.5	3.0	32.4	0.99556833	0.1	1.0
554.01	6.6	2.6	5.0	73.7	0.99999508	2.8	5.0	73.5	0.99993479	0.4	0.2
555.01	27.7	21.5	39.6	112.4	0.55323293	25.7	37.3	115.0	0.055668305	3.0	1.2
557.01	14.7	8.6	13.4	31.1	0.80079204	7.6	12.8	32.8	0.70484591	1.0	1.2
558.01	10.9	5.6	7.2	20.4	0.96186334	6.5	6.3	13.0	0.74857063	0.3	1.2
560.01	14.5	3.4	9.6	13.3	0.99449443	8.5	8.7	11.1	0.4377935	0.5	0.5
561.01	15.9	12.8	22.6	72.1	0.44279582	11.1	22.3	66.0	0.67418681	0.7	1.7
563.01	28.8	16.5	27.0	53.5	0.82315018	16.8	26.3	48.7	0.58760866	0.3	0.3
564.01	16.7	10.1	29.7	63.9	0.72075129	8.6	14.5	27.5	0.5609253	4.2	0.4
566.01	13.8	3.9	7.8	13.1	0.9449868	4.8	6.0	7.7	0.44669861	1.6	0.5
567.01	10.4	4.7	7.0	17.3	0.98224138	3.1	6.2	17.7	0.99705714	1.6	2.2
567.02	15.4	22.8	21.2	32.6	0.003858143	12.7	17.6	27.3	0.14821116	1.7	0.1
567.03	15.5	14.7	13.7	17.7	0.23343857	3.1	3.9	5.9	0.66640614	6.1	1.1
568.01	19.4	12.4	16.5	35.6	0.94957998	13.8	16.1	39.7	0.71725404	0.0	0.0
569.01	19.3	9.1	16.2	25.4	0.88371134	6.2	15.7	32.4	0.84704462	0.1	0.2
571.01	12.5	8.3	8.9	19.1	0.7897387	7.2	8.5	18.5	0.84728549	0.4	0.7
571.02	11.3	7.3	15.3	44.1	0.68292757	12.6	14.3	38.9	0.019455479	0.2	0.3
571.03	13.4	13.4	19.8	35.7	0.022733215	12.5	19.3	39.8	0.053598912	0.2	1.6
572.01	20.2	10.3	14.3	35.6	0.94475941	5.1	10.9	27.8	0.99834263	2.0	0.1
573.01	14.6	11.0	17.5	43.7	0.58739812	13.6	16.5	33.6	0.073152904	1.6	0.3
573.02	35.7	19.7	41.0	145.6	0.99976171	26.5	39.3	159.3	0.70126932	1.9	1.4
574.01	8.5	5.2	10.8	18.6	0.71178134	5.9	8.3	23.5	0.28976079	1.6	0.9
575.01	19.5	17.1	14.3	19.4	0.30343383	12.5	10.4	14.0	0.27689513	2.1	0.9

Table 4—Continued

KOI	σ_{TT} (min)	(E_L5,T2) MAD[a] (min)	WRMS[b] (min)	MAX[c] (min)	$p_{X'^2}$[d]	(E_L2,T2) MAD[a] (min)	WRMS[b] (min)	MAX[c] (min)	$p_{X'^2}$[d]	$\frac{\lvert\Delta\ P\rvert}{\sigma_P}$[e]	$\frac{\lvert\Delta\ E\rvert}{\sigma_E}$[f]
577.01	19.6	4.3	5.6	7.7	0.97390088	1.8	3.0	5.6	0.84140956	3.5	0.4
578.01	7.2	3.8	4.8	10.3	0.98101996	4.4	4.8	9.6	0.82918002	0.2	0.5
579.01	14.0	15.8	24.7	74.6	9.10E-06	16.2	24.1	71.8	7.45E-07	1.3	1.4
580.01	11.9	6.9	8.3	16.1	0.93204412	5.5	8.1	16.8	0.97861458	0.8	1.6
581.01	6.8	5.6	6.7	13.6	0.36455305	5.9	6.6	13.0	0.15632048	0.1	0.1
582.01	11.0	6.9	12.5	39.8	0.90045788	6.3	12.4	38.0	0.90989332	1.1	0.1
583.01	26.3	14.0	26.5	71.8	0.99973042	11.5	25.7	66.2	0.99999766	0.6	1.5
584.01	10.5	4.4	12.9	50.3	0.9906683	8.5	11.3	37.2	0.24644737	1.5	1.2
584.02	12.1	5.6	10.4	15.5	0.89182953	7.4	7.9	11.5	0.40152102	1.3	0.2
585.01	11.5	10.0	15.5	64.0	0.22034811	9.5	15.5	63.1	0.25919888	0.2	0.5
586.01	17.1	7.7	10.8	16.0	0.94408889	6.2	5.9	10.7	0.91825633	1.4	0.5
587.01	11.1	13.1	15.0	30.8	0.023986644	11.4	13.0	24.3	0.038092214	2.1	0.6
588.01	15.3	8.9	13.8	26.8	0.86978571	8.3	11.9	23.0	0.80040135	0.8	0.3
589.01	53.7	17.4	36.1	73.1	0.98577041	23.8	29.4	59.9	0.7615314	0.3	1.0
590.01	19.4	7.7	46.6	164.5	0.99092565	23.5	38.8	124.0	0.003307198	2.5	3.6
590.02	16.2	4.9	5.2	6.9	0.93520145	1.2	1.9	3.7	0.87590504	0.3	0.5
592.01	18.5	10.8	12.7	21.5	0.65779705	10.8	12.7	21.4	0.20488806	4.2	1.3
593.01	20.0	10.1	16.9	36.4	0.95702874	10.0	16.6	31.5	0.88776964	0.5	0.1
596.01	11.8	8.8	17.4	40.2	0.74489082	11.7	16.4	35.3	0.001108231	5.0	1.0
597.01	17.9	15.6	19.3	30.7	0.30998619	6.6	11.4	24.1	0.86695595	2.0	0.8
598.01	12.7	9.4	17.4	72.4	0.59246181	8.2	16.2	65.1	0.68191464	1.8	0.1
599.01	13.6	9.7	17.3	37.4	0.68763644	11.1	12.7	20.9	0.27301256	2.9	0.9
600.01	22.2	19.5	35.7	94.8	0.18718037	14.2	33.2	79.5	0.90743931	2.1	1.7
601.01	32.6	4.1	7.3	24.1	1	4.8	7.2	22.8	1	0.2	0.8
602.01	29.8	0.7	6.5	19.0	1	2.2	6.2	17.0	0.99999906	0.0	0.2
605.01	10.0	3.4	10.1	25.0	1	3.6	10.0	25.9	0.99999999	0.5	1.0
607.01	3.6	3.0	3.4	12.1	0.33647263	3.4	3.3	12.0	0.066900639	1.7	0.5
609.01	2.9	1.5	3.4	50.0	0.99395203	1.5	3.4	50.0	0.98835895	0.9	0.1
610.01	10.2	8.7	15.6	35.0	0.33544229	8.8	15.5	32.5	0.15007542	0.2	1.7
611.01	1.5	0.8	1.4	9.4	0.9996344	0.8	1.4	9.6	0.99701243	0.4	1.3
612.01	12.3	15.6	19.7	34.6	0.020056113	5.4	6.0	11.6	0.76969912	3.6	2.6
614.01	2.1	2.3	3.0	5.5	0.083895717	1.6	2.6	4.3	0.31184152	0.6	0.4

Table 4—Continued

KOI	σ_{TT} (min)	(E_L5,T2) MAD[a] (min)	WRMS[b] (min)	MAX[c] (min)	$p_{X'^2}$[d]	(E_L2,T2) MAD[a] (min)	WRMS[b] (min)	MAX[c] (min)	$p_{X'^2}$[d]	$\frac{\lvert\Delta\ P\rvert}{\sigma_P}$[e]	$\frac{\lvert\Delta\ E\rvert}{\sigma_E}$[f]
618.01	11.1	10.0	22.4	95.2	0.2252401	10.7	22.0	94.1	0.068953687	0.6	1.5
620.01	4.3	1.4	1.8	4.0	0.92593354	1.3	1.0	1.4	0.52056648	2.2	0.0
623.01	21.8	15.3	25.0	61.4	0.67759124	17.0	22.6	44.9	0.31943545	1.6	0.1
623.02	24.8	9.9	30.2	75.3	0.98023467	13.0	25.6	56.2	0.74952058	0.9	1.8
623.03	25.0	15.3	35.1	87.3	0.92350573	19.7	34.7	80.2	0.36287337	0.1	0.1
624.01	14.0	20.1	63.0	148.9	0.006638923	43.7	42.1	159.6	2.22E-16	6.3	3.5
626.01	15.7	14.6	19.9	38.6	0.23101732	19.0	19.1	33.8	0.008043793	0.1	0.8
627.01	12.3	8.2	11.0	22.6	0.75781035	7.4	8.3	13.0	0.7611121	2.1	1.4
628.01	12.4	7.3	10.3	17.5	0.81878895	5.9	9.9	14.3	0.83428191	0.5	0.9
629.01	29.0	6.6	5.5	6.6	0.97009622	1.9	2.1	3.8	0.88620247	2.6	0.2
632.01	16.7	10.1	22.0	48.6	0.90523627	10.0	19.1	43.8	0.82923143	3.0	0.2
635.01	13.0	10.7	15.4	33.2	0.38339267	12.5	14.8	29.7	0.067009608	0.3	0.9
638.01	6.3	2.5	2.5	3.4	0.91379578	2.9	2.3	3.6	0.50725464	0.5	0.8
639.01	13.1	15.5	19.6	39.8	0.050184169	14.5	13.9	21.2	0.022182295	1.9	1.1
640.01	5.5	4.3	4.5	6.5	0.40559975	0.6	0.8	1.1	0.80625758	4.8	1.1
641.01	7.6	5.8	7.4	23.4	0.49572327	6.7	6.8	26.5	0.14232301	0.9	2.5
645.01	20.2	18.2	34.5	82.9	0.21513746	23.5	31.0	60.9	0.003546801	1.9	0.9
645.02	26.4	16.1	24.3	36.6	0.70907193	13.2	23.4	34.3	0.58007334	0.1	0.4
647.01	21.5	16.8	25.8	60.7	0.51119146	17.7	24.6	60.1	0.26593347	2.0	0.3
649.01	18.3	6.9	13.4	25.2	0.9246362	11.2	10.0	13.8	0.30899041	0.5	0.2
650.01	5.8	5.5	5.1	10.8	0.17629864	2.3	4.1	9.0	0.92285347	2.0	2.0
652.01	2.3	1.5	1.2	1.9	0.64900002	0.7	0.6	1.2	0.78271623	1.3	1.1
654.01	20.5	12.7	25.8	57.4	0.8665769	8.9	17.3	36.0	0.98090188	3.5	1.1
655.01	8.0	8.3	8.3	11.6	0.16514122	3.2	3.3	4.7	0.38194961	14.6	2.6
657.01	13.0	9.0	15.0	70.6	0.82549229	10.8	14.8	66.1	0.23638065	0.7	0.5
657.02	9.8	4.4	5.8	24.2	0.94608424	4.0	5.4	24.5	0.87609861	0.0	2.1
658.01	21.5	6.6	10.3	30.5	1	6.6	10.1	31.2	1	2.2	4.6
658.02	12.0	5.5	14.2	43.8	0.99741558	7.7	14.0	42.6	0.78991349	0.3	0.6
659.01	12.9	9.3	9.1	11.0	0.54245699	4.0	4.9	9.7	0.85930531	0.7	0.6
660.01	22.4	19.4	27.1	70.0	0.26902157	20.5	26.7	67.9	0.093102328	0.5	0.1
661.01	16.7	6.9	24.5	70.9	0.97508982	11.7	22.9	61.9	0.40194787	0.5	1.3
662.01	24.9	13.9	22.7	63.2	0.91237762	20.6	20.6	44.0	0.22723412	6.1	5.3

Table 4—Continued

KOI	σ_{TT} (min)	(E_L5,T2) MAD[a] (min)	WRMS[b] (min)	MAX[c] (min)	$p_{X'^2}$[d]	(E_L2,T2) MAD[a] (min)	WRMS[b] (min)	MAX[c] (min)	$p_{X'^2}$[d]	$\frac{\lvert\Delta\ P\rvert}{\sigma_P}$[e]	$\frac{\lvert\Delta\ E\rvert}{\sigma_E}$[f]
663.01	7.9	5.8	8.4	31.8	0.72721528	5.2	8.4	32.8	0.89830242	0.1	0.4
663.02	8.0	12.9	12.2	16.6	0.000431686	4.9	6.7	11.9	0.47028322	4.6	5.5
664.01	18.1	17.4	36.5	59.2	0.18424586	24.8	28.9	51.9	0.000981038	2.9	1.3
665.01	10.2	5.6	9.9	28.4	0.97314145	5.7	9.6	28.2	0.92395857	1.2	1.1
665.02	49.8	26.3	53.0	200.8	0.99999211	31.3	52.0	185.8	0.99208769	2.8	1.2
665.03	78.6	23.0	79.8	300.0	1	28.3	78.9	299.5	0.9999999	1.1	1.6
666.01	7.4	6.3	6.4	9.9	0.33672547	2.4	2.0	3.9	0.72309618	1.8	1.7
667.01	5.2	3.7	4.5	7.1	0.7287436	3.8	4.4	7.2	0.51291028	0.1	1.1
670.01	19.8	16.9	22.8	92.0	0.31074877	13.2	22.2	93.2	0.61105058	1.0	0.6
671.01	24.5	14.0	20.2	49.8	0.98269336	11.6	17.8	44.2	0.99777883	1.9	0.7
672.01	8.5	2.0	6.2	16.1	0.99884468	3.8	5.5	11.7	0.82804446	0.2	0.8
672.02	5.5	4.0	3.0	4.1	0.48448944	0.2	0.2	0.2	0.93746604	2.5	0.1
673.01	20.5	13.8	16.0	40.7	0.85529171	11.1	15.6	38.6	0.97888233	0.8	0.0
674.01	5.0	4.6	4.1	5.9	0.25437459	1.7	2.5	4.7	0.82970521	1.4	0.2
676.01	2.6	2.8	3.4	11.2	0.022798997	2.0	3.0	12.1	0.38428424	1.0	0.4
676.02	3.7	3.5	6.2	114.2	0.040622585	2.1	5.8	115.8	0.99447957	0.4	2.1
679.01	19.9	15.9	21.2	32.3	0.38910658	14.3	18.1	23.2	0.11787075	9.7	5.0
680.01	1.7	1.2	1.8	13.1	0.76781541	1.3	1.7	14.5	0.37065604	1.3	0.5
684.01	8.8	8.7	13.0	42.8	0.02820332	6.6	12.7	40.7	0.54055055	1.6	0.1
685.01	19.7	7.3	19.6	69.6	0.99999982	8.2	19.4	65.4	0.99998498	0.8	0.8
688.01	17.8	13.9	21.5	47.6	0.53428649	16.1	20.1	44.0	0.077313835	0.9	2.1
689.01	9.1	8.1	9.8	15.4	0.28619433	5.7	5.4	8.4	0.28483127	1.5	0.9
691.01	12.3	4.5	11.8	20.1	0.88885309	11.2	11.1	16.1	0.048416866	1.6	0.8
691.02	50.2	47.9	66.1	107.7	0.17678718	46.1	63.1	94.8	0.10144564	0.5	0.9
692.01	27.2	13.8	19.6	71.9	0.99988619	16.4	19.5	68.7	0.98501923	0.6	0.1
693.01	24.1	5.7	10.5	20.0	0.98665767	11.3	9.4	14.2	0.49791979	0.2	1.0
693.02	20.0	25.2	85.1	340.6	0.010546127	68.2	76.8	266.5	0	4.6	1.1
694.01	9.7	4.8	13.7	33.3	0.88961536	12.6	11.2	20.8	0.00294363	2.5	1.7
695.01	8.1	2.3	4.8	7.8	0.94597424	2.1	2.9	4.1	0.57106083	4.0	1.1
697.01	11.4	11.8	18.2	41.1	0.010987102	14.0	17.8	37.2	1.44E-05	0.2	1.6
698.01	1.5	0.7	1.4	3.6	0.90512801	1.0	1.3	3.8	0.36446384	0.5	0.6
700.01	7.6	4.8	6.0	8.5	0.60659192	4.8	5.6	6.6	0.16830753	1.8	0.2

Table 4—Continued

KOI	σ_{TT} (min)	(E_L5,T2) MAD[a] (min)	WRMS[b] (min)	MAX[c] (min)	$p_{X'2}$[d]	(E_L2,T2) MAD[a] (min)	WRMS[b] (min)	MAX[c] (min)	$p_{X'2}$[d]	$\frac{\lvert\Delta P\rvert}{\sigma_P}$[e]	$\frac{\lvert\Delta E\rvert}{\sigma_E}$[f]
700.02	17.5	11.9	34.0	96.9	0.73965246	14.4	26.3	55.1	0.24173034	4.5	0.9
701.01	6.4	5.3	5.7	11.0	0.37444025	4.2	5.4	9.2	0.40058891	0.5	0.9
701.02	12.5	8.5	15.4	39.4	0.79684755	12.5	14.8	37.2	0.026872858	1.2	0.4
703.01	21.7	11.4	22.9	139.3	0.99999931	10.6	22.8	135.7	0.99999996	0.7	0.6
704.01	20.9	20.3	29.9	209.7	0.20572241	20.6	28.1	223.6	0.046453213	0.1	1.0
707.01	13.0	5.4	5.8	13.1	0.90082824	7.8	5.1	8.8	0.32229615	0.3	0.6
707.02	19.6	14.8	18.1	30.3	0.44418267	0.4	0.4	0.5	0.96452968	4.6	0.7
707.03	22.7	18.8	92.8	223.9	0.35992666	72.0	57.7	94.2	5.89E-12	31.1	1.5
707.04	27.5	24.8	22.5	47.4	0.24611997	11.5	20.3	52.1	0.90134562	0.8	0.5
708.01	12.5	6.7	9.8	19.2	0.85068356	6.3	8.7	17.5	0.66209513	0.8	0.4
708.02	20.5	16.4	25.3	54.9	0.44397051	21.8	20.2	35.3	0.015188132	2.2	2.3
709.01	11.7	15.6	28.3	44.1	0.015746422	22.8	26.0	31.8	1.54E-06	1.0	0.1
710.01	22.1	13.6	36.5	132.9	0.92562556	21.3	34.7	124.7	0.043118468	1.5	1.8
711.02	48.3	22.0	33.8	87.5	0.99988764	22.6	33.6	86.8	0.99936969	0.2	0.7
712.01	33.3	16.8	33.4	136.1	0.99997453	15.6	32.2	119.0	0.99999479	2.0	2.1
714.01	5.2	2.7	3.5	9.7	0.99611269	2.2	3.4	10.3	0.99969479	0.3	1.0
716.01	2.9	2.2	2.0	2.8	0.43565268	0.4	0.5	0.6	0.74734986	11.5	1.9
717.01	16.2	5.6	14.9	36.6	0.99320617	10.4	13.6	28.2	0.52473223	1.1	2.3
718.01	14.5	7.7	14.2	41.5	0.99177097	9.4	13.8	37.5	0.83343157	1.0	0.8
718.02	12.0	3.2	21.5	45.8	0.9904169	11.1	20.2	48.9	0.081577643	0.7	1.0
718.03	16.2	9.2	21.7	39.7	0.67557424	13.4	14.9	17.9	0.073052955	6.8	0.6
719.01	5.7	4.3	4.5	12.4	0.56498758	3.4	4.4	12.5	0.79108612	0.4	0.1
720.01	5.7	4.0	5.2	17.0	0.70636158	5.1	5.1	15.9	0.10706464	0.4	0.0
721.01	21.3	29.5	35.8	72.1	0.003450789	25.6	25.7	39.1	0.007142762	2.8	1.0
723.01	9.0	6.5	8.9	32.1	0.75626006	6.0	8.7	33.9	0.82221327	0.8	1.2
723.02	14.9	13.9	11.2	16.0	0.24873919	3.8	6.5	29.6	0.58290866	3.5	1.7
723.03	7.2	3.1	9.4	27.6	0.9891969	4.9	8.3	23.1	0.55999049	0.1	1.2
725.01	7.4	6.9	10.1	98.8	0.14646203	8.4	9.9	100.0	0.002936057	1.7	3.7
728.01	1.9	1.0	2.0	5.1	0.96644712	1.2	1.9	5.4	0.77484183	0.9	1.7
730.01	27.8	25.4	24.5	34.0	0.23166345	29.0	24.2	37.6	0.033331062	1.0	2.0
730.02	47.2	41.6	46.5	90.1	0.26147693	33.3	42.4	108.4	0.49825497	0.0	1.4
730.03	37.6	50.7	50.1	87.9	0.000395502	36.3	42.0	90.0	0.06112336	0.3	2.0

Table 4—Continued

KOI	σ_{TT} (min)	(E_L5,T2) MAD[a] (min)	WRMS[b] (min)	MAX[c] (min)	$p_{X'^2}$[d]	(E_L2,T2) MAD[a] (min)	WRMS[b] (min)	MAX[c] (min)	$p_{X'^2}$[d]	$\frac{\lvert\Delta\ P\rvert}{\sigma_P}$[e]	$\frac{\lvert\Delta\ E\rvert}{\sigma_E}$[f]
730.04	61.2	29.4	67.8	164.7	0.98743301	29.4	66.3	152.3	0.9638556	0.9	0.3
732.01	9.5	6.9	10.5	26.5	0.86683028	6.8	10.1	30.1	0.89346459	2.1	2.1
733.01	10.6	3.6	15.0	99.8	0.99995797	5.5	14.5	94.5	0.9657352	1.8	0.3
733.02	14.5	5.9	9.5	23.3	0.98943032	6.9	9.5	24.1	0.89827727	0.0	0.0
733.03	27.7	16.3	28.6	67.8	0.99035225	19.2	27.2	70.9	0.81017278	1.8	0.4
734.01	16.2	5.9	8.6	19.5	0.93462876	10.1	6.9	10.6	0.29190885	0.6	1.1
735.01	9.4	26.6	20.1	27.9	4.05E-10	11.5	16.5	33.7	0.00937252	2.7	0.7
736.01	14.2	7.1	6.8	12.1	0.88099968	6.3	6.0	11.0	0.76003091	1.1	2.5
736.02	24.1	10.8	31.1	71.7	0.99651661	19.1	29.8	61.7	0.32952173	0.3	0.9
737.01	6.5	4.2	3.9	5.3	0.70371149	1.7	2.2	4.6	0.95596439	1.3	1.0
738.01	14.2	9.6	10.9	20.6	0.7285779	8.9	8.8	17.3	0.65510302	2.4	2.9
738.02	18.7	12.3	26.3	55.1	0.73052401	11.8	25.2	54.7	0.59019257	0.3	1.2
739.01	13.0	10.6	18.4	47.4	0.3881949	9.8	17.9	50.9	0.73889948	2.0	2.8
740.01	21.0	13.3	17.8	39.3	0.7078978	11.8	17.4	37.0	0.56196379	0.2	1.3
741.01	0.9	0.3	0.4	0.6	0.86356459	0.1	0.1	0.2	0.79215343	10.5	0.9
743.01	5.1	10.2	17.4	102.9	8.79E-06	4.0	15.9	108.5	0.18371644	0.1	10.7
745.01	6.5	3.9	9.9	30.6	0.72597566	8.6	9.3	28.9	0.00370927	0.8	0.5
746.01	9.9	5.0	12.6	36.1	0.96355132	7.6	11.0	28.8	0.3468364	1.8	0.3
747.01	9.8	6.7	10.6	29.7	0.78315551	8.0	10.6	28.2	0.27636752	1.0	1.4
749.01	15.4	12.1	18.6	46.0	0.50867735	13.9	16.7	47.9	0.11706862	2.0	2.0
749.02	31.5	18.2	35.8	137.2	0.98138533	19.9	31.7	113.6	0.89108624	2.9	0.3
750.01	15.2	19.7	22.2	29.5	0.031465881	6.4	5.4	7.0	0.57678667	0.4	2.3
751.01	17.3	23.5	28.1	66.4	4.84E-05	22.2	27.1	69.4	0.000104399	1.8	0.9
752.01	20.9	13.3	21.7	46.0	0.82473595	15.3	18.3	38.3	0.45592354	2.7	0.5
753.01	3.8	1.5	16.6	84.7	0.95941041	6.8	15.3	70.3	6.22E-06	4.2	1.5
755.01	17.5	7.2	11.1	26.2	0.99999481	7.1	10.7	26.4	0.99998531	1.2	0.1
756.01	12.0	2.5	8.0	16.8	0.99956472	3.0	7.5	16.1	0.98321391	0.5	0.1
756.02	21.6	30.8	35.3	77.8	1.57E-06	30.3	34.6	73.3	9.95E-07	1.1	0.6
756.03	50.9	30.9	49.0	196.0	0.96975208	26.5	45.9	173.9	0.9944966	0.6	0.9
757.01	3.3	2.5	2.8	4.6	0.47192841	2.3	2.4	4.2	0.38287818	1.0	0.3
757.02	8.2	10.7	22.0	41.6	0.044764645	7.7	8.1	9.4	0.040264053	25.7	1.6
757.03	19.3	11.3	30.5	95.8	0.93950777	20.4	27.7	73.1	0.011362602	1.3	0.2

Table 4—Continued

KOI	σ_{TT} (min)	(E_L5,T2) MAD[a] (min)	WRMS[b] (min)	MAX[c] (min)	$p_{X'^2}$[d]	(E_L2,T2) MAD[a] (min)	WRMS[b] (min)	MAX[c] (min)	$p_{X'^2}$[d]	$\frac{\lvert\Delta\ P\rvert}{\sigma_P}$[e]	$\frac{\lvert\Delta\ E\rvert}{\sigma_E}$[f]
758.01	14.7	7.0	10.1	17.8	0.92921085	6.1	9.2	19.8	0.86115968	2.0	1.3
760.01	1.3	0.8	1.2	4.1	0.97127181	0.6	1.2	3.7	0.99608261	0.4	1.5
762.01	45.2	13.3	34.5	82.7	0.99999995	17.7	33.7	76.4	0.99989706	0.9	0.3
763.01	2.0	1.4	1.5	2.0	0.56952689	1.5	1.3	2.0	0.1547063	0.6	0.4
765.01	15.6	8.9	13.5	28.5	0.92746917	12.7	12.7	22.4	0.26520226	0.4	2.0
766.01	9.3	4.3	6.9	17.9	0.99786525	4.8	6.8	16.9	0.97879306	0.4	1.1
767.01	1.1	0.5	0.8	2.1	0.99995821	0.6	0.8	2.3	0.99687157	137.4	104.2
769.01	16.5	11.9	15.5	37.9	0.7265314	12.9	15.3	33.6	0.40624572	0.3	0.5
773.01	18.3	2.1	20.2	32.7	0.99577172	15.0	16.2	20.6	0.074187404	0.4	0.9
774.01	1.8	1.0	0.9	3.5	0.94897018	1.0	0.9	3.8	0.90683059	0.8	0.3
775.01	15.0	21.4	22.7	36.4	0.002066526	19.7	21.2	28.7	0.001867103	1.5	0.2
775.02	10.4	10.7	23.4	85.0	0.060192657	10.5	20.0	69.2	0.035142974	2.0	3.5
776.01	3.3	2.3	2.6	6.8	0.84946257	2.1	2.6	6.0	0.87855676	0.7	1.7
778.01	10.6	8.1	13.2	29.6	0.63551978	9.1	12.8	32.8	0.15812187	0.8	1.7
779.01	1.7	0.8	1.4	2.5	0.9443865	1.3	1.2	2.3	0.25034684	0.6	0.4
780.01	12.4	8.7	21.0	52.3	0.88419141	10.1	20.5	50.6	0.31987738	1.8	0.8
781.01	8.2	3.6	7.1	17.9	0.97547288	5.7	5.3	11.8	0.45094451	2.0	1.6
782.01	5.7	3.3	4.7	13.1	0.9449617	3.7	4.4	9.6	0.75402124	0.5	2.5
783.01	5.4	4.2	4.8	10.4	0.49614465	4.6	4.5	7.8	0.19865289	0.9	0.3
784.01	15.1	10.0	10.2	13.4	0.59368429	6.8	6.9	11.4	0.53113323	1.3	2.6
785.01	20.3	14.1	18.7	44.3	0.64129141	14.3	12.3	26.3	0.39268499	1.8	1.4
786.01	20.0	18.1	32.6	71.5	0.12654554	23.4	31.9	64.2	6.68E-05	2.0	0.2
787.01	17.5	9.8	13.2	23.0	0.98442658	11.9	12.5	26.5	0.75353018	2.0	1.0
787.02	24.0	18.0	31.4	94.5	0.61465712	18.7	28.3	90.4	0.38209942	2.3	1.0
788.01	9.9	5.9	5.5	7.0	0.69382383	4.5	4.5	5.8	0.52620281	1.0	1.0
790.01	19.2	11.5	14.3	32.4	0.86797079	10.7	13.6	26.1	0.82577381	1.1	0.4
791.01	3.4	1.3	3.7	34.3	0.98852926	1.8	3.6	33.5	0.73859464	0.9	0.2
794.01	30.2	21.9	35.9	82.3	0.78880299	19.6	35.8	80.6	0.93882363	0.8	0.4
795.01	11.0	6.6	12.5	24.0	0.9156746	5.1	11.9	27.4	0.9842977	0.3	1.5
797.01	3.8	3.9	4.8	8.6	0.10268556	3.6	4.5	8.5	0.071226725	1.6	0.3
799.01	9.7	7.1	13.8	69.5	0.85196716	6.9	13.8	69.2	0.88982764	0.7	0.5
800.01	19.7	11.7	22.5	52.7	0.99260018	11.9	22.1	46.1	0.98038661	0.6	1.8

Table 4—Continued

KOI	σ_{TT} (min)	(E_L5,T2) MAD[a] (min)	WRMS[b] (min)	MAX[c] (min)	$p_{X'^2}$[d]	(E_L2,T2) MAD[a] (min)	WRMS[b] (min)	MAX[c] (min)	$p_{X'^2}$[d]	$\frac{\lvert\Delta\ P\rvert}{\sigma_P}$[e]	$\frac{\lvert\Delta\ E\rvert}{\sigma_E}$[f]
800.02	23.7	10.6	47.7	183.6	0.99285361	17.5	46.1	170.2	0.45153898	2.6	5.0
801.01	1.9	1.3	1.9	13.8	0.97321865	1.3	1.9	13.9	0.92776199	0.3	0.3
802.01	1.1	0.8	0.8	1.4	0.53658852	0.7	0.7	1.1	0.28294623	1.2	1.0
804.01	16.4	6.8	10.0	23.1	0.99346819	4.4	9.4	19.7	0.99930454	0.2	1.9
805.01	2.6	0.3	1.7	4.2	0.99999979	0.5	1.7	4.2	0.99911779	0.3	0.3
806.03	25.6	35.4	28.0	52.5	0.017351992	8.0	9.6	20.9	0.73353516	3.4	1.3
809.01	1.2	0.6	1.2	2.9	0.99999425	0.8	1.1	3.0	0.97879622	2.0	0.0
810.01	13.2	9.1	14.9	28.7	0.81399704	9.2	14.4	34.2	0.69868204	1.9	0.1
811.01	8.2	3.8	7.5	12.3	0.896375	7.1	7.2	11.7	0.1203836	0.4	1.2
812.01	11.6	7.6	11.4	28.6	0.93093597	8.2	10.9	30.1	0.74320217	0.9	0.5
812.02	15.5	14.6	30.9	59.2	0.22815322	11.4	19.6	38.1	0.23884434	3.1	1.3
813.01	2.2	1.3	2.3	5.2	0.97088948	1.2	2.3	5.4	0.99294816	0.1	0.5
814.01	21.2	16.8	15.9	20.9	0.41237735	12.8	12.9	24.3	0.31380808	0.8	0.2
815.01	3.9	3.2	3.4	4.1	0.37591529	1.2	1.0	1.2	0.52197557	5.2	0.4
816.01	7.0	5.6	9.2	19.2	0.42632742	4.5	4.7	8.7	0.58206989	3.5	0.4
817.01	17.9	17.2	17.4	35.3	0.21658262	17.7	15.9	27.2	0.047082194	0.1	1.1
818.01	12.1	6.7	22.0	87.4	0.94575556	10.6	18.4	66.2	0.15475427	4.1	0.3
821.01	18.1	22.2	19.7	26.8	0.050703808	18.6	15.6	18.9	0.035593182	1.4	1.0
822.01	2.1	1.6	2.8	6.9	0.53811185	1.4	2.7	6.4	0.5594307	1.9	3.4
823.01	10.7	2.4	8.2	106.2	1	1.9	7.9	101.6	1	1.3	3.0
824.01	2.6	1.9	1.4	2.5	0.56079932	2.0	1.4	2.3	0.26762106	0.2	0.0
825.01	19.8	5.2	14.4	26.6	0.99997121	9.0	12.3	24.8	0.9641028	1.2	0.0
826.01	14.3	7.3	11.3	25.3	0.98827223	7.4	11.2	26.7	0.9684589	1.1	0.5
827.01	17.5	7.9	13.1	29.8	0.99763534	8.0	12.9	28.3	0.99178864	0.2	1.5
829.01	13.1	8.0	9.2	15.4	0.70816511	2.2	2.8	4.9	0.97290141	1.5	0.1
829.02	31.2	17.5	28.9	53.3	0.92028795	17.6	27.0	59.8	0.81791683	1.0	0.3
829.03	17.8	11.9	23.4	60.9	0.55094452	8.2	5.9	10.3	0.31853048	21.5	2.4
830.01	0.7	0.4	0.5	1.0	0.95214925	0.4	0.4	1.1	0.91514348	0.6	0.3
833.01	5.7	5.0	6.3	21.7	0.20264687	5.3	6.1	19.0	0.047852858	0.8	1.8
834.01	4.2	3.7	5.6	9.3	0.30438516	3.2	3.3	5.4	0.16628808	2.8	2.1
834.02	27.2	24.6	33.1	61.7	0.24789266	17.7	32.5	67.8	0.49936573	0.1	0.5
834.03	40.9	22.3	49.0	89.3	0.97891677	31.3	32.8	53.1	0.43296361	4.2	0.0

Table 4—Continued

KOI	σ_{TT} (min)	(E_L5,T2) MAD[a] (min)	WRMS[b] (min)	MAX[c] (min)	$p_{X'^2}$[d]	(E_L2,T2) MAD[a] (min)	WRMS[b] (min)	MAX[c] (min)	$p_{X'^2}$[d]	$\frac{\lvert\Delta P\rvert}{\sigma_P}$[e]	$\frac{\lvert\Delta E\rvert}{\sigma_E}$[f]
834.04	36.8	37.8	60.8	218.7	0.001481828	32.0	59.9	223.3	0.11786888	2.3	0.9
835.01	13.5	5.6	9.7	24.1	0.98249433	4.8	8.7	21.3	0.97066256	0.5	1.1
837.01	14.9	8.9	11.2	20.6	0.87471589	9.4	9.2	15.6	0.68125823	1.7	0.1
837.02	29.0	18.1	26.9	101.2	0.94496753	19.5	26.9	103.5	0.79512926	0.0	0.4
838.01	3.3	2.1	3.7	41.0	0.86709451	1.8	3.6	40.0	0.94742189	0.4	2.3
840.01	1.6	0.9	1.4	3.7	0.99311392	0.9	1.4	3.7	0.98775378	0.1	0.1
841.01	6.9	5.4	5.5	12.1	0.46017737	1.9	4.1	10.1	0.97276599	2.5	1.7
841.02	6.8	3.0	5.2	9.4	0.87702918	4.5	4.6	6.6	0.25179264	2.4	2.2
842.01	11.8	5.2	28.3	123.1	0.9738289	13.9	26.5	106.5	0.006747627	3.1	1.3
843.01	4.3	3.6	5.8	25.0	0.35676436	4.4	5.7	23.9	0.008037314	0.0	0.4
844.01	9.4	7.0	13.8	31.7	0.67524016	10.1	12.5	27.8	0.001731806	2.9	1.2
845.01	13.6	13.2	20.1	32.0	0.17602103	10.7	16.1	32.1	0.21064596	2.0	0.9
846.01	1.0	1.1	0.9	1.1	0.14548225	0.6	0.7	1.1	0.22902481	8.6	1.0
849.01	14.0	9.9	15.7	42.4	0.6481183	6.4	12.1	32.7	0.93168517	2.3	0.9
850.01	1.5	1.3	1.6	3.1	0.27325131	1.5	1.3	2.2	0.030547178	2.2	3.2
851.01	4.4	2.2	4.7	16.3	0.99769797	2.1	4.5	15.0	0.99712876	0.9	0.4
852.01	27.8	10.4	33.8	120.4	0.99999787	14.0	31.9	103.3	0.99634949	2.1	0.3
853.01	11.4	10.2	16.4	47.3	0.22643731	10.9	16.3	45.8	0.064849299	1.0	0.8
853.02	20.7	25.3	28.4	46.2	0.021565909	18.8	18.7	36.6	0.10484616	2.4	0.8
856.01	1.7	1.2	1.5	2.3	0.5180426	0.1	0.1	0.1	0.93374764	7.1	3.9
857.01	11.8	9.8	14.9	38.6	0.35392696	8.1	14.5	42.1	0.665613	0.1	0.8
858.01	3.0	2.4	2.2	9.5	0.45617672	2.4	2.1	9.3	0.21241668	0.4	0.5
861.01	28.9	15.4	25.5	114.9	0.99976382	20.9	24.2	114.3	0.74320075	1.3	2.0
863.01	14.8	7.8	19.1	49.1	0.99874082	10.9	17.4	44.3	0.63620462	2.6	0.7
864.01	13.4	6.8	16.1	31.6	0.98996915	9.7	15.0	29.6	0.54341325	1.3	1.8
864.02	23.3	13.1	21.1	41.1	0.73844404	15.9	20.1	35.9	0.23114582	0.3	0.8
864.03	20.0	13.9	18.2	27.9	0.64023548	16.6	17.3	29.9	0.19051429	1.1	1.1
867.01	7.3	11.2	12.2	17.2	0.000492991	9.6	9.2	14.4	0.001972779	2.0	2.8
869.01	17.7	8.4	14.9	31.2	0.98658117	11.8	13.9	24.5	0.6353122	1.1	0.6
870.01	21.8	11.0	14.5	39.4	0.98793459	3.6	10.1	32.3	0.99999999	1.6	0.1
870.02	18.2	16.0	19.8	31.3	0.26664385	9.5	14.2	29.5	0.87895246	2.3	1.0
871.01	1.5	0.3	0.4	1.7	0.99978449	0.4	0.3	1.7	0.97064687	0.1	0.0

Table 4—Continued

KOI	σ_{TT} (min)	(E_L5,T2) MAD[a] (min)	WRMS[b] (min)	MAX[c] (min)	$p_{X'^2}$[d]	(E_L2,T2) MAD[a] (min)	WRMS[b] (min)	MAX[c] (min)	$p_{X'^2}$[d]	$\frac{\lvert\Delta\ P\rvert}{\sigma_P}$[e]	$\frac{\lvert\Delta\ E\rvert}{\sigma_E}$[f]
872.01	2.3	19.1	23.9	35.7	0	7.3	9.4	14.7	1.78E-12	49.8	0.4
873.01	21.1	15.1	25.9	47.8	0.75507656	17.9	23.7	48.7	0.20252003	0.1	3.1
874.01	13.9	10.3	11.9	30.1	0.66935551	8.9	11.6	33.3	0.85593832	0.4	0.2
875.01	6.8	4.6	6.7	20.8	0.84949437	4.9	6.7	21.0	0.62329222	0.1	0.3
876.01	2.5	1.3	1.4	7.3	0.98858437	1.1	1.3	6.7	0.99391229	0.4	0.2
877.01	11.7	6.8	11.7	30.6	0.94759706	4.4	11.5	28.2	0.99887603	1.0	0.4
877.02	11.1	5.3	8.6	17.7	0.95551745	9.0	7.5	17.4	0.23544618	1.6	0.4
878.01	16.6	23.7	31.1	47.6	0.012379551	26.4	22.3	26.9	0.000367726	4.3	0.8
880.01	6.3	9.7	10.6	17.1	0.011829054	0.4	0.4	0.4	0.87922104	14.2	0.1
880.03	13.7	6.3	17.8	61.8	0.99685817	7.2	17.0	60.3	0.96364035	1.8	0.2
880.04	29.4	21.3	34.6	118.5	0.79728118	21.7	34.0	108.1	0.67520979	1.3	0.2
881.01	12.8	6.9	8.3	11.3	0.7678982	7.6	6.2	10.4	0.33087702	0.2	1.7
882.01	5.0	1.1	2.6	6.5	1	1.3	2.1	7.4	1	1.9	1.4
883.01	2.2	0.8	0.8	2.3	1	0.7	0.8	2.5	1	0.0	0.4
884.01	5.0	1.6	3.2	7.3	0.99911293	2.5	2.9	5.8	0.89613426	0.8	0.1
884.02	4.8	22.7	41.1	58.8	0	4.8	7.2	10.9	0.049741965	13.3	4.7
884.03	24.2	16.5	29.5	70.2	0.87374257	16.5	28.8	76.4	0.81593169	0.4	0.3
886.01	15.1	8.9	10.6	20.8	0.90693115	9.0	10.6	20.6	0.79199617	1.4	2.1
887.01	14.3	8.3	15.7	35.2	0.9187923	8.7	15.4	30.0	0.77837458	0.9	0.4
889.01	1.8	1.4	1.4	3.3	0.43198718	0.9	1.1	3.0	0.90521018	2.5	1.3
890.01	3.1	2.4	2.7	4.8	0.54533248	2.3	2.6	4.5	0.48151228	0.8	0.5
891.01	19.4	15.5	22.0	60.2	0.44769772	17.0	22.0	58.7	0.1548479	0.8	1.4
892.01	10.2	5.6	6.8	20.9	0.90509742	6.9	6.5	17.0	0.50944463	0.5	0.6
893.01	29.2	17.7	23.2	53.9	0.92967159	16.8	23.0	50.3	0.91906908	0.3	0.0
895.01	12.3	2.4	2.4	7.9	1	2.2	2.3	7.7	1	0.4	0.3
896.01	5.9	3.4	4.2	7.1	0.81179879	2.2	4.1	6.8	0.90359359	0.5	0.1
896.02	9.4	6.5	8.4	14.1	0.76152301	7.7	8.1	14.6	0.27424225	1.3	0.1
897.01	1.1	0.5	0.9	2.3	0.99999992	0.6	0.9	2.2	0.99937124	0.8	1.9
898.01	12.0	10.5	14.8	28.1	0.27431856	7.4	13.1	32.9	0.6848606	1.7	0.2
898.02	20.3	14.3	18.8	46.5	0.74967752	13.9	18.4	53.2	0.69776255	1.2	0.1
898.03	17.7	13.6	17.1	24.7	0.45927837	4.5	6.0	10.2	0.91893005	2.0	0.6
899.01	11.7	10.3	12.7	24.7	0.2549669	9.2	12.7	24.4	0.34136087	1.2	1.0

Table 4—Continued

KOI	σ_{TT} (min)	(E_L5,T2) MAD[a] (min)	WRMS[b] (min)	MAX[c] (min)	$p_{X'^2}$[d]	(E_L2,T2) MAD[a] (min)	WRMS[b] (min)	MAX[c] (min)	$p_{X'^2}$[d]	$\frac{\lvert\Delta\ P\rvert}{\sigma_P}$[e]	$\frac{\lvert\Delta\ E\rvert}{\sigma_E}$[f]
899.02	20.5	11.5	24.0	69.4	0.99565577	11.1	23.3	71.4	0.99535708	1.4	1.5
899.03	13.8	8.1	12.0	27.4	0.82571133	7.1	11.3	26.2	0.76724218	0.7	0.0
900.01	14.8	9.5	16.3	34.0	0.7374602	9.0	10.7	18.0	0.58949351	2.0	2.0
901.01	2.7	0.8	1.3	2.0	0.99857737	1.2	1.2	2.4	0.90710262	0.4	0.2
903.01	3.5	1.0	4.7	59.2	0.99999983	1.0	4.7	59.2	0.99999841	0.6	1.3
904.01	26.8	10.6	32.3	108.0	1	16.3	30.7	97.3	0.98942186	1.9	0.6
904.02	12.2	8.3	7.6	10.6	0.52990904	4.4	6.5	10.8	0.42980441	6.7	0.4
905.01	5.9	7.4	10.7	21.8	0.000400577	7.4	10.1	18.1	0.000112966	0.7	0.1
906.01	17.3	10.0	16.4	31.4	0.92874402	13.1	15.7	28.6	0.41384523	1.2	1.4
907.01	16.6	10.7	9.9	16.4	0.6858282	8.6	8.4	12.9	0.6450321	0.4	0.7
907.02	18.6	12.0	12.2	16.1	0.57954212	3.9	4.1	5.0	0.64544978	6.7	1.4
907.03	41.3	22.6	44.4	146.5	0.98848131	30.9	39.7	158.5	0.52482871	2.0	0.7
908.01	1.8	0.4	1.0	5.3	1	0.4	1.0	5.4	1	0.4	0.4
910.01	10.7	8.5	12.1	23.9	0.47811705	9.6	12.1	23.9	0.11674001	0.1	0.7
911.01	21.9	12.9	18.7	46.4	0.97646337	13.9	18.5	43.4	0.88133612	0.5	1.0
912.01	9.2	2.4	4.1	6.9	0.99946983	2.7	3.7	6.8	0.99082273	0.4	0.0
913.01	0.8	0.5	0.8	5.4	0.98204904	0.6	0.8	5.6	0.82566461	0.1	1.7
914.01	34.0	10.8	38.9	218.8	0.99999997	17.4	35.3	191.5	0.99530463	2.6	1.4
916.01	6.7	7.1	10.0	35.9	0.004529219	5.1	9.7	32.2	0.54719264	2.8	1.2
917.01	13.1	8.1	15.9	32.2	0.89468388	11.4	14.7	33.0	0.16434534	1.8	1.4
920.01	14.0	12.6	16.1	24.9	0.28188209	6.2	7.1	9.7	0.53662737	0.2	3.5
921.01	13.8	11.6	16.6	37.0	0.33603873	7.0	13.8	44.7	0.87538691	1.5	1.0
921.02	10.3	7.7	13.3	19.8	0.48886753	8.1	13.3	20.2	0.1776538	0.1	0.0
921.03	29.2	22.9	27.7	58.7	0.52268978	20.8	27.6	59.6	0.70181315	0.3	0.6
922.01	20.0	7.4	32.1	107.1	0.99994421	10.3	31.8	103.2	0.97667044	0.1	1.2
923.01	15.0	5.3	9.7	39.3	0.99995868	5.2	9.4	35.5	0.99986447	0.5	1.8
924.01	14.9	15.7	15.9	17.2	0.15619294	17.1	14.8	21.6	0.013134228	2.2	2.3
926.01	12.7	9.3	17.5	50.0	0.6866659	11.0	17.2	46.9	0.16646444	0.1	1.0
928.01	15.3	20.8	31.6	79.8	2.66E-10	15.1	24.8	59.7	0.00810768	7.7	2.1
929.01	2.7	3.0	2.6	4.7	0.023308282	2.8	2.5	5.2	0.03071683	0.2	0.3
931.01	1.3	1.1	1.1	4.0	0.4626938	1.0	1.1	3.9	0.50301808	0.0	1.1
934.01	11.2	6.3	12.6	37.3	0.96261984	9.7	12.3	35.7	0.16382857	1.0	0.1

Table 4—Continued

KOI	σ_{TT} (min)	(E_L5,T2) MAD[a] (min)	WRMS[b] (min)	MAX[c] (min)	$p_{X'^2}$[d]	(E_L2,T2) MAD[a] (min)	WRMS[b] (min)	MAX[c] (min)	$p_{X'^2}$[d]	$\frac{\lvert\Delta\ P\rvert}{\sigma_P}$[e]	$\frac{\lvert\Delta\ E\rvert}{\sigma_E}$[f]
934.02	36.4	9.7	14.2	32.7	0.99941878	5.6	12.7	22.9	0.99985851	0.6	0.1
934.03	22.5	10.5	39.6	82.9	0.88928853	21.9	37.1	70.4	0.060086392	0.3	1.2
935.01	6.4	4.0	4.6	7.3	0.70140527	4.0	4.0	6.2	0.38894739	0.4	0.9
935.02	8.5	2.4	3.1	9.4	0.94525561	0.8	2.1	7.7	0.83685256	1.3	0.3
936.01	6.1	2.3	3.7	11.0	0.99650326	3.0	2.9	7.1	0.90276486	1.6	1.7
936.02	14.5	8.1	14.0	67.5	0.99999983	7.7	13.7	66.2	0.99999998	2.0	0.8
937.01	15.0	7.5	12.3	29.7	0.84981867	5.0	8.5	20.6	0.83059263	0.9	0.3
938.01	16.6	10.5	24.4	74.7	0.81254383	9.2	20.4	59.2	0.81106413	1.4	0.9
938.02	55.5	25.8	41.6	215.9	0.99996979	27.9	37.6	248.6	0.99940011	1.8	1.1
939.01	30.8	23.3	31.1	85.1	0.63760088	20.3	28.7	71.9	0.87350937	1.4	1.0
940.01	4.3	2.7	30.0	221.8	0.86454075	5.5	29.6	216.1	8.10E-05	1.9	4.6
941.01	6.1	2.4	4.2	8.1	0.99919409	1.3	4.1	7.9	0.99999833	0.1	0.2
941.02	17.9	10.0	19.2	62.9	0.99890792	9.1	18.1	53.2	0.99981743	2.3	0.3
941.03	5.9	8.4	6.2	12.4	0.012242093	5.4	4.7	11.2	0.075407927	0.1	0.3
942.01	10.7	8.3	17.8	56.2	0.47890711	10.5	13.6	34.0	0.053184752	3.6	0.9
943.01	15.5	11.8	19.7	40.7	0.59436884	12.8	18.8	37.9	0.27278827	2.3	1.6
944.01	6.2	5.2	6.6	15.0	0.29746397	4.7	6.5	15.1	0.5709972	0.6	0.0
945.01	29.7	19.3	21.1	40.0	0.61985651	23.3	20.3	30.3	0.14528133	0.7	0.4
945.02	20.4	4.5	21.6	33.6	0.97203183	5.5	8.9	15.7	0.56108234	7.6	1.0
947.01	7.5	5.4	4.8	8.1	0.52323328	5.9	4.7	8.1	0.14126285	0.3	3.3
949.01	12.5	8.4	8.9	16.8	0.6737156	6.5	6.4	10.6	0.74942419	0.7	0.6
951.01	5.0	2.1	4.1	7.0	0.98095214	2.4	4.0	7.7	0.85695829	0.8	1.2
952.01	11.0	5.9	12.2	26.1	0.97283853	8.2	10.5	20.8	0.45982427	1.7	0.2
952.02	12.5	12.2	17.2	31.4	0.10971322	12.4	14.2	26.1	0.045988832	1.8	1.1
952.03	11.2	12.8	22.7	61.6	0.066427078	7.2	16.6	44.5	0.35738618	3.1	0.9
952.04	37.9	25.1	43.7	196.9	0.93220755	25.8	43.3	200.8	0.85216154	1.1	0.5
953.01	5.9	3.6	6.1	20.1	0.95086863	3.4	6.0	20.6	0.95098951	0.1	0.7
954.01	14.5	9.5	26.0	79.6	0.78116457	10.6	20.6	51.5	0.43108222	4.4	0.4
954.02	14.7	2.6	5.8	9.1	0.98631622	1.2	1.4	2.0	0.86368129	3.0	0.9
955.01	20.0	9.2	19.4	51.6	0.99246425	10.3	17.8	45.9	0.93588537	1.1	1.0
956.01	6.5	3.4	5.5	10.4	0.95822764	3.2	5.4	11.5	0.93240384	0.2	1.3
960.01	0.7	0.6	0.8	1.3	0.37674328	0.5	0.6	1.6	0.32588536	2.5	0.1

Table 4—Continued

KOI	σ_{TT} (min)	(E_L5,T2) MAD[a] (min)	WRMS[b] (min)	MAX[c] (min)	$p_{X'^2}$[d]	(E_L2,T2) MAD[a] (min)	WRMS[b] (min)	MAX[c] (min)	$p_{X'^2}$[d]	$\frac{\lvert\Delta\ P\rvert}{\sigma_P}$[e]	$\frac{\lvert\Delta\ E\rvert}{\sigma_E}$[f]
961.01	7.9	4.0	8.8	40.8	0.99999999	4.1	8.7	41.8	0.99999976	6.9	12.7
972.01	2.6	4.1	3.3	4.7	0.000469826	2.3	2.7	5.2	0.10081544	1.4	2.2
975.01	19.8	9.1	21.0	108.6	0.99998368	9.4	20.8	111.9	0.99989883	0.5	0.3
977.01	41.6	151.4	2,067.1	3,096.0	0	366.8	387.3	957.9	0	222.2	121.1
981.01	103.8	54.5	92.5	232.2	0.9965663	50.7	77.8	276.4	0.99752774	2.4	8.1
984.01	291.0	1,026.8	1,460.0	21,420.5	0	1,053.0	837.9	3,072.4	0	251.3	184.8
986.01	18.6	11.0	14.8	31.3	0.90617149	7.8	13.1	26.9	0.98533582	1.4	0.5
987.01	21.8	8.4	13.0	54.6	0.99999948	8.4	12.2	54.3	0.99999817	0.0	0.2
988.01	21.8	15.0	22.5	63.1	0.71160084	22.9	21.6	62.7	0.022471457	0.8	0.7
991.01	14.5	5.5	7.4	16.3	0.99412848	5.0	7.4	17.1	0.98435225	0.1	0.0
992.01	45.1	18.3	69.9	164.0	0.99480954	19.7	69.0	160.3	0.96413767	0.6	0.6
993.01	23.1	5.0	7.5	14.2	0.99610865	3.3	7.0	13.5	0.98399636	0.3	0.5
999.01	20.9	17.9	19.7	46.7	0.32606594	7.4	10.0	28.0	0.9281686	2.8	1.9
1001.01	52.1	56.7	222.4	569.9	0.072391402	129.8	179.1	395.0	2.45E-13	4.3	4.1
1002.01	17.3	17.1	28.9	62.7	0.023430107	17.6	28.7	65.4	0.006461492	0.2	0.5
1003.01	8.3	2.8	178.6	973.6	0.99771024	46.0	166.9	853.7	0	21.0	16.4
1013.01	13.4	7.0	12.7	74.3	1	7.0	12.7	74.9	1	0.2	2.2
1014.01	14.3	2.8	5.3	13.9	0.99966073	3.6	5.1	13.1	0.9821248	0.3	0.1
1015.01	15.7	5.9	11.5	18.6	0.87877807	1.2	1.7	2.6	0.86879269	35.0	0.0
1015.02	36.7	17.8	43.5	87.4	0.93670349	25.0	41.7	108.6	0.44045963	0.9	0.6
1017.01	18.1	8.9	13.4	23.0	0.91523524	9.4	12.2	19.2	0.70422167	0.2	0.6
1019.01	41.1	45.3	80.5	215.4	0.000175146	45.8	77.9	202.1	4.64E-05	1.8	1.6
1022.01	32.5	20.2	18.9	35.8	0.65607089	17.6	17.7	34.3	0.39804116	0.3	1.3
1024.01	12.8	7.4	14.1	51.7	0.9563353	8.8	12.8	49.7	0.66141307	2.1	0.8
1030.01	28.5	34.0	42.5	119.1	0.010152508	30.3	41.7	119.6	0.020439739	0.5	1.1
1031.01	67.8	8.0	78.0	253.7	0.99999774	31.9	73.6	211.2	0.83557534	1.0	0.3
1050.01	13.4	10.9	17.3	60.6	0.38977527	10.5	17.3	60.2	0.49837828	0.5	0.3
1051.01	24.1	11.8	28.0	84.6	0.98968273	12.8	27.2	78.1	0.9410789	0.9	0.0
1052.01	25.0	11.4	26.3	70.4	0.94362972	14.0	26.1	67.9	0.63424054	0.1	0.3
1053.01	31.0	20.4	40.8	213.2	0.99209744	21.7	40.7	210.9	0.9388723	0.0	0.1
1054.01	34.0	70.6	116.7	310.7	0	52.4	112.9	290.1	7.70E-14	5.6	0.2
1059.01	17.6	17.6	27.9	75.1	7.11E-05	20.0	27.4	82.4	2.08E-10	2.2	0.7

Table 4—Continued

KOI	σ_{TT} (min)	(E_L5,T2) MAD[a] (min)	WRMS[b] (min)	MAX[c] (min)	$p_{X'^2}$[d]	(E_L2,T2) MAD[a] (min)	WRMS[b] (min)	MAX[c] (min)	$p_{X'^2}$[d]	$\frac{\lvert\Delta P\rvert}{\sigma_P}$[e]	$\frac{\lvert\Delta E\rvert}{\sigma_E}$[f]
1060.01	32.8	11.3	23.9	56.4	0.99718189	13.7	21.7	48.8	0.94924986	1.0	0.1
1060.02	64.8	33.2	65.7	148.5	0.99575624	23.9	53.2	197.9	0.99994638	2.2	1.7
1061.01	22.5	9.4	21.8	35.9	0.84583519	7.0	9.0	12.1	0.49919026	7.8	0.1
1072.01	26.8	2.9	8.8	18.8	0.99656873	5.1	7.1	13.7	0.67857763	2.0	0.4
1078.01	12.7	11.4	22.3	103.7	0.1426801	9.5	20.5	86.0	0.56809706	3.3	1.8
1081.01	27.7	24.7	29.1	45.7	0.23648349	21.8	23.5	48.2	0.31674943	0.7	2.4
1082.01	30.3	24.2	49.1	126.6	0.45731276	17.9	47.0	110.4	0.87633869	2.1	0.1
1083.01	31.8	31.7	57.2	153.9	0.076188945	30.9	52.2	115.9	0.051879022	2.0	1.6
1085.01	41.1	16.7	45.7	129.4	0.99865253	19.1	45.0	123.5	0.97928412	0.5	0.4
1086.01	22.3	8.1	13.1	23.6	0.95966173	8.2	12.7	21.5	0.78415897	1.0	1.0
1089.02	7.2	5.4	6.0	10.3	0.56254226	4.6	5.4	10.1	0.61369922	1.4	3.6
1094.01	38.2	11.9	23.8	57.9	0.99999528	10.5	23.1	61.2	0.9999953	0.7	1.1
1101.01	64.9	27.6	49.2	176.7	0.99999827	21.4	48.6	186.0	1	0.7	0.4
1102.01	23.2	25.1	25.7	38.4	0.048355313	24.6	23.9	41.0	0.023701609	1.5	0.8
1102.02	276.2	25.2	51.1	106.3	1	26.3	39.5	76.2	1	0.1	1.0
1106.01	152.1	43.2	50.0	92.4	0.97284525	55.5	46.5	62.7	0.65769158	0.3	0.1
1108.01	23.5	17.8	38.4	90.3	0.54584529	23.1	33.8	70.2	0.053392324	0.6	1.9
1109.01	80.3	45.9	136.5	359.1	0.94779566	84.9	105.3	239.5	0.01234075	2.4	3.3
1110.01	35.9	36.3	48.8	100.4	0.069679642	40.1	47.8	90.7	0.006608499	0.9	1.7
1111.01	36.7	37.1	76.3	198.5	0.091546194	64.5	72.3	158.8	2.47E-08	1.6	0.7
1112.01	27.9	45.7	40.1	53.8	0.00553938	0.8	0.9	1.1	0.9500977	15.3	0.3
1113.01	28.0	6.6	18.9	25.0	0.99442486	9.4	10.1	23.2	0.8294393	1.2	0.1
1114.01	24.6	22.9	28.8	81.6	0.15197341	26.4	28.6	78.2	0.011764248	0.1	0.5
1115.01	37.2	14.9	39.8	103.8	0.99071283	23.2	36.1	79.1	0.63405046	1.4	0.1
1116.01	19.4	9.2	24.6	83.1	0.9996574	10.5	22.9	92.5	0.98946239	0.2	1.3
1117.01	29.4	8.9	18.9	49.2	0.99909185	12.3	15.1	28.6	0.9490812	1.1	0.4
1118.01	26.1	12.2	18.4	44.4	0.99050138	11.9	16.4	37.9	0.97759697	1.1	1.1
1128.01	12.0	12.2	20.4	70.5	0.001411978	12.7	20.3	73.4	0.000121867	1.1	1.3
1129.01	21.9	15.5	27.0	61.6	0.75324019	14.5	26.6	57.7	0.78242908	0.6	0.0
1141.01	31.6	36.3	50.6	93.3	0.002225982	32.1	49.5	102.6	0.016967135	1.6	0.0
1144.01	39.9	23.4	62.4	203.8	0.99610441	26.1	57.8	170.0	0.93618545	3.7	0.4
1145.01	18.7	19.3	21.7	32.3	0.15424175	3.9	3.3	5.3	0.87390256	2.1	2.8

Table 4—Continued

KOI	σ_{TT} (min)	(E_L5,T2) MAD[a] (min)	WRMS[b] (min)	MAX[c] (min)	$p_{X'^2}$[d]	(E_L2,T2) MAD[a] (min)	WRMS[b] (min)	MAX[c] (min)	$p_{X'^2}$[d]	$\frac{\lvert\Delta\ P\rvert}{\sigma_P}$[e]	$\frac{\lvert\Delta\ E\rvert}{\sigma_E}$[f]
1146.01	22.4	27.4	34.7	76.5	0.001077701	26.3	29.8	60.9	0.001081326	0.0	0.7
1148.01	35.3	19.8	42.1	113.1	0.90771639	12.6	30.5	75.8	0.98768263	2.5	0.8
1150.01	93.1	71.9	73.6	167.9	0.50098584	53.3	70.0	148.8	0.77275173	0.8	1.4
1151.01	37.0	32.7	43.1	181.3	0.20747804	29.7	42.0	180.2	0.32722545	1.2	1.6
1151.02	34.5	21.3	34.7	69.7	0.88780763	26.9	34.2	62.6	0.35495599	0.2	0.1
1152.01	2.9	1.2	1.4	3.0	0.99827076	1.4	1.4	2.7	0.97423442	0.2	0.5
1160.01	22.2	13.1	15.5	21.4	0.81972107	8.9	9.2	21.4	0.91987838	0.0	1.4
1161.01	29.1	21.4	39.8	103.1	0.6589125	24.6	39.0	95.0	0.2113547	0.0	1.5
1163.01	23.0	16.7	41.1	168.4	0.77497441	14.2	40.4	165.5	0.95942781	1.0	0.9
1163.02	28.4	21.0	44.5	72.1	0.59822318	19.5	43.3	71.7	0.5655128	1.0	0.8
1164.01	51.7	26.6	72.4	326.9	0.99978456	29.4	72.0	318.5	0.99463937	0.1	0.6
1165.01	11.5	3.1	10.5	24.8	0.9999989	6.3	9.4	23.4	0.93196403	1.8	0.2
1166.01	16.5	9.9	13.8	34.4	0.91533237	10.5	12.9	32.8	0.76767366	1.1	0.2
1169.01	108.7	16.7	119.4	3,714.8	1	15.8	42.9	250.4	1	1.1	7.2
1170.01	12.3	7.4	17.2	42.5	0.90834005	9.7	16.3	33.3	0.33378302	1.4	0.8
1175.01	52.0	47.5	39.6	54.4	0.26309111	25.0	31.9	65.4	0.48439615	0.8	0.8
1176.01	1.3	0.5	1.1	12.9	0.99999999	0.6	1.0	13.0	0.99930912	1.2	0.5
1177.01	19.6	11.0	11.5	46.5	0.98468516	3.4	6.4	55.9	1	3.0	1.8
1187.01	4.1	2.7	4.2	20.1	0.99999899	2.5	4.2	19.7	0.99999999	1.5	1.3
1198.01	32.9	27.7	41.9	88.7	0.34592401	34.3	41.3	90.9	0.033758685	0.7	0.0
1198.02	49.8	14.7	70.9	186.4	0.99978734	32.3	64.7	160.0	0.63579198	2.1	0.5
1199.01	11.9	23.9	27.1	39.0	0.000290474	12.1	18.8	30.5	0.027895914	10.5	0.9
1201.01	15.2	14.2	24.7	58.2	0.052342173	16.2	23.7	50.8	0.000608547	3.0	0.1
1202.01	28.3	19.1	34.7	118.9	0.99298494	19.1	34.7	117.6	0.99018312	0.3	0.5
1203.01	23.9	17.6	16.0	22.3	0.48977279	12.0	11.5	15.5	0.45099686	0.8	0.2
1203.02	28.3	9.1	41.4	165.5	0.99729035	24.2	37.1	130.1	0.17103525	2.1	0.0
1204.01	58.6	46.2	79.1	159.3	0.47765338	45.9	72.1	139.0	0.33946859	1.4	1.5
1205.01	37.3	8.7	25.3	61.8	0.99998337	11.4	23.1	47.9	0.99793491	0.9	0.7
1207.01	17.9	22.8	36.4	85.8	0.008785765	14.3	25.2	55.6	0.23609623	3.1	2.5
1210.01	35.0	7.3	16.7	30.7	0.99992736	5.4	16.5	34.1	0.999857	0.2	0.0
1212.01	38.4	26.8	30.7	46.0	0.66031745	14.6	25.5	67.3	0.97109998	0.9	0.7
1214.01	63.2	34.5	69.4	138.5	0.99233623	40.5	68.2	159.5	0.87409998	0.9	0.5

Table 4—Continued

KOI	σ_{TT} (min)	(E_L5,T2) MAD[a] (min)	WRMS[b] (min)	MAX[c] (min)	$p_{X'^2}$[d]	(E_L2,T2) MAD[a] (min)	WRMS[b] (min)	MAX[c] (min)	$p_{X'^2}$[d]	$\frac{\lvert\Delta P\rvert}{\sigma_P}$[e]	$\frac{\lvert\Delta E\rvert}{\sigma_E}$[f]
1215.01	22.2	19.9	41.5	78.0	0.27001188	17.4	16.2	23.6	0.23837475	2.0	3.2
1215.02	22.5	25.8	24.7	35.6	0.082801771	8.1	6.6	9.7	0.66376272	2.0	1.5
1216.01	28.1	29.0	34.8	63.2	0.073588894	21.6	34.2	57.9	0.33348048	0.2	0.9
1218.01	15.5	8.3	9.0	12.2	0.81629029	4.1	7.1	13.7	0.90676342	0.6	0.2
1219.01	76.1	34.9	78.5	174.4	0.99993476	37.0	67.1	173.7	0.99930653	3.4	2.0
1220.01	25.3	24.3	38.7	102.8	0.1005205	23.5	35.2	88.6	0.08235055	1.8	0.7
1221.01	25.2	27.2	23.0	28.1	0.13802028	3.5	3.9	5.8	0.76471209	7.5	0.3
1221.02	40.9	4.3	3.8	4.7	0.99679328	0.7	0.8	1.4	0.97222484	0.1	0.2
1222.01	34.3	22.6	71.9	163.1	0.89177319	33.7	69.3	145.0	0.023690682	0.0	0.7
1227.01	7.3	1.6	8.1	67.0	1	2.4	7.9	63.7	1	3.3	0.5
1236.01	12.2	17.0	18.0	30.6	0.02732072	1.0	0.9	1.0	0.86034733	19.7	0.8
1236.02	26.0	47.5	104.7	486.4	7.49E-13	52.3	98.8	443.3	0	5.2	0.6
1238.01	19.7	10.4	11.6	17.2	0.78199133	7.1	6.3	10.3	0.6620329	0.8	0.3
1240.01	25.3	14.0	31.2	117.4	0.9996427	12.7	31.0	117.4	0.99996625	1.0	1.2
1241.01	20.9	33.3	61.5	91.1	0.001310734	29.2	41.7	67.1	0.001617233	3.1	2.2
1241.02	43.8	48.1	164.9	479.6	0.034972298	73.2	144.5	386.0	2.18E-07	4.2	3.7
1244.01	20.9	5.6	27.4	82.4	0.99984058	10.7	17.4	53.2	0.87335347	2.6	1.7
1245.01	25.4	13.6	24.5	44.0	0.87207098	14.5	23.2	54.8	0.61002098	0.5	0.5
1246.01	22.1	8.9	14.3	30.3	0.93803501	7.7	9.0	18.2	0.81109797	1.2	1.4
1258.01	7.0	8.1	7.4	9.9	0.10126764	0.5	0.6	0.9	0.87524615	12.4	0.6
1264.01	18.0	10.5	15.1	27.8	0.85381378	9.4	13.3	30.6	0.80018945	1.2	0.2
1266.01	17.4	6.7	13.7	42.1	0.99312423	9.2	13.1	39.9	0.81889255	0.2	0.6
1270.01	8.4	9.5	11.3	25.0	0.004627814	10.3	11.0	23.5	0.000192562	0.7	0.6
1273.01	11.2	2.8	2.8	2.9	0.96073183	1.2	1.3	2.6	0.81032845	2.0	0.1
1276.01	18.4	6.0	12.7	25.8	0.98528902	9.2	12.3	24.9	0.67201872	0.3	0.1
1278.01	41.7	22.7	42.0	75.9	0.89854265	32.8	35.5	47.9	0.2724472	0.3	1.0
1278.02	20.2	21.7	17.3	27.2	0.14084354	8.5	7.4	11.5	0.36173625	6.4	1.4
1279.01	16.5	7.8	9.3	15.0	0.94688877	6.4	8.2	13.2	0.92909687	0.4	0.4
1281.01	13.2	5.6	6.2	7.8	0.8387711	1.5	1.2	1.5	0.80534892	1.0	0.9
1282.01	15.9	16.1	31.3	73.4	0.17156305	17.4	14.2	21.2	0.023700682	2.6	2.1
1283.01	46.2	21.4	33.7	157.5	0.99148808	20.6	29.8	172.3	0.9813829	0.7	1.5
1285.01	12.3	4.5	7.7	68.2	1	1.8	6.2	67.7	1	2.7	4.0

Table 4—Continued

KOI	σ_{TT} (min)	(E_L5,T2) MAD[a] (min)	WRMS[b] (min)	MAX[c] (min)	$p_{X'^2}$[d]	(E_L2,T2) MAD[a] (min)	WRMS[b] (min)	MAX[c] (min)	$p_{X'^2}$[d]	$\frac{\lvert\Delta P\rvert}{\sigma_P}$[e]	$\frac{\lvert\Delta E\rvert}{\sigma_E}$[f]
1298.01	9.8	10.2	11.3	17.4	0.084443755	11.3	11.0	16.6	0.009093844	1.1	1.3
1300.01	11.6	6.6	12.7	47.3	1	6.6	12.6	48.1	1	1.3	0.6
1301.01	21.7	6.7	23.6	34.2	0.98931179	13.4	14.1	19.8	0.46233326	1.0	1.7
1303.01	37.0	25.1	21.1	40.8	0.57704676	13.5	16.3	37.7	0.65608775	0.5	0.7
1304.01	36.8	16.7	33.3	99.1	0.9994596	17.4	32.9	96.8	0.99668469	0.4	0.1
1305.01	31.2	13.3	38.7	182.4	0.99999915	13.9	37.9	182.6	0.99998788	0.9	1.5
1306.01	24.8	23.7	32.3	139.4	0.013388426	23.9	32.0	142.1	0.005635702	1.1	0.9
1306.02	31.9	20.5	38.6	115.0	0.94575557	14.6	36.8	110.9	0.99980828	1.8	0.4
1306.03	43.6	38.1	57.2	131.5	0.23506952	29.5	54.0	103.6	0.71737885	1.5	0.8
1307.02	11.9	9.0	10.4	17.1	0.50083748	11.5	9.9	16.3	0.066306191	0.2	0.0
1308.01	18.5	15.1	28.8	78.1	0.39025884	13.1	21.2	43.3	0.26959394	3.2	2.3
1309.01	19.5	13.8	23.2	52.7	0.64967349	14.6	19.3	36.8	0.37875661	2.1	1.0
1310.01	21.1	4.5	7.2	16.9	0.99944466	6.3	5.8	9.6	0.96444514	0.6	1.0
1312.01	23.2	21.0	42.0	113.1	0.18153892	22.6	40.9	104.3	0.041390048	1.1	1.9
1314.01	42.8	32.9	49.1	92.6	0.51644668	33.6	48.5	95.9	0.31467237	0.6	0.0
1315.01	22.9	14.8	37.0	79.6	0.85050583	18.7	36.8	82.1	0.27590341	0.3	0.1
1316.01	55.7	15.0	48.1	132.3	0.99998998	24.5	40.5	117.0	0.98374822	1.4	1.3
1325.01	5.8	3.2	3.9	9.6	0.93273003	2.4	3.9	8.9	0.97757025	0.2	0.2
1329.01	18.7	8.4	8.5	13.3	0.86924112	11.2	6.6	14.9	0.32623027	0.4	0.6
1336.01	25.8	26.0	44.5	94.1	0.093937533	21.1	42.3	85.9	0.23959658	1.8	0.2
1337.01	39.5	21.3	40.1	149.6	0.99990112	24.6	39.5	153.7	0.98792174	1.2	0.7
1338.01	36.8	23.4	38.4	101.2	0.92147606	25.5	33.6	68.6	0.71758708	2.1	1.8
1339.01	47.4	21.5	40.4	96.2	0.99973805	25.6	40.0	100.8	0.98517417	1.2	1.9
1341.01	54.6	16.3	18.6	28.1	0.99922215	18.2	16.4	33.4	0.98757075	0.3	0.9
1342.01	39.7	20.3	33.8	82.3	0.99850081	16.5	33.3	79.0	0.99993594	0.4	1.4
1344.01	26.5	29.0	38.3	66.5	0.004089481	32.3	35.5	67.4	5.05E-05	2.7	1.1
1355.01	8.1	4.7	10.3	13.1	0.66939359	5.1	4.2	10.5	0.1761757	6.9	2.3
1360.01	12.8	7.0	10.3	12.7	0.70043786	4.1	5.4	12.0	0.48562155	5.3	0.8
1360.02	19.1	13.9	14.3	27.9	0.58031538	12.4	12.6	25.8	0.5027724	1.2	0.3
1363.01	36.4	14.7	37.0	100.0	0.99999568	18.5	36.3	93.4	0.99761271	0.1	1.2
1364.01	22.1	15.5	19.8	30.0	0.54520542	17.2	15.0	18.5	0.15033554	0.4	1.5
1364.02	22.7	14.1	20.8	46.5	0.7938846	17.3	19.6	40.4	0.31562962	0.0	1.7

Table 4—Continued

KOI	σ_{TT} (min)	(E_L5,T2) MAD[a] (min)	WRMS[b] (min)	MAX[c] (min)	$p_{X'^2}$[d]	(E_L2,T2) MAD[a] (min)	WRMS[b] (min)	MAX[c] (min)	$p_{X'^2}$[d]	$\frac{\lvert\Delta P\rvert}{\sigma_P}$[e]	$\frac{\lvert\Delta E\rvert}{\sigma_E}$[f]
1366.01	17.7	8.0	22.3	36.5	0.90061336	3.8	10.3	29.1	0.94948735	2.1	4.2
1367.01	38.3	11.7	26.1	138.4	1	11.7	26.0	137.2	1	0.6	1.7
1369.01	26.7	18.8	30.7	70.7	0.83549698	19.9	29.8	79.2	0.60114974	1.5	0.3
1370.01	32.8	11.6	26.5	76.8	0.99984486	10.8	26.5	79.2	0.99968366	0.1	0.1
1376.01	15.4	15.1	25.0	62.9	0.11293887	14.1	24.8	58.1	0.10794717	0.7	0.1
1377.01	40.9	30.2	43.6	105.7	0.57263574	28.5	43.5	102.0	0.47310142	0.2	0.0
1378.01	17.8	18.0	16.5	34.7	0.12407712	6.2	13.1	39.3	0.93281771	1.0	1.1
1379.01	23.2	15.7	19.0	48.2	0.82453493	12.8	18.8	49.1	0.95346987	0.3	0.8
1382.01	4.0	2.2	4.0	113.1	0.97448277	1.7	3.8	113.7	0.99739944	0.5	0.8
1385.01	1.6	0.5	0.6	1.7	0.9921217	0.5	0.5	1.3	0.94348082	0.6	1.0
1387.01	1.3	1.0	0.6	2.2	0.44876699	1.1	0.4	1.6	0.11903893	1.0	2.9
1391.01	6.3	2.1	15.6	57.3	0.99975404	5.4	14.5	46.8	0.18392874	3.2	1.7
1395.01	17.5	6.8	11.9	23.7	0.99650671	5.3	10.3	24.2	0.99793741	0.9	0.5
1396.01	21.7	12.1	24.5	64.8	0.92096394	10.0	22.4	48.1	0.9456261	1.0	1.2
1396.02	41.4	51.1	53.8	181.9	0.000260834	54.3	53.7	178.2	8.94E-06	0.4	0.5
1401.01	23.5	13.4	28.2	179.7	1	13.4	28.2	179.2	1	1.1	2.5
1402.01	41.4	19.3	29.1	73.1	0.99295373	24.4	25.0	58.2	0.84653496	0.0	1.0
1403.01	18.4	9.1	11.8	18.8	0.91446618	8.3	9.5	15.5	0.81785662	0.1	0.4
1404.01	43.8	15.9	35.2	97.2	0.99979129	13.3	34.5	90.1	0.99988573	0.7	0.4
1405.01	31.0	29.3	39.7	68.6	0.19955106	15.1	32.3	71.2	0.75932624	2.0	0.7
1406.01	18.2	9.5	13.4	24.2	0.93522628	8.4	11.3	20.6	0.91044509	1.1	0.5
1408.01	24.7	19.0	31.3	65.5	0.48925805	32.2	29.8	55.4	0.001559721	1.2	0.8
1409.01	15.8	23.6	25.3	49.7	0.00183048	19.7	25.1	52.9	0.005244895	0.7	0.9
1410.01	52.6	11.1	29.5	61.5	0.99654845	14.9	26.1	55.7	0.88906889	0.6	2.2
1412.01	17.0	7.1	8.8	14.8	0.89600208	4.2	4.2	5.1	0.82694108	0.9	0.4
1413.01	40.8	44.6	61.6	117.2	0.043097254	50.5	46.9	72.9	0.002254188	3.1	0.2
1419.01	6.7	4.6	8.4	30.9	0.9483493	4.2	8.2	32.9	0.9877565	1.1	2.3
1422.01	14.4	14.4	17.6	38.2	0.05528909	14.5	17.5	37.5	0.024902249	0.3	0.4
1422.02	13.1	11.3	12.0	23.0	0.31615562	11.0	11.3	17.7	0.17748545	0.8	0.7
1422.03	23.5	21.8	48.8	116.2	0.08912444	25.0	46.2	98.2	0.001881282	3.9	0.0
1424.01	16.2	10.7	20.9	79.1	0.9918561	11.1	20.9	79.9	0.96060053	1.0	1.0
1425.01	95.7	18.1	40.7	168.3	1	21.1	39.4	163.3	1	0.0	1.0

Table 4—Continued

KOI	σ_{TT} (min)	(E_L5,T2) MAD[a] (min)	WRMS[b] (min)	MAX[c] (min)	$p_{X'^2}$[d]	(E_L2,T2) MAD[a] (min)	WRMS[b] (min)	MAX[c] (min)	$p_{X'^2}$[d]	$\frac{\lvert\Delta P\rvert}{\sigma_P}$[e]	$\frac{\lvert\Delta E\rvert}{\sigma_E}$[f]
1426.01	8.7	10.9	8.6	11.0	0.061191962	2.9	2.5	3.0	0.47294199	1.8	1.6
1427.01	33.4	16.5	25.3	108.6	0.99995148	13.9	25.0	105.0	0.99999922	0.7	0.4
1428.01	11.7	7.8	18.6	73.6	0.9961766	7.3	18.5	76.7	0.99959056	1.1	0.5
1430.01	15.7	8.9	10.8	20.4	0.91611485	7.7	7.7	18.1	0.91892787	0.8	1.7
1432.01	24.0	19.1	36.9	112.6	0.46486464	13.7	34.5	101.0	0.89151781	1.0	1.6
1433.01	28.7	9.1	9.1	17.5	0.98787147	5.1	7.3	15.6	0.99026624	0.3	0.5
1434.01	42.3	21.4	35.6	214.6	1	18.8	36.4	214.6	0.99999135	0.1	0.7
1435.01	20.3	14.9	20.0	33.0	0.46832162	14.9	15.8	24.4	0.11098411	2.7	1.2
1436.01	33.5	16.4	35.7	115.1	0.99995807	18.0	35.4	107.1	0.99886085	0.9	0.2
1437.01	39.8	28.4	50.0	147.0	0.68378657	35.1	48.7	142.2	0.14289436	0.8	0.4
1438.01	31.5	28.3	44.1	103.9	0.19881381	20.9	43.6	105.4	0.71446002	0.8	0.3
1440.01	35.0	8.8	30.4	84.7	0.99999913	13.2	27.3	75.6	0.99835626	0.9	0.6
1441.01	30.8	15.0	26.0	76.9	0.98179398	10.6	25.6	74.4	0.99762786	0.6	0.1
1442.01	36.1	14.7	26.8	96.8	1	14.6	26.6	99.0	1	0.1	0.9
1444.01	21.6	14.7	15.7	26.6	0.53517523	18.5	15.2	18.9	0.062139722	1.4	0.2
1445.01	28.0	23.2	38.4	86.5	0.37009244	27.8	32.1	67.3	0.033973525	2.8	1.8
1448.01	9.8	2.3	21.0	339.1	1	3.8	20.8	334.6	0.99999994	2.3	0.9
1452.01	13.4	5.1	20.1	274.1	1	5.2	19.9	278.9	1	2.8	1.0
1459.01	4.9	2.6	5.2	55.9	1	2.5	5.2	56.1	1	0.6	0.2
1465.01	6.6	32.0	26.4	67.5	0	31.1	25.8	74.1	0	0.4	4.4
1468.01	12.6	17.9	26.4	58.8	3.00E-05	16.9	24.4	62.8	6.26E-05	2.3	1.7
1475.02	34.1	17.3	44.6	98.1	0.919274	19.4	43.8	91.2	0.66700742	0.1	0.4
1480.01	11.7	5.2	13.1	24.4	0.90217539	8.7	12.9	22.2	0.22786583	0.4	0.1
1486.02	24.0	2.9	8.4	28.0	0.99896616	6.0	7.8	24.1	0.82060871	0.2	0.2
1488.01	12.9	11.2	16.7	45.1	0.23804645	9.9	15.6	41.5	0.47404195	2.4	0.7
1489.01	17.7	10.9	10.0	21.9	0.78069525	8.8	9.5	16.6	0.79350678	0.5	0.1
1494.01	26.5	16.2	29.2	42.0	0.67115605	10.6	10.6	22.4	0.60109128	2.1	1.2
1495.01	21.2	8.3	9.6	16.3	0.96218565	5.3	5.1	6.9	0.96423943	0.8	0.5
1498.01	34.1	20.4	33.3	89.2	0.94106756	22.4	27.1	66.8	0.76142647	2.6	0.1
1499.01	10.3	5.1	10.5	18.5	0.9095181	4.5	9.5	17.6	0.83888061	1.0	0.2
1502.01	17.4	12.5	25.9	74.6	0.85632427	12.9	25.9	76.4	0.70374294	0.1	1.0
1505.01	29.7	21.6	31.9	93.3	0.68926517	22.6	30.8	89.4	0.46064732	1.0	0.4

Table 4—Continued

KOI	σ_{TT} (min)	(E_L5,T2) MAD[a] (min)	WRMS[b] (min)	MAX[c] (min)	$p_{X'^2}$[d]	(E_L2,T2) MAD[a] (min)	WRMS[b] (min)	MAX[c] (min)	$p_{X'^2}$[d]	$\frac{\lvert\Delta P\rvert}{\sigma_P}$[e]	$\frac{\lvert\Delta E\rvert}{\sigma_E}$[f]
1506.01	15.0	8.9	7.4	9.6	0.65074879	0.5	0.6	0.8	0.94209465	4.3	0.0
1507.01	34.0	36.3	41.8	80.7	0.097771858	35.7	37.7	68.5	0.034698826	1.2	0.7
1508.01	21.8	14.1	52.4	112.9	0.68650258	30.7	30.2	43.5	0.000921422	4.5	0.2
1510.01	17.7	12.6	17.8	82.8	0.93369868	12.6	17.7	81.4	0.91372515	1.5	0.5
1511.01	23.0	13.1	25.7	151.1	0.99733402	16.4	23.4	158.6	0.77744038	2.2	1.5
1512.01	15.3	13.2	41.4	131.3	0.30069959	23.9	37.8	102.5	6.52E-07	4.1	0.6
1515.01	20.6	18.9	30.5	107.4	0.047233567	15.8	29.6	105.6	0.57034058	2.7	0.5
1516.01	23.8	19.0	50.8	113.9	0.42254884	32.2	45.9	95.3	0.001757162	1.9	1.0
1517.01	9.5	5.8	8.3	14.0	0.63295483	4.9	5.5	6.9	0.25960988	7.2	0.2
1518.01	25.9	20.9	14.7	20.9	0.39524792	13.8	10.9	25.4	0.41189278	0.2	0.8
1519.01	39.8	18.3	31.9	69.8	0.9993126	15.1	31.5	73.8	0.99990987	0.6	0.0
1520.01	14.4	18.8	14.6	20.0	0.013398347	18.1	14.5	20.0	0.004869325	0.1	0.2
1521.01	19.0	25.3	22.0	28.2	0.039524241	14.4	15.6	23.0	0.10004854	10.1	0.5
1522.01	14.7	5.4	9.8	15.1	0.88537977	1.2	1.4	2.0	0.85650939	4.2	0.6
1523.01	37.6	47.4	82.4	150.5	0.001107588	41.2	75.8	148.9	0.008131062	1.9	1.4
1525.01	26.2	12.5	71.0	277.0	0.99279178	21.5	68.5	248.9	0.26728463	3.0	0.3
1526.01	46.3	25.6	31.0	78.1	0.98793914	28.2	30.9	81.0	0.91593186	0.0	0.1
1528.01	23.5	9.2	17.7	40.8	0.99999344	8.5	16.6	45.7	0.99999593	0.2	0.4
1529.01	20.9	20.1	35.3	70.5	0.19072422	27.2	27.6	73.4	0.00305531	1.9	1.6
1530.01	17.9	6.8	13.3	32.9	0.98613972	9.6	11.2	25.9	0.73413923	0.1	1.0
1531.01	22.9	10.7	14.7	30.3	0.99702396	11.1	14.5	30.4	0.98662816	0.4	0.8
1532.01	21.4	22.2	25.2	83.5	0.1186063	15.4	21.2	59.9	0.30078278	1.6	0.2
1533.01	30.5	14.7	43.3	131.0	0.9945817	10.4	38.4	95.8	0.99980664	2.6	1.1
1534.01	28.6	20.0	19.6	24.5	0.57081614	17.3	18.7	29.6	0.40977323	0.0	0.1
1536.01	38.7	20.4	29.0	84.8	0.99735397	19.0	28.9	84.4	0.99807444	0.1	0.2
1537.01	43.0	18.6	34.1	96.8	0.98730457	13.1	32.0	116.7	0.99629662	0.4	0.7
1540.01	12.4	2.1	6.0	82.6	1	2.1	6.0	83.0	1	42.5	71.5
1541.01	1.7	0.6	1.0	7.4	1	0.8	1.0	7.6	0.99999191	0.9	0.5
1543.01	2.0	0.7	1.0	2.7	0.99999983	0.8	0.9	2.5	0.99997346	0.5	0.8
1546.01	11.9	2.7	6.2	71.9	1	2.1	5.5	69.8	1	2.9	0.9
1557.01	6.9	4.8	5.7	11.3	0.86726745	4.8	5.6	11.9	0.80886619	0.9	0.1
1561.01	11.9	5.3	17.6	55.6	0.9608563	9.8	16.1	48.8	0.20196117	0.2	2.0

Table 4—Continued

KOI	σ_{TT} (min)	(E_L5,T2) MAD[a] (min)	WRMS[b] (min)	MAX[c] (min)	$p_{X'^2}$[d]	(E_L2,T2) MAD[a] (min)	WRMS[b] (min)	MAX[c] (min)	$p_{X'^2}$[d]	$\frac{\lvert\Delta P\rvert}{\sigma_P}$[e]	$\frac{\lvert\Delta E\rvert}{\sigma_E}$[f]
1564.01	5.9	2.8	2.4	5.2	0.78248324	0.0	0.0	0.1	0.99254795	5.4	0.4
1569.01	18.4	11.9	11.3	17.4	0.74722669	7.4	9.1	15.5	0.93990739	1.2	0.1
1573.01	7.7	5.7	7.5	9.8	0.47905482	1.6	1.3	5.0	0.8667736	1.2	2.5
1576.01	7.5	3.7	5.0	10.8	0.97403058	3.8	4.5	9.7	0.90298095	0.2	1.2
1581.01	54.7	18.1	67.3	143.3	0.95288515	67.5	49.1	74.1	0.008408237	1.2	1.7
1583.01	34.0	18.5	42.5	160.7	0.95827003	19.5	41.4	146.9	0.85915401	0.9	0.5
1584.01	24.4	18.4	27.3	68.0	0.58929937	15.4	24.6	58.1	0.80914813	0.4	1.5
1585.01	23.6	11.4	12.8	18.9	0.92117756	8.2	10.5	18.0	0.93094001	0.8	0.1
1586.01	14.6	6.8	8.9	23.8	0.99579786	4.6	8.5	22.8	0.99989885	0.7	0.4
1588.01	18.3	8.4	13.0	35.4	0.99989025	11.6	12.7	31.4	0.91516599	0.9	0.2
1589.01	24.3	16.8	38.7	115.6	0.71848227	15.2	29.3	74.0	0.71239097	3.3	0.9
1589.02	24.4	25.4	31.9	72.2	0.074559444	20.8	27.5	66.5	0.1820699	1.9	0.8
1590.01	36.1	3.0	6.9	9.7	0.99842471	5.6	5.6	7.5	0.7373081	0.9	1.0
1590.02	29.7	25.7	32.1	88.3	0.21404264	18.9	30.4	77.7	0.91948554	0.3	1.3
1591.01	14.1	7.8	22.4	46.9	0.82494409	14.9	18.7	34.1	0.031208828	2.1	0.8
1593.01	30.1	8.8	24.0	47.4	0.99174407	5.1	19.4	32.1	0.9914722	1.2	0.4
1596.01	24.5	16.0	36.7	92.6	0.85685508	21.6	34.9	87.4	0.13828802	0.9	1.3
1597.01	16.8	9.7	22.8	79.7	0.92873104	8.6	19.9	60.8	0.94210726	2.0	1.1
1598.01	8.6	3.0	8.2	20.9	0.90392115	3.8	3.8	6.3	0.34638362	5.2	1.2
1599.01	24.3	27.8	38.5	67.4	0.055725096	23.1	29.6	41.2	0.073863061	1.2	2.0
1601.01	38.1	18.9	45.5	150.8	0.97504361	16.5	43.5	144.4	0.97437679	1.3	0.1
1602.01	52.4	36.4	72.3	178.6	0.69287429	35.4	72.0	166.1	0.56951525	0.6	0.6
1603.01	28.2	20.6	41.2	165.2	0.75275146	17.8	40.6	157.7	0.94927952	0.7	1.3
1605.01	39.5	23.5	65.1	153.4	0.96318673	27.6	64.4	147.1	0.69145198	3.7	11.9
1606.01	27.1	13.3	23.4	50.6	0.99736961	16.3	23.2	51.0	0.91282459	0.6	0.3
1608.01	28.0	25.0	42.0	82.6	0.24251848	19.4	38.0	83.8	0.50375951	2.0	0.7

Note. — Table 4 is published in its entirety in the electronic edition of the *Astrophysical Journal Supplement*. A portion is shown here for guidance regarding its form and content.

[a]Median Absolute Deviation of transit times in Q0-2 from ephemeris

[b]Weighted Root Mean Square deviation of transit times in Q0-2 from ephemeris

[c]MAXimum absolute deviation of transit times in Q0-2 from ephemeris

[d]p-value for a χ^2-like-test assuming X'^2 follows a χ^2 distribution, as described in § 3.1

[e]Absolute value of difference of best-fit periods for L_2,T2 and L_5,T2 ephemerides normalized by formal uncertainty

[f]Absolute value of difference of best-fit transit epochs for L_2,T2 and L_5,T2 ephemerides normalized by formal uncertainty

Table 6. Notes for *Kepler* Planet Candidates with Putative Transit Timing Variations.

KOI	P (d)	R_p[a] ($R_\oplus$)	S/N[b]	T_{dur}[c] (hr)	nTT[d]	nPC[e]	TTV[f] Flag	Comment
10.01	3.52230	10.5	22.6	3.3	35	1	2	epoch offset
13.01	1.76359	20.4	130.7	3.2	35	1	3	outlier
42.01	17.83278	2.6	10.8	4.5	5	1	2	quadratic?
94.02	10.42361	4.0	10.1	5.3	3	3	2	offset
103.01	14.91155	2.3	14.5	3.4	7	1	1	Period & epoch differ
124.02	31.71954	2.8	10.7	5.1	4	2	4	few TTs; quadratic?
131.01	5.01418	9.0	78.6	4.7	16	1	3	plausible
137.01	7.6415774	6.0	22.0	3.5	16	3	5	if clipped
137.02	14.85901	8.6	59.3	3.8	7	3	2	offset; trend?
142.01	10.91478	2.5	18.1	3.7	10	1	1	cubic
148.03	42.89554	2.0	12.3	5.6	3	3	2	offset
151.01	13.44739	4.6	10.8	2.7	10	1	2	Period differs
153.01	8.92503	3.2	8.9	2.7	12	2	3	plausible
156.02	5.18856	1.6	3.1	2.5	21	3	3	no obvious pattern
168.01	10.7435565	3.7	7.2	6.1	11	3	2	offset
172.01	13.72288	1.6	8.9	5.0	8	1	3	plausible
179.01	20.74007	3.3	21.7	10.3	6	1	3	outlier
190.01	12.2650109	16.2	91.8	4.4	9	1	6	if clipped
209.01	50.78974	7.5	74.0	10.9	3	2	4	few TTs
209.02	18.7956661	4.9	33.7	7.1	5	2	6	if clipped
217.01	3.90509	10.4	83.0	2.8	30	1	2	epoch offset?
226.01	8.30890	1.6	5.6	3.0	15	1	2	Period differs
227.01	17.66076	2.9	13.4	4.7	7	1	1	large amplitude; quadratic
238.01	17.23217	2.5	6.5	4.4	8	1	2	Period differs
241.01	13.82145	1.7	9.3	3.5	10	1	3	plausible
244.02	6.23855	2.6	20.4	3.6	18	2	2	systematically low; long-term trend
245.01	39.79454	2.1	30.3	4.7	3	1	2	few TTs; offset
248.01	7.20349	2.9	7.4	2.6	17	3	2	Period differs
248.02	10.9140064	2.5	4.9	2.1	11	3	6	if clipped
258.01	4.15764	4.5	4.5	5.3	27	1	2	period & epoch change; pattern?
260.01	10.49577	1.2	3.4	4.5	10	2	3	outlier
261.01	16.23844	5.6	9.6	3.9	7	1	3	no obvious pattern
270.01	12.58084	0.9	5.8	5.9	9	2	3	low amplitude
277.01	16.23675	2.1	19.9	7.7	7	1	1	quadratic
279.01	28.45557	4.9	50.8	8.1	3	2	2	few TTs; offset
281.01	19.55687	3.7	14.3	8.1	5	1	2	outlier
288.01	10.27540	1.5	9.9	6.3	10	1	3	no obvious pattern; outliers
295.01	5.31741	2.0	2.5	2.9	20	1	2	Period differs
312.01	11.57898	1.6	4.2	2.7	10	1	3	no obvious pattern
314.01	13.7810484	1.9	8.0	2.5	8	2	2	offset; quadratic?
323.01	5.83674	2.9	1.4	3.4	21	1	5	long-term trend; despite low SNR; but is it spots?
331.01	18.68416	1.1	7.0	6.4	6	1	3	fit affected by a few outliers
339.02	6.41681	1.1	2.4	3.1	18	2	4	Period differs; but lo SNR
346.01	12.92463	3.4	3.7	2.8	9	1	4	possible periodicicty; outliers
348.01	28.51109	5.3	30.0	4.6	3	1	4	few TTs

Table 6—Continued

KOI	P (d)	R_p[a] ($R_\oplus$)	S/N[b]	T_{dur}[c] (hr)	nTT[d]	nPC[e]	TTV[f] Flag	Comment
355.01	4.90345	2.0	4.4	2.8	23	1	3	outlier
360.01	5.94042	1.3	2.6	4.6	17	1	5	offset; low SNR
377.02	38.91160	6.2	37.3	5.0	3	3	2	few TTs; offset
388.01	6.14974	0.6	4.4	5.4	18	1	2	epoch offset? Large TT uncertainties
417.01	19.19311	9.0	45.0	2.5	6	1	2	epoch offset?
418.01	22.41834	12.6	157.6	4.9	4	1	4	epoch offset?
420.01	6.01040	4.3	24.4	2.3	19	1	2	epoch offset?
423.01	21.08739	9.6	62.3	6.0	4	1	4	few TTs; outliers?
443.01	16.21718	2.2	9.1	4.7	6	1	2	epoch offset
467.01	18.00891	5.0	30.4	4.9	4	1	4	few TTs; quadratic?
473.01	12.70512	2.2	6.6	2.4	8	1	2	epoch offset? or outlier?
477.01	16.54318	2.6	6.0	3.8	7	1	2	outlier?
486.01	22.18310	1.4	7.4	5.1	4	1	4	few TTs
505.01	13.76725	3.1	6.2	3.0	9	1	2	epoch offset?; chopping?
524.01	4.59252	2.3	6.2	2.4	25	1	2	Period & epoch differ
528.01	9.57676	3.1	6.1	3.4	11	3	1	cubic?
528.03	20.55273	3.2	5.4	2.5	5	3	3	fift affected by outlier?
531.01	3.68746	4.2	15.7	1.3	31	1	5	short duration and PDC likely affecting TTs
564.01	21.05821	2.4	6.6	7.4	5	2	2	Period differs
579.01	2.02000	1.5	2.3	1.9	58	1	4	low SNR; short duraiton; no obvious pattern
596.01	1.68271	1.7	2.8	1.3	70	1	5	short transit durations may affect TTs; Period differs
607.01	5.8940278	6.8	12.7	1.6	18	1	6	if clipped
624.01	17.78948	2.1	5.1	4.4	5	1	2	outlier
649.01	23.44942	2.0	7.3	8.1	4	1	4	few TTs; quadratic?
658.01	3.16267	1.5	6.1	1.9	37	2	2	short duraiton; offset?
662.01	10.21362	1.5	6.2	5.5	11	1	2	Period & epoch differ
663.02	20.30708	1.7	10.1	2.8	6	2	2	no obvious pattern
664.01	13.13755	2.1	4.0	4.7	7	1	3	no obvious pattern
679.01	31.80485	1.8	10.4	8.1	3	1	2	few TTs; offset?
693.02	15.66002	1.7	7.3	7.0	8	2	3	fit affected by outlier
697.01	3.03219	4.0	6.0	3.6	29	1	3	plausible
700.02	9.36127	1.9	3.0	3.3	13	2	2	Period differs
707.03	31.78453	2.5	6.4	8.6	3	4	4	few TTs; outlier
709.01	21.38418	2.2	7.5	3.8	5	1	2	large amplitude; alternating?
725.01	7.30500	6.7	4.4	3.4	17	1	3	outlier
735.01	22.34101	5.0	6.9	4.8	4	1	5	few TTs; large amplitude; active star
743.01	19.40335	10.9	44.6	10.5	5	1	5	active star; possible periodicicty; fit affected by outliers
751.01	4.99682	3.2	2.4	2.1	17	1	4	lo SNR; no obvious pattern
753.01	19.89939	6.9	10.8	1.9	6	1	5	short duraiton; outlier
756.02	4.13463	2.6	2.7	3.1	20	3	4	lo SNR; no obvious pattern
767.01	2.81651	14.2	79.9	2.6	40	1	5	inaccurate ephemeris in B11
775.02	7.8776054	2.5	3.5	2.4	14	2	6	if clipped
786.01	3.68995	1.8	1.9	2.3	32	1	4	low SNR; plausibly small amplitude
799.01	1.6266615	4.5	4.6	1.6	74	1	6	if clipped
800.02	7.21227	2.5	3.8	4.0	14	2	4	offset?; but outlier; low SNR

Table 6—Continued

KOI	P (d)	R_p[a] ($R_\oplus$)	S/N[b]	T_{dur}[c] (hr)	nTT[d]	nPC[e]	TTV[f] Flag	Comment
806.03	29.1654328	3.1	4.0	4.6	4	3	6	if clipped
818.01	8.11429	3.6	5.0	2.4	14	1	2	Period differs
822.01	7.91937	11.5	43.4	3.1	15	1	2	epoch offset?
834.03	6.15542	1.4	2.3	4.6	20	4	2	Period differs
850.01	10.52631	8.7	52.8	2.7	10	1	2	epoch offset?
856.01	39.74897	13.1	105.8	5.7	3	1	4	epoch offset?
867.01	16.08561	3.4	9.2	3.7	7	1	3	no obvious pattern
870.02	8.985971	3.4	4.4	4.4	12	2	6	if clipped
872.01	33.60167	7.4	38.5	4.4	3	1	4	few TTs
878.01	23.58879	5.2	8.6	4.5	4	1	4	outlier?
884.02	20.47687	2.7	10.8	3.5	5	3	1	quadratic
905.01	5.79511	2.0	6.5	2.4	19	1	3	no obvious pattern
917.01	6.7197208	3.2	3.0	2.2	17	1	6	if clipped
920.01	21.80587	1.9	5.7	2.9	4	1	4	epoch offset?
928.01	2.49409	2.3	2.2	1.8	45	1	1	short duraiton; periodic in Q¡=2?
935.01	20.85987	3.6	14.1	5.2	5	3	2	quadratic
940.01	6.10484	3.5	23.5	4.7	18	1	2	outlier
941.03	24.7	6.6	9.6	3.3	4	3	2	offset; quadratic?
947.01	28.59891	2.7	8.8	3.7	4	1	4	epoch offset?
952.02	8.7524615	2.3	4.4	2.3	13	4	6	if clipped
954.01	8.11522	2.3	4.3	2.9	12	2	2	Period differs
960.01	15.8011094	13.9	237.4	6.2	6	1	2	offset; quadratic?
961.01	1.21377	3.9	3.4	0.5	98	3	5	short transit durations may affect TTs; Period differs
972.01	13.11893	5.3	30.0	4.5	6	1	5	pulsations may affect TTs
977.01	1.35366	0.8	2.5	3.6	86	1	5	phase linked variations
984.01	4.28899	4.4	1.2	2.9	28	1	5	noisy star; likely dominates apparent TTVs; low SNR
1001.01	20.40241	2.6	4.3	12.8	7	1	2	major outliers
1003.01	8.36062	14.1	24.7	7.3	10	1	2	outlier
1019.01	2.49677	1.2	0.7	2.6	47	1	5	low SNR
1054.01	3.32361	2.0	1.4	3.8	36	1	5	variable star; low SNR; messy TTVs suggest false alarm
1059.01	1.02267	1.4	0.8	1.4	114	1	5	low SNR; short transit duration
1089.02	12.2182202	5.7	11.0	2.9	10	2	2	offset
1111.01	10.26494	1.6	1.7	3.8	11	1	4	low SNR; fit likely affected by outliers
1128.01	0.97488	1.0	3.2	1.7	61	1	5	some transits affected by thermal events; short duraiton
1169.01	0.68921	1.2	2.1	1.6	171	1	5	low SNR; short duration
1199.01	53.52962	2.7	8.2	5.6	3	1	4	few TTs
1201.01	2.75753	1.4	1.0	1.0	43	1	5	low SNR; short duration
1204.01	8.39776	1.7	1.9	6.5	15	1	4	low SNR; periodic?
1215.01	17.3229827	2.2	5.5	7.5	7	2	2	offset
1236.02	6.15488	1.7	2.6	5.7	19	2	4	low SNR
1241.02	10.49447	7.0	3.6	12.7	11	2	2	plausible
1258.01	36.3392096	4.2	17.4	6.3	3	1	6	if clipped
1270.01	5.72943	2.0	3.6	1.2	20	1	5	short transit duration
1285.01	0.93742	8.0	4.7	1.7	124	1	5	spotted star; short duraiton; epoch offset? Trend?
1308.01	23.584268	2.0	6.8	5.5	5	1	2	period & epoch differ

Table 6—Continued

KOI	P (d)	R_p[a] ($R_\oplus$)	S/N[b]	T_{dur}[c] (hr)	nTT[d]	nPC[e]	TTV[f] Flag	Comment
1310.01	19.12903	2.0	3.9	3.7	7	1	2	F test suggests quadratic; but TTs consistent w/ linear
1344.01	4.48761	1.1	1.7	2.6	26	1	5	low SNR
1366.01	19.25493	2.4	6.4	4.5	5	1	2	epoch offset?
1376.01	7.1390621	2.8	3.1	2.6	12	1	6	if clipped
1396.02	3.70128	1.9	1.2	2.6	22	2	5	low SNR
1465.01	9.77142	4.9	10.5	1.7	13	1	5	PDF artificacts; short duraiton; TTs unreliable
1468.01	8.48084	3.7	9.5	6.2	15	1	3	possible periodicicty; fit affected by outliers
1508.01	22.04698	1.6	3.6	4.6	6	1	2	outlier?
1512.01	9.04184	2.1	3.1	2.1	13	1	2	fit affected by outlier
1525.01	7.7146748	2.1	3.1	4.5	17	1	6	if clipped
1529.01	17.9761922	1.7	3.4	3.5	6	1	6	if clipped
1540.01	1.20785	19.2	22.0	3.0	71	1	5	inaccurate ephemeris in B11
1573.01	24.8076159	3.8	16.7	3.4	4	1	6	if clipped
1605.01	4.93916	1.8	3.3	1.4	25	1	5	offset; but low SNR and short duration may affect TTs

[a]Putative radius of planet in Earth radii (from B11)

[b]Typical Signal to Noise Ratio of an individual transit

[c]Transit duration (from B11)

[d]Number of transit times measured in Q0-2

[e]Number of transiting planet candidates for host star

[f]1=pattern to eye, 2=trend or periodicity, 3=excess scatter and no trend, 4=low S/N per transit and/or few transits, 5=note about difficulty measuring TTs, 6=excess scatter significant only after clipping

Table 7. Predicted Transit Time Variation Magnitude for *Kepler* Transiting Planet Candidates

KOI	RMS Q2 (s)	Min-to-Max Q2 (s)	RMS 3.5yr (s)	Min-to-Max 3.5yr (s)	RMS 7yr (s)	Min-to-Max 7yr (s)
70.01	1.2	3.5	1.3	5.1	1.3	5.2
70.02	1.4	5	1.3	6	1.3	6
70.03	···	···	3.4	9.7	3.4	10
70.04	23	71	23	91	23	94
72.01	0.0003	0.001	0.003	0.01	0.01	0.05
72.02	0.01	0.03	0.2	0.5	0.2	0.5
82.01	161	484	183	612	185	609
82.02	442	1303	484	1624	485	1639
85.01	33	133	35	134	35	134
85.02	1.2	4.1	1.2	4.3	1.2	4.5
85.03	119	416	123	419	123	420
89.01	···	···	7118	25131	7700	29300
89.02	···	···	5536	18234	5926	21552
94.01	21	58	43	149	42	156
94.02	533	1924	851	2668	845	2624
94.03	···	···	97	305	150	447
111.01	15	42	61	188	62	182
111.02	9.7	22	38	114	39	113
111.04	···	···	5.8	21	6.6	25
112.01	···	···	0.7	2	0.7	2
112.02	0.04	0.1	0.04	0.1	0.04	0.1
115.01	72	295	80	344	81	365
115.02	218	893	270	1055	273	1116
116.01	6.3	22	7.9	27	7.9	27
116.02	···	···	10	31	10	30
117.01	1.5	4.3	1.7	5.8	1.7	6.1
117.02	12	37	12	40	12	41
117.03	8.1	27	8.2	27	8.2	27
117.04	32	97	36	125	36	126
123.01	0.9	3.5	1	3.5	1	3.5
123.02	1.2	3.4	1.2	3.5	1.2	3.4
124.01	9.7	26	9.9	25	10	26
124.02	0.3	0.7	0.4	0.8	0.4	0.9
137.01	296	1066	1457	4372	1435	4219
137.02	120	401	633	1870	622	1806
137.03	54	162	53	171	53	173
139.01	···	···	0.5	1.2	0.5	1.4
139.02	0.003	0.01	0.006	0.02	0.008	0.03
148.01	9.9	41	186	608	189	563
148.02	5.3	19	66	221	68	201
148.03	5.1	11	4.7	14	4.8	17
150.01	2.7	9.2	2.7	9.2	2.7	9.2
150.02	3.5	9.3	3.9	11	3.9	11
152.01	17	36	123	366	124	384
152.02	106	322	690	2278	705	2286

Table 7—Continued

KOI	RMS Q2 (s)	Min-to-Max Q2 (s)	RMS 3.5yr (s)	Min-to-Max 3.5yr (s)	RMS 7yr (s)	Min-to-Max 7yr (s)
152.03	11	32	195	586	197	618
153.01	34	113	35	106	36	104
153.02	53	176	55	167	55	164
156.01	103	352	237	910	238	918
156.02	37	141	40	156	40	156
156.03	70	241	169	517	170	529
157.01	58	186	191	803	209	1053
157.02	263	779	662	2520	678	2867
157.03	53	105	699	2687	690	2693
157.04	291	617	1917	6452	1811	6339
157.05	···	···	26	83	29	107
157.06	212	846	436	1853	487	2240
168.01	54	177	321	1029	328	1001
168.02	55	199	52	221	54	278
168.03	137	499	763	2489	786	2470
209.01	···	···	10	34	10	33
209.02	70	228	67	228	68	230
220.01	0.6	2	0.6	2	0.6	2
220.02	9.8	33	9.8	33	9.8	33
222.01	4.6	13	85	256	84	268
222.02	2.4	8	67	199	66	207
223.01	0.02	0.06	0.02	0.07	0.02	0.08
223.02	0.01	0.02	1.8	5.5	1.9	5.4
232.01	2.5	7.7	2.5	7.3	2.5	7.1
232.02	32	108	33	103	33	100
244.01	0.7	2.6	17	50	18	51
244.02	29	107	207	617	210	620
248.01	107	406	357	1240	425	1581
248.02	136	414	678	2226	812	2894
248.03	2.2	8.1	2.2	8.1	2.2	8.5
250.01	547	1819	546	2042	515	2044
250.02	774	2178	756	2456	708	2459
250.03	2.1	7.6	2.1	9.4	2.1	9.5
260.01	0.07	0.3	0.08	0.3	0.08	0.3
260.02	···	···	0.8	2.3	0.8	2.4
270.01	1	3.4	1.1	3.5	1	3.5
270.02	0.3	0.8	0.3	0.8	0.3	0.8
271.01	···	···	51	191	52	188
271.02	88	219	66	213	67	219
279.01	21	53	33	100	34	100
279.02	192	504	276	832	278	832
282.01	0.2	0.5	0.2	0.6	0.2	0.7
282.02	1.9	6.5	1.9	6.5	1.9	6.5
291.01	0.04	0.1	0.4	1.2	0.4	1.2
291.02	0.3	0.8	0.3	0.9	0.3	0.9

Table 7—Continued

KOI	RMS Q2 (s)	Min-to-Max Q2 (s)	RMS 3.5yr (s)	Min-to-Max 3.5yr (s)	RMS 7yr (s)	Min-to-Max 7yr (s)
313.01	3.9	12	4.2	12	4.2	12
313.02	25	76	25	78	25	78
314.01	33	96	41	126	40	125
314.02	50	132	61	198	59	195
339.01	0.06	0.2	0.06	0.2	0.06	0.2
339.02	0.2	0.5	0.2	0.5	0.2	0.5
341.01	44	142	75	238	75	236
341.02	64	233	104	340	104	336
343.01	0.2	0.6	0.2	0.6	0.2	0.6
343.02	1.5	4.9	1.5	4.9	1.5	4.9
351.01	···	···	5934	15686	7355	21462
351.02	···	···	11655	34240	12674	37917
351.03	···	···	52	182	51	213
377.01	51	132	2691	9568	4732	13959
377.02	9.5	20	3748	11547	5629	17018
377.03	0.07	0.2	0.07	0.3	0.08	0.3
386.01	16	42	28	92	28	94
386.02	···	···	4.4	14	4.4	15
398.01	1	2.2	3.8	11	3.9	11
398.02	0.4	1.3	0.4	1.6	0.4	1.7
398.03	3.1	9.9	3.1	10	3.1	10
401.01	7.6	15	7.9	26	7.8	26
401.02	···	···	66	157	73	170
408.01	36	111	37	117	37	118
408.02	52	169	52	195	52	198
408.03	3.4	7.2	4.9	16	4.8	17
416.01	1.5	4.6	1.4	4.6	1.4	4.6
416.02	···	···	9.1	27	9	27
431.01	24	61	25	86	26	86
431.02	0.4	0.8	1.4	5.4	3.2	10
433.01	0.001	0.005	0.03	0.1	0.03	0.1
433.02	···	···	12	32	18	52
440.01	1	2.9	1.1	3.2	1.1	3.2
440.02	1.3	4.6	1.3	4.5	1.3	4.5
442.01	0.2	0.6	0.2	0.6	0.2	0.6
442.02	0.02	0.05	0.02	0.06	0.02	0.08
446.01	38	119	40	126	40	125
446.02	50	129	66	220	65	220
448.01	2.7	9.8	2.7	9.2	2.7	9.1
448.02	···	···	4.2	12	4.2	12
456.01	0.4	1.2	0.4	1.3	0.4	1.3
456.02	1.1	4.2	1.3	4.4	1.3	4.4
459.01	0.3	1	0.3	1	0.3	0.9
459.02	4.5	16	4.9	17	4.9	17
464.01	0.1	0.3	2.5	7.2	2.6	7.2

Table 7—Continued

KOI	RMS Q2 (s)	Min-to-Max Q2 (s)	RMS 3.5yr (s)	Min-to-Max 3.5yr (s)	RMS 7yr (s)	Min-to-Max 7yr (s)
464.02	0.4	1.3	0.4	1.3	0.4	1.3
474.01	4	13	4	13	4	13
474.02	1.3	3.4	1.2	3.9	1.2	3.8
475.01	58	160	57	170	56	171
475.02	31	86	31	94	31	91
481.01	0.8	2.3	0.8	3.2	0.8	3.2
481.02	0.08	0.3	0.08	0.3	0.08	0.3
481.03	0.5	1.1	2.4	7.1	2.4	7.3
490.01	15	49	16	49	16	49
490.03	14	48	14	48	14	48
497.01	0.008	0.03	0.4	1.3	0.4	1.2
497.02	1.3	3.4	1.1	3.5	1.1	3.5
500.01	252	864	2342	9320	4127	13597
500.02	218	671	945	4256	2415	7680
500.03	95	336	2422	8064	2733	12365
500.04	109	505	3685	13150	3562	12555
500.05	0.1	0.6	0.1	0.6	0.1	0.6
508.01	28	105	72	211	72	212
508.02	19	56	37	105	37	105
509.01	2	6.6	2.1	7	2.1	7
509.02	0.8	2.4	0.8	2.5	0.8	2.5
510.01	8.6	26	8.7	27	8.7	26
510.02	3.4	9.4	3.4	9.8	3.4	9.7
518.01	1.3	4	1.9	6.7	1.9	6.7
518.02	0.5	1.2	3.5	11	3.6	11
520.01	17	45	574	1994	643	1980
520.02	9.4	30	9.3	30	9.3	31
520.03	6.4	16	625	2062	672	2021
523.01	177	376	3377	11772	4369	14545
523.02	544	1153	21346	76692	27676	92156
528.01	39	133	48	146	48	146
528.02	···	···	12	46	12	46
528.03	17	51	21	62	21	64
534.01	0.3	0.7	0.2	0.7	0.2	0.7
534.02	2.3	7.9	2.3	7.3	2.3	7.3
543.01	21	74	22	75	22	75
543.02	25	97	26	99	26	98
551.01	6.5	20	18	51	18	51
551.02	15	55	46	137	47	138
555.01	0.007	0.02	0.007	0.02	0.009	0.04
555.02	···	···	0.7	2.2	0.7	2.2
564.01	2.3	6.3	2.5	8.4	2.5	8.4
564.02	···	···	2.7	9.3	6	18
567.01	33	113	61	208	89	375
567.02	93	290	226	880	372	1637

Table 7—Continued

KOI	RMS Q2 (s)	Min-to-Max Q2 (s)	RMS 3.5yr (s)	Min-to-Max 3.5yr (s)	RMS 7yr (s)	Min-to-Max 7yr (s)
567.03	88	225	260	842	337	1382
571.01	48	148	45	172	45	172
571.02	21	66	22	72	22	71
571.03	20	58	20	61	20	62
573.01	0.3	0.9	0.3	0.8	0.3	0.8
573.02	0.9	3	0.9	3	0.9	3
584.01	7.8	29	13	39	13	38
584.02	5	13	6.2	18	6.2	18
590.01	0.6	1.8	0.5	1.9	0.5	1.9
590.02	···	···	2.3	6.5	2.2	6.6
597.01	0.2	0.6	0.2	0.6	0.2	0.6
597.02	0.03	0.1	0.03	0.1	0.03	0.1
612.01	25	73	60	186	60	190
612.02	···	···	15	48	15	47
623.01	15	47	90	314	91	303
623.02	20	54	206	664	207	656
623.03	15	51	16	53	16	56
638.01	24	64	19	69	20	68
638.02	···	···	16	50	16	49
645.01	2.5	8.1	2.5	8.4	2.5	8.4
645.02	1.4	3.9	1.5	4.5	1.5	4.6
657.01	0.2	0.7	0.3	0.7	0.3	0.8
657.02	8.00E-05	0.0002	0.009	0.03	0.05	0.2
658.01	9	30	9.4	29	9.4	29
658.02	3.6	12	3.7	13	3.8	12
663.01	0.04	0.1	0.04	0.1	0.04	0.2
663.02	0.9	2.3	0.9	2.7	1	2.7
665.01	1.4	4.5	1.5	4.4	1.5	4.5
665.02	1.1	4.1	1.1	3.8	1.1	3.9
665.03	16	56	18	53	18	56
672.01	26	68	25	82	25	82
672.02	4.3	9.1	4.2	14	4.2	14
676.01	1.3	3.7	1.4	3.8	1.4	3.9
676.02	2.3	8.3	2.3	8	2.3	8
691.01	8.8	20	13	40	13	39
691.02	43	134	91	286	92	277
693.01	14	33	23	69	23	72
693.02	24	59	35	105	35	107
700.01	1.4	3.5	1.3	3.8	1.3	3.9
700.02	2.2	7.2	2.3	7.7	2.2	7.7
701.01	0.7	1.9	0.7	2.5	0.7	2.5
701.02	1.1	3.6	1.1	3.7	1.1	3.7
701.03	···	···	6.1	20	6.5	20
707.01	87	282	385	1486	408	1656
707.02	18	39	873	2934	881	3682

Table 7—Continued

KOI	RMS Q2 (s)	Min-to-Max Q2 (s)	RMS 3.5yr (s)	Min-to-Max 3.5yr (s)	RMS 7yr (s)	Min-to-Max 7yr (s)
707.03	833	2150	1229	5113	1388	6794
707.04	48	193	88	329	92	349
708.01	1.6	4.4	1.5	4.5	1.5	4.5
708.02	8.1	25	8.3	26	8.3	26
711.01	4.6	9.7	16	57	17	58
711.02	0.03	0.1	0.03	0.1	0.03	0.1
711.03	···	···	8.6	26	9.3	28
718.01	0.1	0.4	0.1	0.4	0.1	0.4
718.02	6.2	13	33	101	34	102
718.03	0.2	0.5	21	61	22	63
723.01	3.8	13	3.9	13	3.9	13
723.02	4.3	11	3.7	13	3.8	13
723.03	4.9	17	5.1	17	5.1	18
730.01	162	487	8382	33786	17883	74103
730.02	80	267	16621	66072	24803	104129
730.03	329	969	15160	47329	18483	65726
730.04	275	986	11247	38638	27649	96231
733.01	29	97	34	109	33	111
733.02	23	78	29	85	29	85
733.03	19	59	19	58	19	58
736.01	1.2	3.9	1.2	3.8	1.2	3.8
736.02	4.5	14	4.4	15	4.4	15
738.01	175	688	208	894	2586	11784
738.02	286	986	320	1383	4117	18482
749.01	27	102	27	92	27	93
749.02	45	179	44	164	44	165
752.01	0.6	1.9	0.6	2	0.6	2
752.02	···	···	3.6	10	3.6	10
756.01	1	2.9	0.8	2.8	0.8	2.9
756.02	7.5	29	7.2	33	7.1	33
756.03	12	41	12	43	12	43
757.01	17	61	18	61	18	62
757.02	0.8	1.6	7.2	29	7	29
757.03	16	52	15	52	15	52
775.01	12	37	41	119	42	120
775.02	20	77	61	184	62	185
787.01	58	240	66	281	67	278
787.02	126	480	146	575	147	569
800.01	1.2	4	1.2	3.9	1.2	3.9
800.02	0.5	1.4	0.4	1.4	0.4	1.4
806.01	···	···	329	1014	309	1022
806.02	···	···	859	3193	896	3389
806.03	302	656	5950	17563	5811	19928
812.01	0.1	0.6	0.1	0.6	0.1	0.6
812.02	15	45	34	110	34	110

Table 7—Continued

KOI	RMS Q2 (s)	Min-to-Max Q2 (s)	RMS 3.5yr (s)	Min-to-Max 3.5yr (s)	RMS 7yr (s)	Min-to-Max 7yr (s)
812.03	...	...	9.1	33	9.6	34
829.01	31	85	172	559	171	558
829.02	38	118	81	251	81	247
829.03	9.9	20	85	256	84	240
834.01	20	54	23	75	23	72
834.02	225	677	218	676	217	670
834.03	10	34	10	39	10	38
834.04	0.2	0.8	0.2	0.8	0.2	0.8
837.01	8.7	26	8.8	26	8.8	26
837.02	23	69	23	67	23	67
841.01	56	156	758	2402	816	2420
841.02	3.5	8.3	293	890	312	947
842.01	7.1	23	8.5	29	8.6	29
842.02	1.3	2.8	4.1	12	4	12
853.01	27	88	27	83	27	83
853.02	35	128	39	124	39	125
864.01	3.7	12	3.7	12	3.7	12
864.02	4.2	11	27	84	27	78
864.03	11	38	52	168	52	155
869.01	1.3	4.4	1.3	4.3	1.3	4.3
869.02	1.2	2.5	4.1	12	4.2	12
870.01	75	268	125	505	168	754
870.02	113	378	237	836	298	1176
877.01	10	35	198	652	211	625
877.02	14	42	160	516	166	493
880.01	80	215	2073	6486	2074	6146
880.02	40	85	1145	3558	1160	3448
880.03	1.6	5.2	1.6	6	1.6	6.5
880.04	2	6.7	2	6.8	2	6.8
881.01	0.2	0.6	0.6	1.8	0.6	1.8
881.02	...	...	11	28	10	30
884.01	39	111	38	116	38	116
884.02	18	52	19	55	19	54
884.03	1.9	6.7	2	7	2	7.1
896.01	0.9	2.8	0.9	3	0.9	3
896.02	9.3	30	9	30	9	30
898.01	64	195	164	516	163	554
898.02	82	245	86	256	85	256
898.03	22	53	111	318	109	330
899.01	22	67	22	73	22	75
899.02	11	36	11	33	11	33
899.03	8.5	25	9	27	9	27
904.01	0.03	0.1	0.03	0.1	0.03	0.1
904.02	1	2.4	1	2.9	1	2.9
907.01	100	301	134	436	135	410

Table 7—Continued

KOI	RMS Q2 (s)	Min-to-Max Q2 (s)	RMS 3.5yr (s)	Min-to-Max 3.5yr (s)	RMS 7yr (s)	Min-to-Max 7yr (s)
907.02	85	234	103	339	104	318
907.03	1.3	4.3	1.3	5.1	1.3	5.2
921.01	52	173	54	167	54	168
921.02	30	97	31	100	31	100
921.03	1.5	5.1	1.5	5.6	1.5	5.7
934.01	14	40	14	44	14	44
934.02	47	142	269	900	283	1021
934.03	28	78	308	917	321	1064
935.01	14	36	418	1192	395	1208
935.02	7.7	16	570	1730	486	1843
935.03	···	···	214	680	277	849
936.01	0.5	1.3	0.5	1.4	0.5	1.4
936.02	0.03	0.1	0.03	0.1	0.04	0.2
938.01	0.06	0.2	0.1	0.3	0.1	0.3
938.02	0.02	0.05	0.02	0.06	0.02	0.09
941.01	5.5	19	5.5	21	5.5	21
941.02	4.2	14	4.3	15	4.3	15
941.03	8.5	22	9.3	30	9.4	31
945.01	46	119	159	538	162	559
945.02	6.5	14	120	404	122	424
952.01	71	269	461	1510	432	1496
952.02	76	265	646	2000	610	1957
952.03	1.7	5	3.3	13	3.3	14
952.04	69	221	77	239	77	234
954.01	0.5	1.6	0.5	1.6	0.5	1.6
954.02	0.008	0.02	2.1	6.2	2.2	6.3
961.01	695	2502	808	4159	902	4654
961.02	1.7	8.3	11	50	19	62
961.03	127	415	127	585	126	575
1015.01	0.5	1.5	0.5	1.5	0.5	1.5
1015.02	4.3	13	4.2	13	4.2	13
1060.01	0.08	0.3	0.09	0.3	0.09	0.3
1060.02	0.9	3.1	0.9	3	0.9	3
1089.01	···	···	23	63	22	67
1089.02	3.8	12	3.9	13	3.9	13
1102.01	5	16	60	188	61	181
1102.02	51	199	491	1577	495	1512
1113.01	6	16	5.7	19	5.5	19
1113.02	···	···	6.4	19	6.5	19
1151.01	11	42	12	43	11	43
1151.02	16	51	16	52	16	52
1163.01	0.6	1.9	0.6	1.9	0.6	1.9
1163.02	0.3	0.8	0.3	0.8	0.3	0.8
1198.01	21	63	33	112	33	112
1198.02	31	103	44	148	43	149

Table 7—Continued

KOI	RMS Q2 (s)	Min-to-Max Q2 (s)	RMS 3.5yr (s)	Min-to-Max 3.5yr (s)	RMS 7yr (s)	Min-to-Max 7yr (s)
1203.01	4.4	11	6.3	19	6.3	19
1203.02	15	49	21	68	21	68
1215.01	9.1	27	77	228	78	235
1215.02	0.5	1	54	162	55	167
1221.01	161	408	408	1260	405	1298
1221.02	31	65	322	1053	319	1060
1236.01	0.5	1.1	0.8	2.3	0.8	2.3
1236.02	0.2	0.7	0.2	0.8	0.2	0.8
1241.01	74	186	914	2647	857	2632
1241.02	55	187	1669	5404	1551	5292
1278.01	1.3	4.1	1.4	4.7	1.4	4.7
1278.02	0.0009	0.002	1.2	3.6	1.2	3.5
1301.01	3.6	9.7	3.3	11	3	10
1301.02	0.04	0.1	1.5	4.7	1.6	4.7
1306.01	12	38	12	36	12	38
1306.02	9.9	35	9.8	38	9.9	43
1306.03	8.4	28	8.3	28	8.6	32
1307.01	9.9	21	19	55	19	56
1307.02	33	83	57	177	58	178
1360.01	1	2.1	1.2	3.8	1.2	3.9
1360.02	12	36	13	42	13	42
1364.01	0.5	1.2	1.8	6.2	1.9	5.7
1364.02	2	6.5	2.4	8.5	2.4	8.5
1396.01	6	20	6.2	19	6.2	20
1396.02	15	46	15	47	15	48
1422.01	24	78	23	85	23	85
1422.02	4	11	4.6	16	4.6	16
1422.03	50	164	49	161	49	161
1426.01	376	1009	3920	11828	4220	13975
1426.02	···	···	9178	33482	85203	296827
1426.03	···	···	4126	12096	38889	126515
1475.01	0.07	0.2	0.07	0.2	0.07	0.3
1475.02	0.5	1.5	0.5	1.4	0.5	1.4
1486.01	···	···	10	27	9.2	28
1486.02	0.8	2.2	5.3	18	5.3	18
1589.01	69	228	160	525	161	534
1589.02	92	295	237	709	237	725
1590.01	0.02	0.04	0.6	1.9	0.6	1.8
1590.02	0.03	0.1	0.03	0.1	0.03	0.1
1596.01	0.05	0.2	0.05	0.1	0.05	0.2
1596.02	···	···	2.9	7.7	2.8	8.5

Note. — We report the magnitude (root mean square and min-to-max) of transit timing variations expected based on n-body integrations using estimated nominal masses and initially circular orbits (Lissauer et al. 2011b). We assume that all members of multiple planet candidate systems are true planets and orbit the same star. Integrations extend for the duration of the first two quarters of *Kepler* data, the nominal 3.5 year mission life time and 7.5 years, representative of a hypothetical extended mission. Eccentric models can dramatically affect

both the predicted TTV magnitude and timescale. Table 7 is published in its entirety in the electronic edition of the *Astrophysical Journal Supplement*. A portion is shown here for guidance regarding its form and content.

Appendix

Here we provide an appendix (online only) of TTVs for several *Kepler* planet candidates of particular interest. The TT are plotted relative to the E_L5 ephemeris provided by B11. Using the Q0-Q2 ephemeris would cause the weighted average of TTVs was zero. Thus, an offset of the weighted average of plotted TTVs (relative to zero) and/or a slope of the TTVs may indicate a gradual change in the orbital period between the ephemeris measured based on Q0-2 and the ephemeris based on Q0-5 data and provided in B11.

TTV Candidates

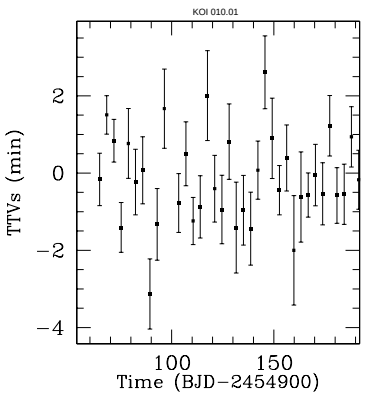

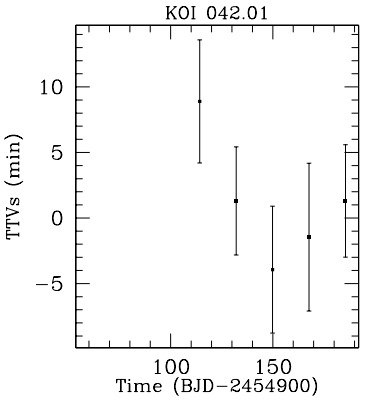

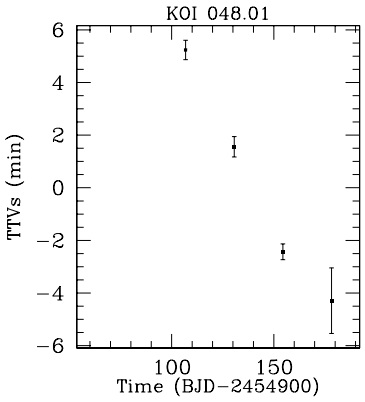
KOI 048.01
TTVs (min)
6
4
2
0
−2
−4
−6
100
150
Time (BJD−2454900)

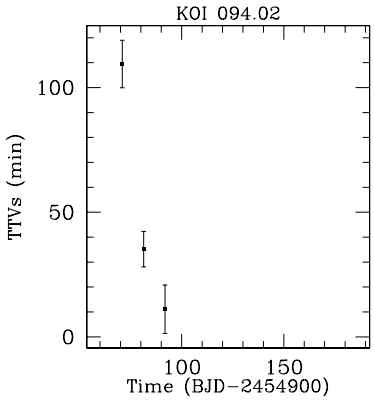
KOI 094.02
TTVs (min)
100
50
0
100
150
Time (BJD−2454900)

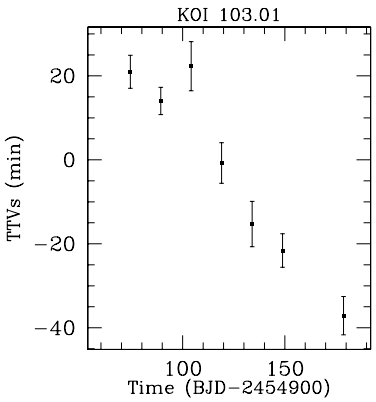
KOI 103.01
TTVs (min)
20
0
−20
−40
100
150
Time (BJD−2454900)

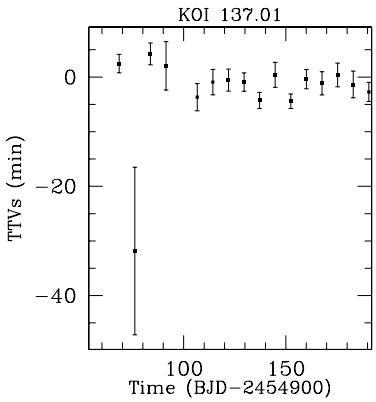
KOI 137.01
TTVs (min)
0
−20
−40
100
150
Time (BJD−2454900)

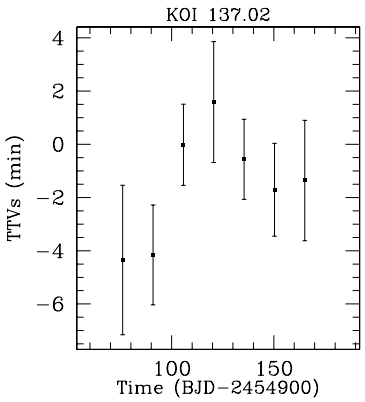
KOI 137.02
TTVs (min)
4
2
0
−2
−4
−6
100
150
Time (BJD−2454900)

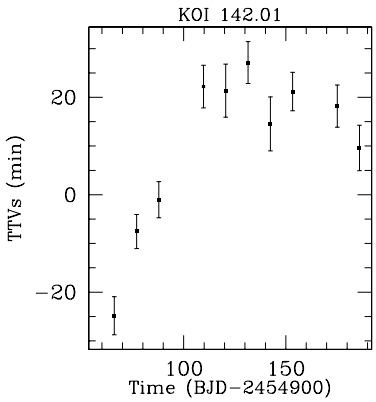
KOI 142.01
TTVs (min)
20
0
−20
100
150
Time (BJD−2454900)

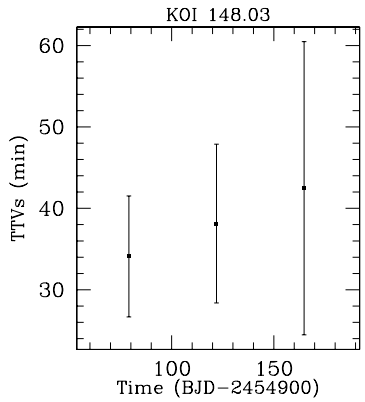
KOI 148.03
TTVs (min)
60
50
40
30
100
150
Time (BJD−2454900)

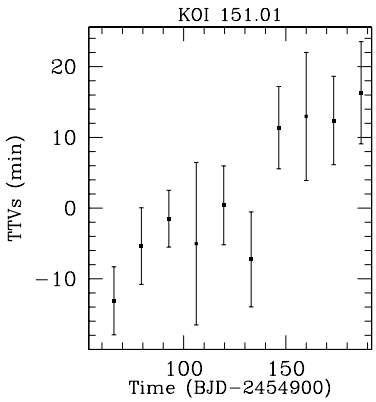
KOI 151.01
TTVs (min)
20
10
0
−10
100
150
Time (BJD−2454900)

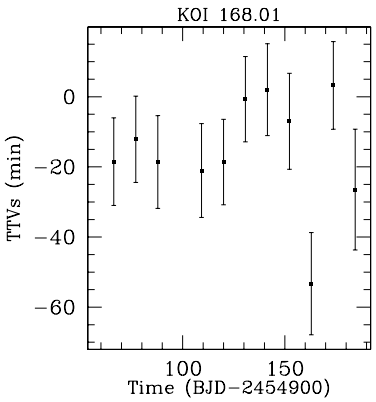
KOI 168.01
TTVs (min)
0
−20
−40
−60
100
150
Time (BJD−2454900)

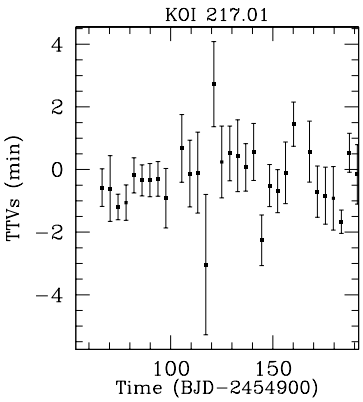
KOI 217.01
TTVs (min)
4
2
0
−2
−4
100
150
Time (BJD−2454900)

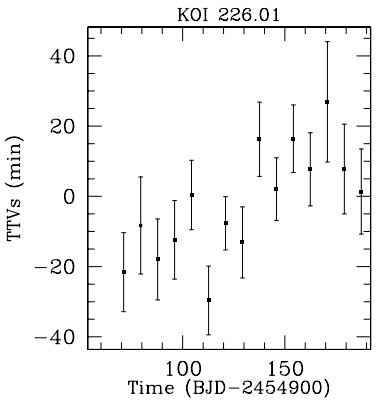
KOI 226.01
TTVs (min)
40
20
0
−20
−40
100
150
Time (BJD−2454900)

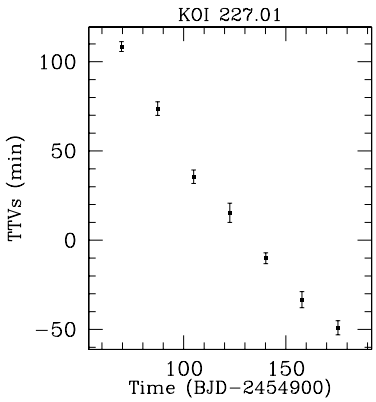
KOI 227.01
TTVs (min)
100
50
0
−50
100
150
Time (BJD−2454900)

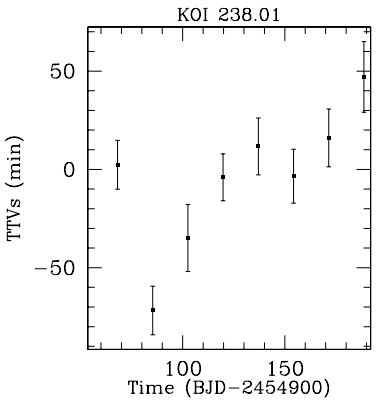
KOI 238.01
TTVs (min)
50
0
−50
100
150
Time (BJD−2454900)

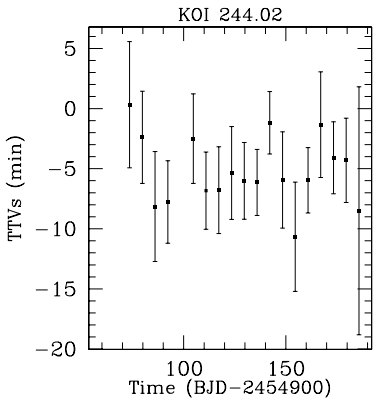
KOI 244.02
TTVs (min)
5
0
−5
−10
−15
−20
100
150
Time (BJD−2454900)

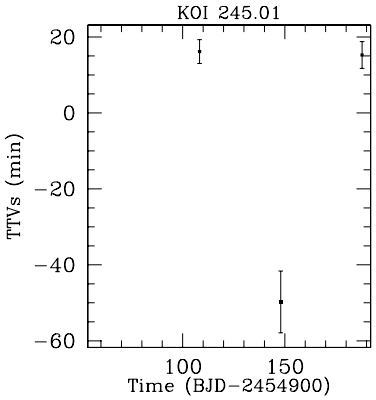
KOI 245.01
TTVs (min)
Time (BJD−2454900)

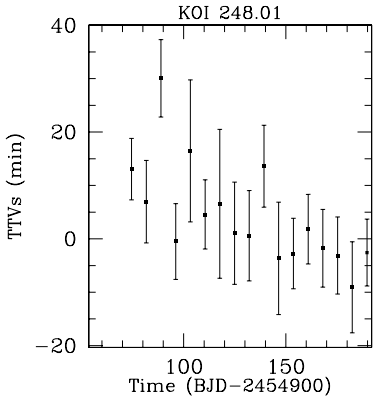
KOI 248.01
TTVs (min)
Time (BJD−2454900)

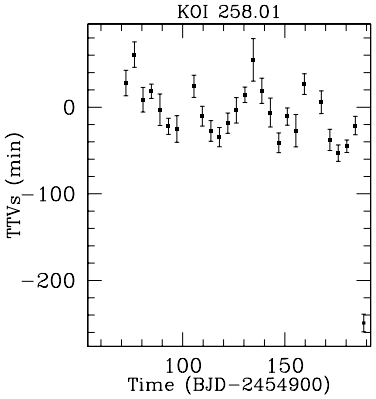
KOI 258.01
TTVs (min)
Time (BJD−2454900)

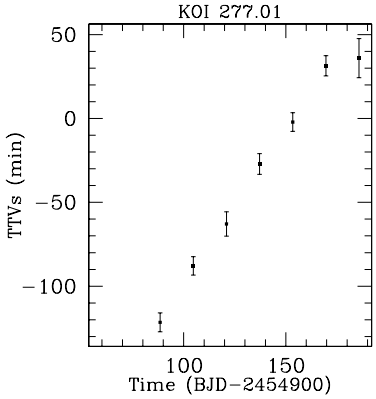
KOI 277.01
TTVs (min)
Time (BJD−2454900)

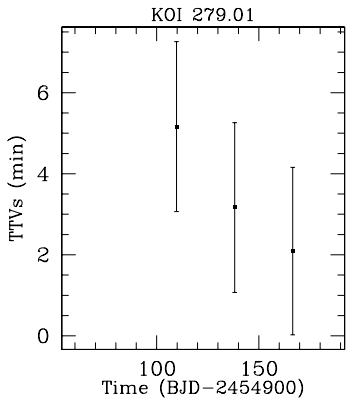
KOI 279.01
TTVs (min)
6
4
2
0
100
150
Time (BJD−2454900)

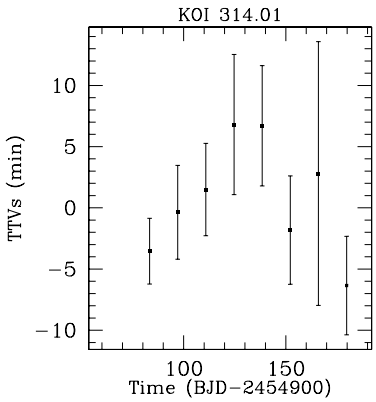
KOI 314.01
TTVs (min)
10
5
0
−5
−10
100
150
Time (BJD−2454900)

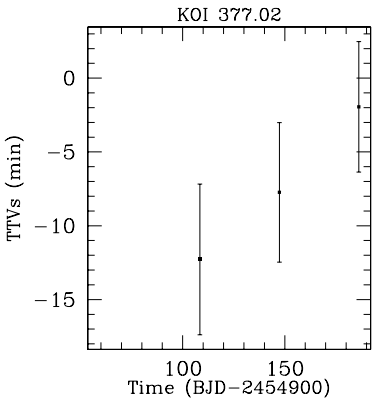
KOI 377.02
TTVs (min)
0
−5
−10
−15
100
150
Time (BJD−2454900)

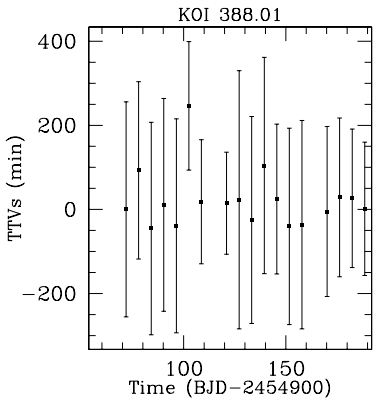
KOI 388.01
TTVs (min)
400
200
0
−200
100
150
Time (BJD−2454900)

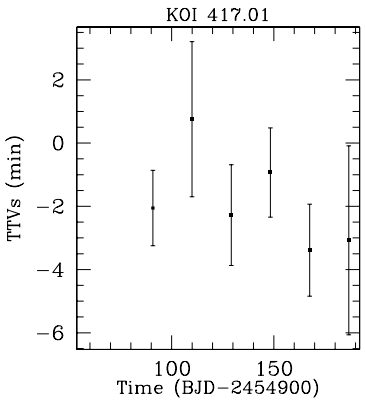
KOI 417.01
TTVs (min)
2
0
−2
−4
−6
100
150
Time (BJD−2454900)

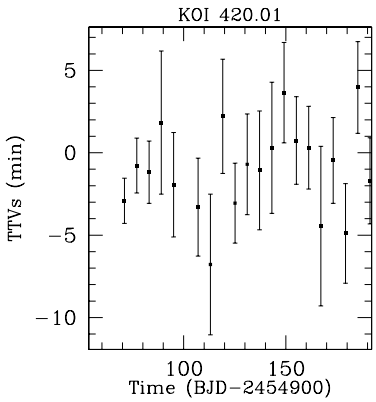
KOI 420.01
TTVs (min)
5
0
−5
−10
100
150
Time (BJD−2454900)

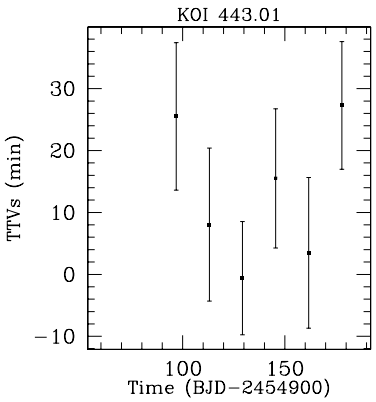
KOI 443.01
TTVs (min)
30
20
10
0
−10
100
150
Time (BJD−2454900)

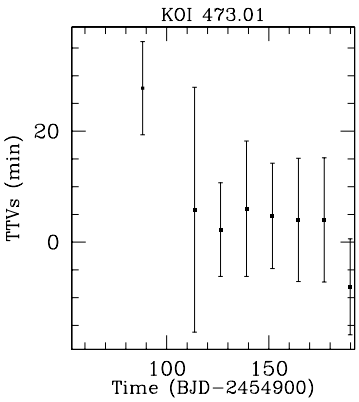
KOI 473.01
TTVs (min)
20
0
100
150
Time (BJD−2454900)

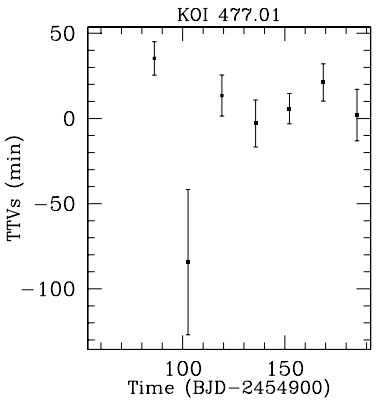
KOI 477.01
TTVs (min)
50
0
−50
−100
100
150
Time (BJD−2454900)

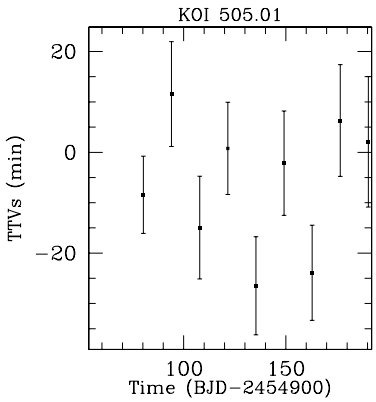
KOI 505.01
TTVs (min)
20
0
−20
100
150
Time (BJD−2454900)

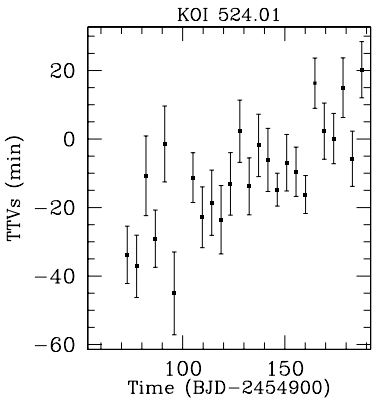
KOI 524.01
TTVs (min)
20
0
−20
−40
−60
100
150
Time (BJD−2454900)

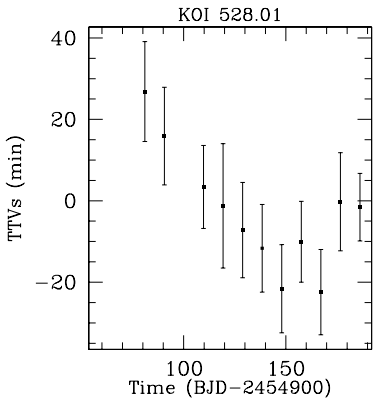
KOI 528.01
TTVs (min)
40
20
0
−20
100
150
Time (BJD−2454900)

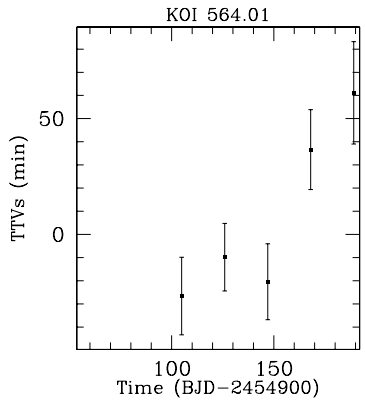
KOI 564.01
TTVs (min)
50
0
100
150
Time (BJD−2454900)

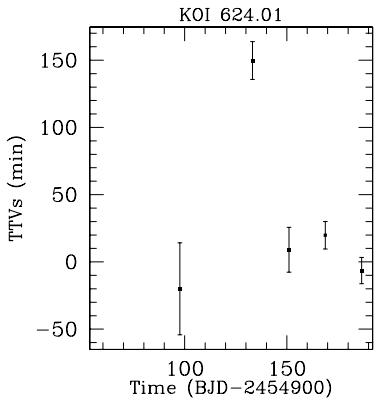
KOI 624.01
TTVs (min)
150
100
50
0
−50
100
150
Time (BJD−2454900)

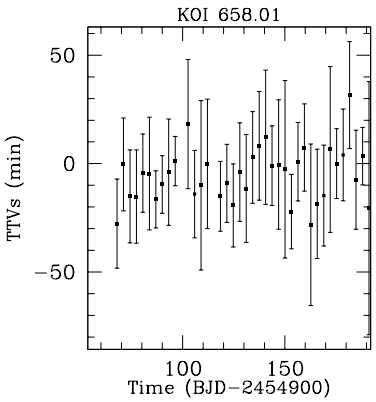
KOI 658.01
TTVs (min)
50
0
−50
100
150
Time (BJD−2454900)

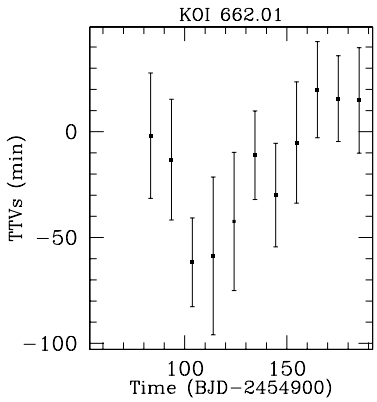
KOI 662.01
TTVs (min)
0
−50
−100
100
150
Time (BJD−2454900)

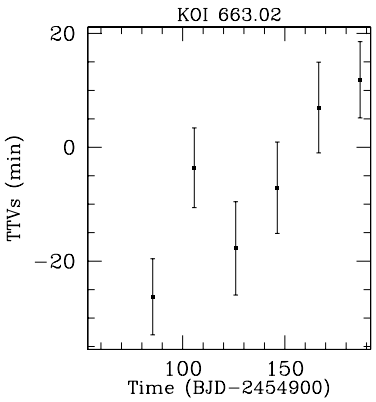
KOI 663.02
TTVs (min)
20
0
−20
100
150
Time (BJD−2454900)

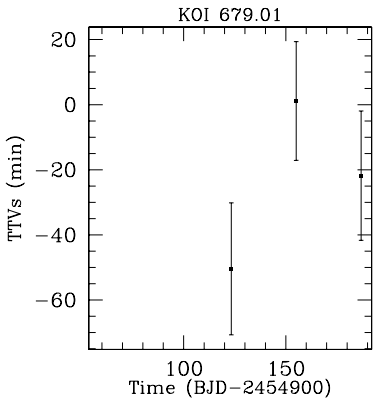
KOI 679.01
TTVs (min)
20
0
−20
−40
−60
100
150
Time (BJD−2454900)

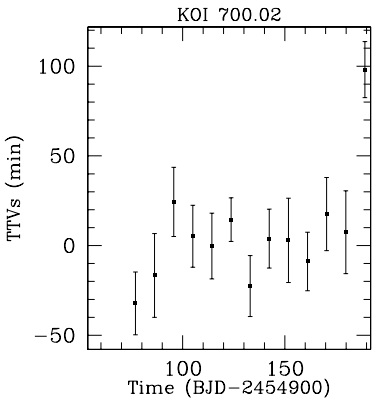
KOI 700.02
TTVs (min)
100
50
0
−50
100
150
Time (BJD−2454900)

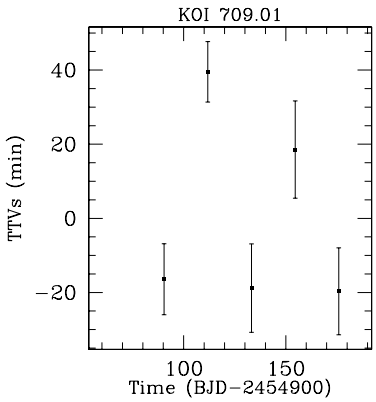
KOI 709.01
TTVs (min)
40
20
0
−20
100
150
Time (BJD−2454900)

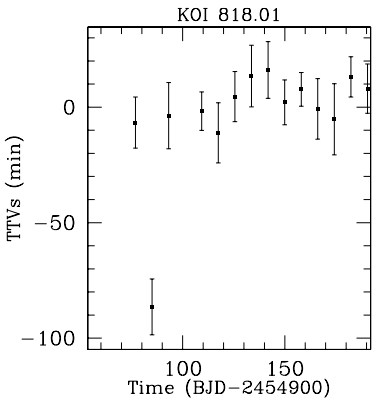
KOI 818.01
TTVs (min)
0
−50
−100
100
150
Time (BJD−2454900)

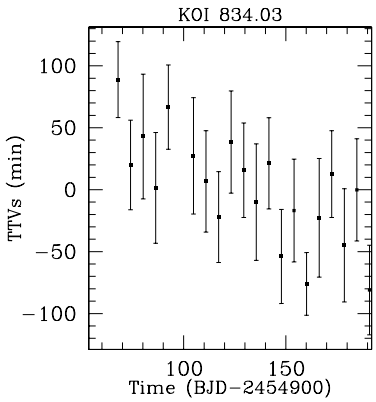
KOI 834.03
TTVs (min)
100
50
0
−50
−100
100
150
Time (BJD−2454900)

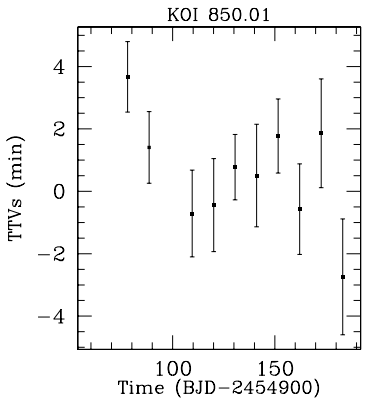
KOI 850.01
TTVs (min)
4
2
0
−2
−4
100
150
Time (BJD−2454900)

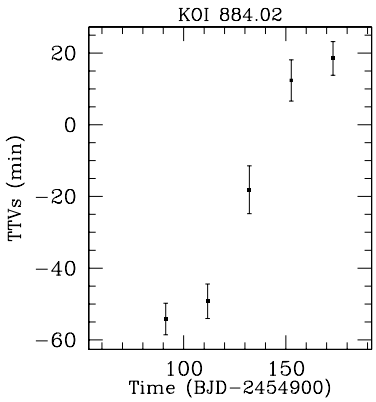
KOI 884.02
TTVs (min)
20
0
−20
−40
−60
100
150
Time (BJD−2454900)

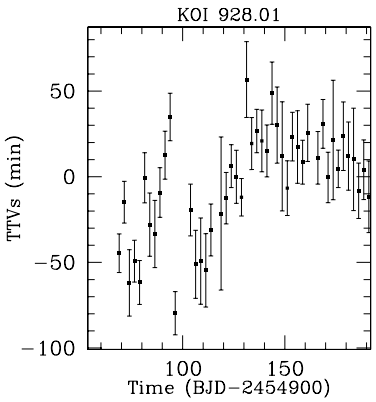
KOI 928.01
TTVs (min)
50
0
−50
−100
100
150
Time (BJD−2454900)

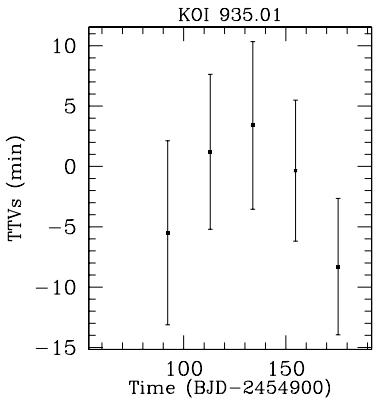
KOI 935.01
TTVs (min)
10
5
0
−5
−10
−15
100
150
Time (BJD−2454900)

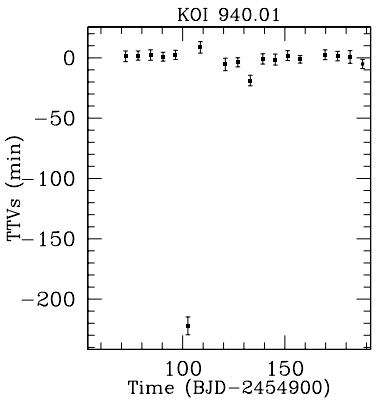
KOI 940.01
TTVs (min)
0
−50
−100
−150
−200
100
150
Time (BJD−2454900)

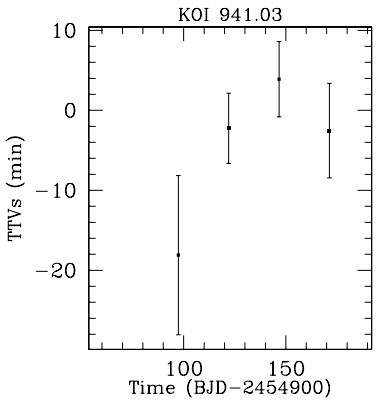
KOI 941.03
TTVs (min)
10
0
−10
−20
100
150
Time (BJD−2454900)

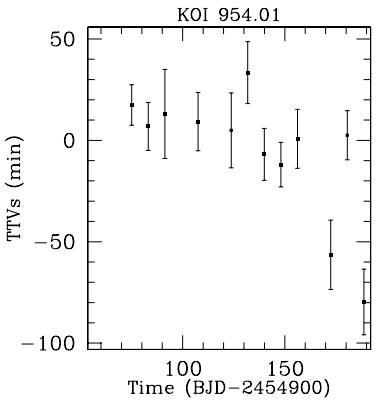
KOI 954.01
TTVs (min)
50
0
−50
−100
100
150
Time (BJD−2454900)

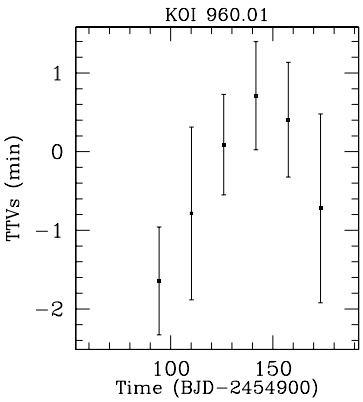
KOI 960.01
TTVs (min)
1
0
−1
−2
100
150
Time (BJD−2454900)

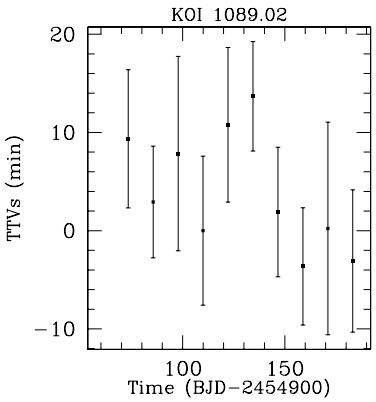
KOI 1089.02
TTVs (min)
20
10
0
−10
100
150
Time (BJD−2454900)

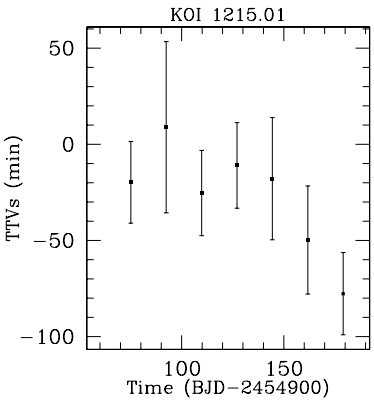
KOI 1215.01
TTVs (min)
50
0
−50
−100
100
150
Time (BJD−2454900)

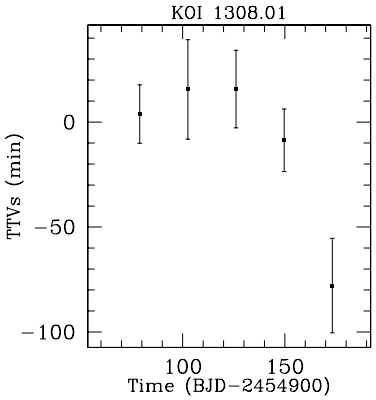
KOI 1308.01
TTVs (min)
0
−50
−100
100
150
Time (BJD−2454900)

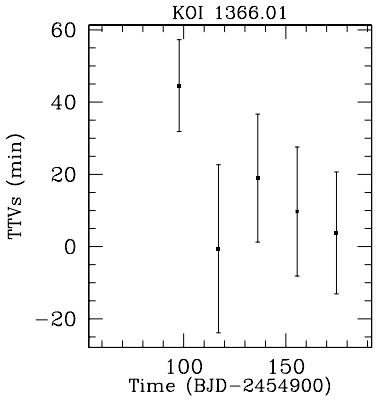
KOI 1366.01
TTVs (min)
60
40
20
0
−20
100
150
Time (BJD−2454900)

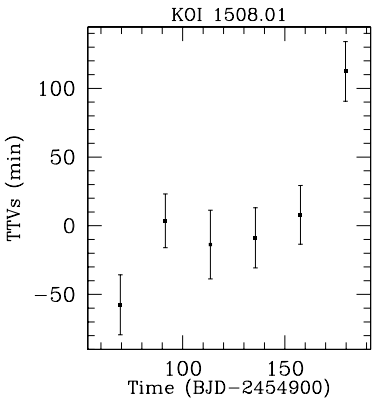
KOI 1508.01
TTVs (min)
100
50
0
−50
100
150
Time (BJD−2454900)

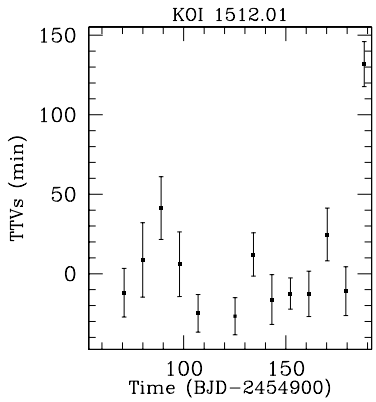
KOI 1512.01
TTVs (min)
150
100
50
0
100
150
Time (BJD−2454900)

Weak TTV Candidates

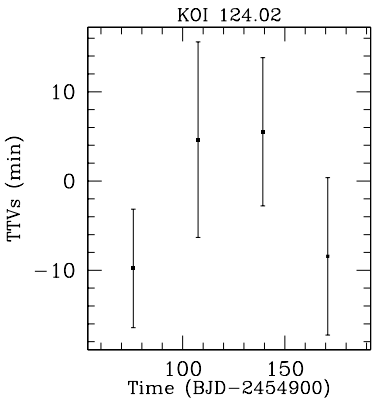

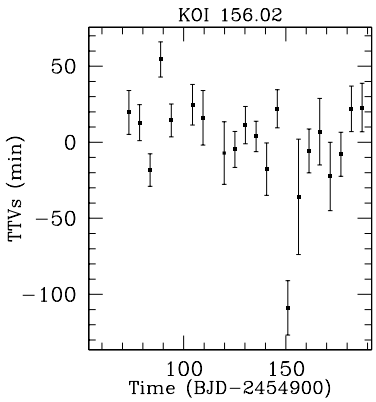

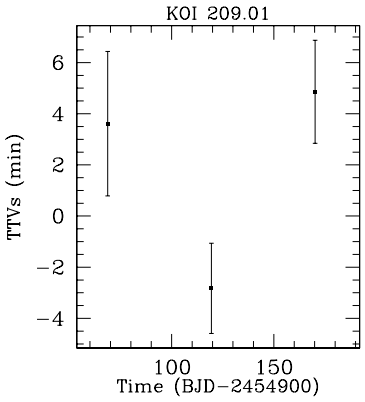
KOI 209.01
TTVs (min)
6
4
2
0
−2
−4
100
150
Time (BJD−2454900)

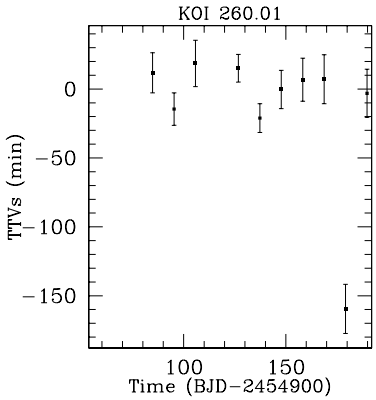
KOI 260.01
TTVs (min)
0
−50
−100
−150
100
150
Time (BJD−2454900)

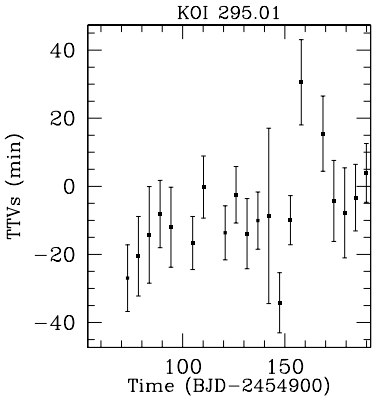
KOI 295.01
TTVs (min)
40
20
0
−20
−40
100
150
Time (BJD−2454900)

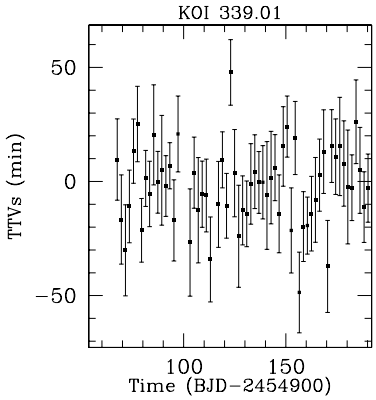
KOI 339.01
TTVs (min)
50
0
−50
100
150
Time (BJD−2454900)

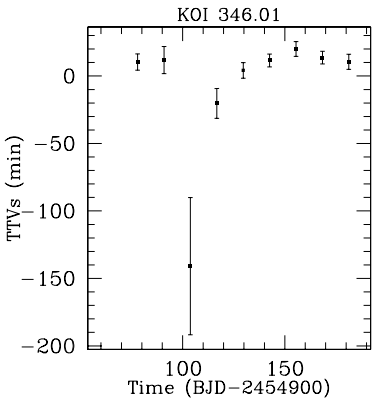
KOI 346.01
TTVs (min)
0
−50
−100
−150
−200
100
150
Time (BJD−2454900)

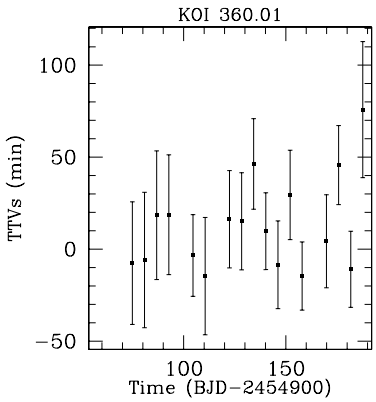
KOI 360.01
TTVs (min)
100
50
0
−50
100
150
Time (BJD−2454900)

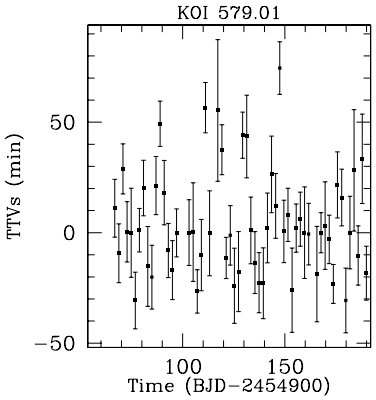
KOI 579.01
TTVs (min)
50
0
−50
100
150
Time (BJD−2454900)

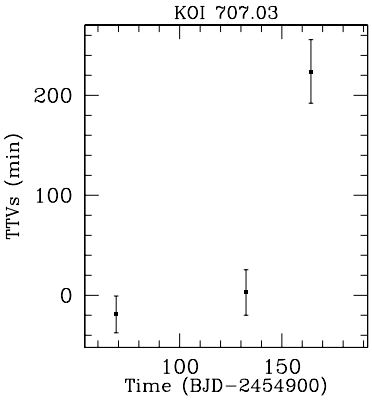
KOI 707.03
TTVs (min)
200
100
0
100
150
Time (BJD−2454900)

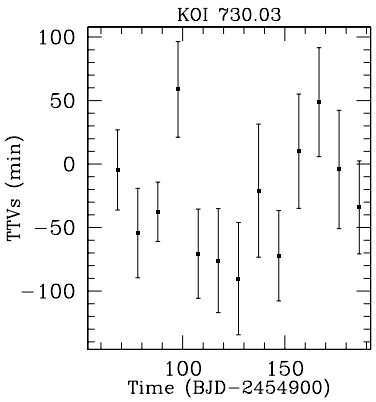
KOI 730.03
TTVs (min)
100
50
0
−50
−100
100
150
Time (BJD−2454900)

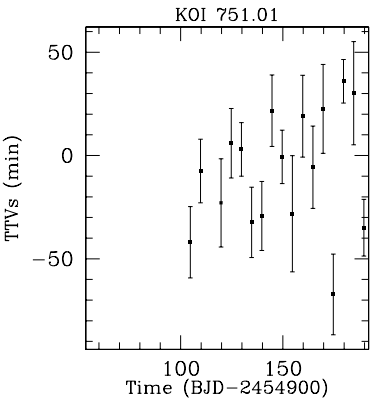
KOI 751.01
TTVs (min)
50
0
−50
100
150
Time (BJD−2454900)

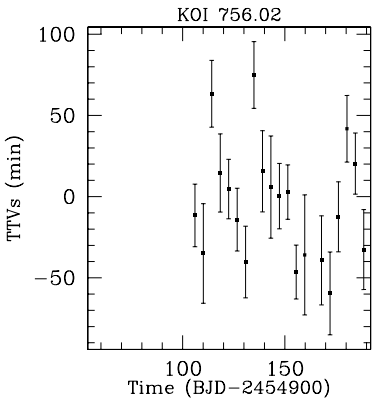
KOI 756.02
TTVs (min)
100
50
0
−50
100
150
Time (BJD−2454900)

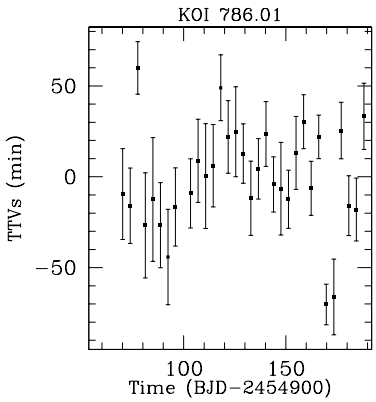
KOI 786.01
TTVs (min)
50
0
−50
100
150
Time (BJD−2454900)

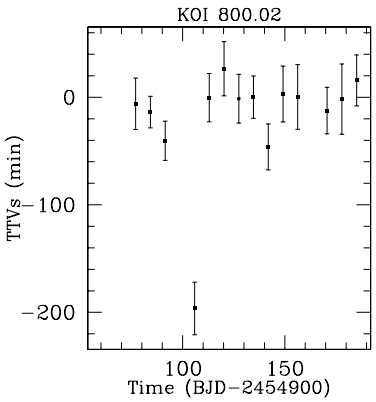
KOI 800.02
TTVs (min)
0
−100
−200
100
150
Time (BJD−2454900)

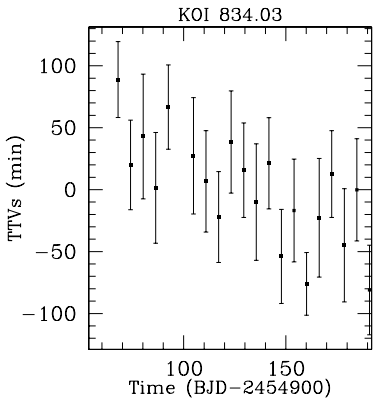
KOI 834.03
TTVs (min)
100
50
0
−50
−100
100
150
Time (BJD−2454900)

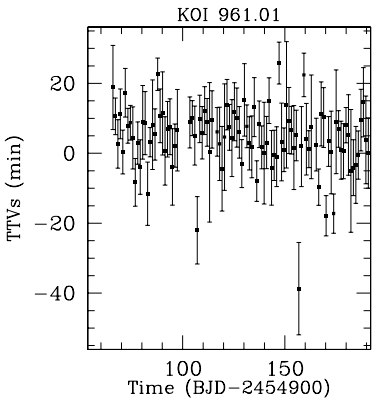
KOI 961.01
TTVs (min)
20
0
−20
−40
100
150
Time (BJD−2454900)

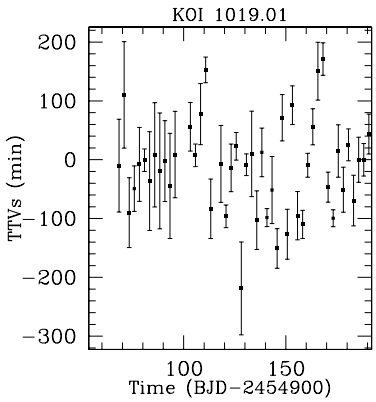
KOI 1019.01
TTVs (min)
200
100
0
−100
−200
−300
100
150
Time (BJD−2454900)

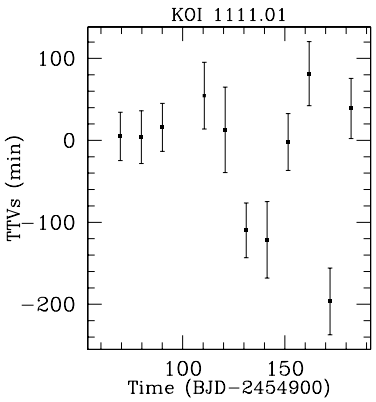
KOI 1111.01
TTVs (min)
100
0
−100
−200
100
150
Time (BJD−2454900)

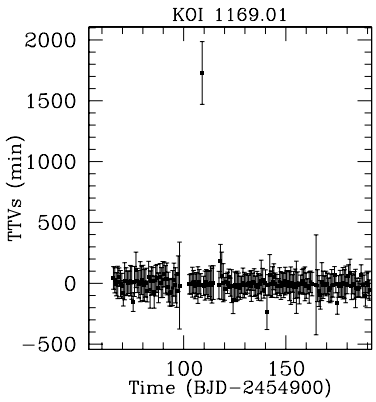
KOI 1169.01
TTVs (min)
2000
1500
1000
500
0
−500
100
150
Time (BJD−2454900)

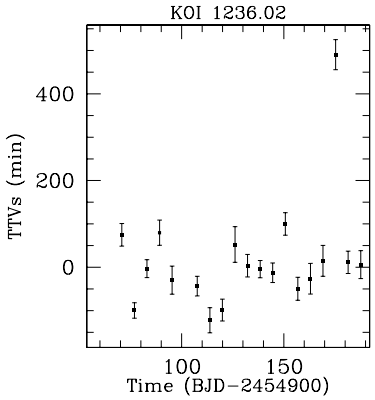
KOI 1236.02
TTVs (min)
400
200
0
100
150
Time (BJD−2454900)

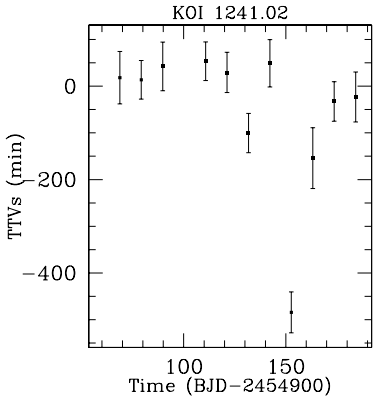
KOI 1241.02
TTVs (min)
0
−200
−400
100
150
Time (BJD−2454900)

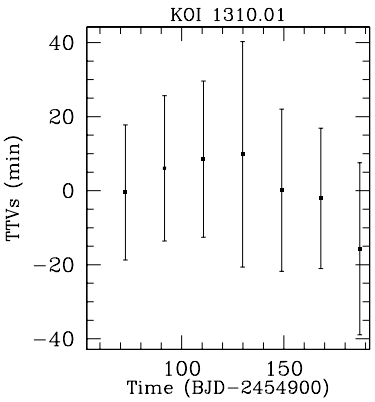
KOI 1310.01
TTVs (min)
40
20
0
−20
−40
100
150
Time (BJD−2454900)

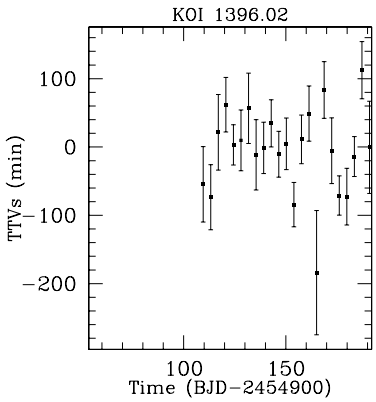
KOI 1396.02
TTVs (min)
100
0
−100
−200
100
150
Time (BJD−2454900)

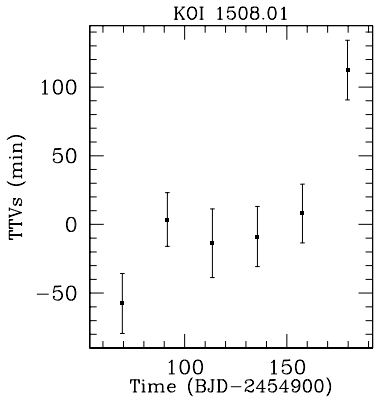
KOI 1508.01
TTVs (min)
100
50
0
−50
100
150
Time (BJD−2454900)

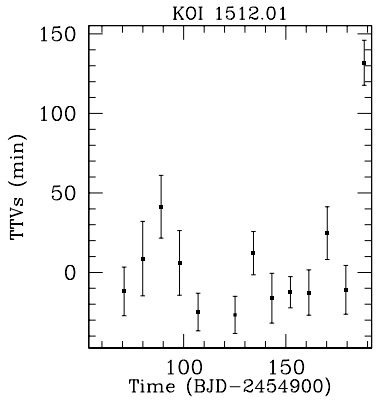
KOI 1512.01
TTVs (min)
150
100
50
0
100
150
Time (BJD−2454900)

Non-Detections of TTVs

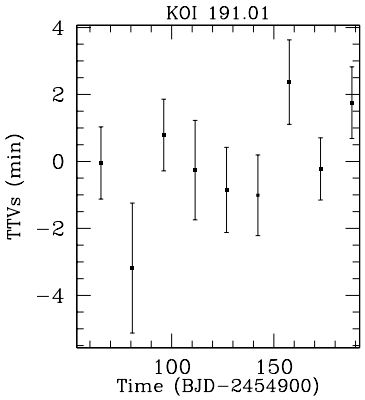

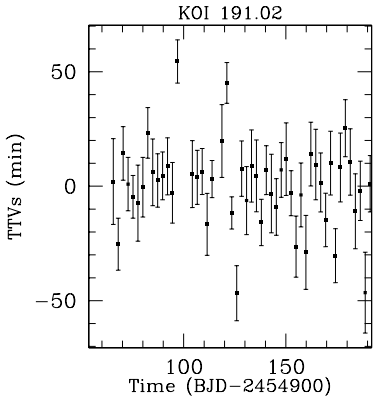

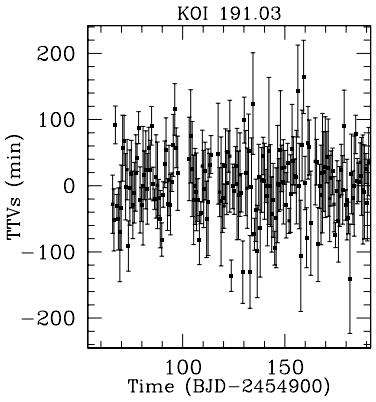
KOI 191.03
TTVs (min)
200
100
0
−100
−200
100
150
Time (BJD−2454900)

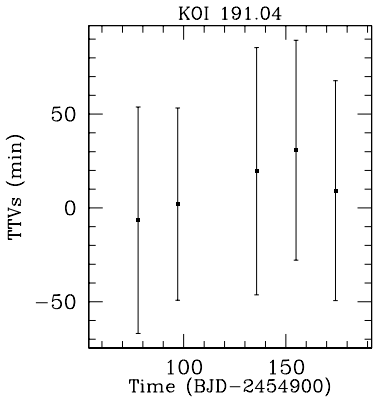
KOI 191.04
TTVs (min)
50
0
−50
100
150
Time (BJD−2454900)

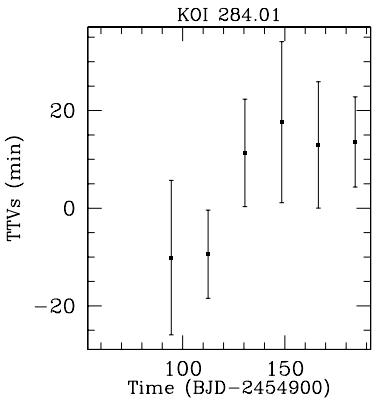
KOI 284.01
TTVs (min)
20
0
−20
100
150
Time (BJD−2454900)

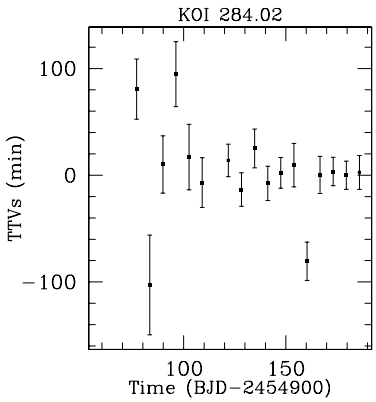
KOI 284.02
TTVs (min)
100
0
−100
100
150
Time (BJD−2454900)

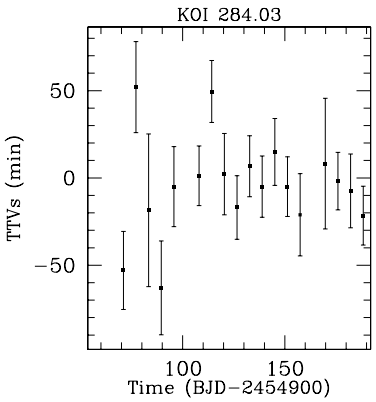
KOI 284.03
TTVs (min)
50
0
−50
100
150
Time (BJD−2454900)

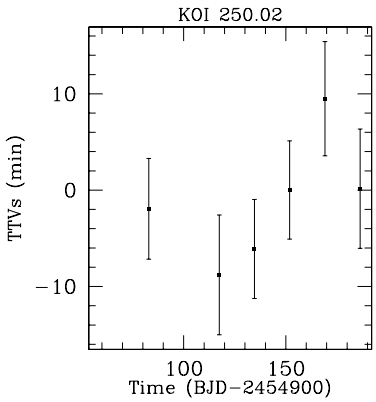
KOI 250.02
TTVs (min)
10
0
−10
100
150
Time (BJD−2454900)